

**A Novel Approach to Free Radical
Polymerization Focusing on Acrylic
Polymers for Commercial
Applications.**

By

Bertram Barnswell

Matriculation Number: 2975

**A Thesis Submitted For The Partially
Fulfillment Of The Requirements For
Doctor of Philosophy Degree
St. Clements University.**

Table of contents

Chapter 1

Introduction

- 1.1 The history of polymers 1
- 1.2 Free-radical polymerization 1
- 1.3 Controlled or 'Living' free-radical polymerization 2
- 1.4 Emulsion polymerization 3
- 1.5 Objective and outline 5
- 1.6 References 6

Chapter 2

controlled radical polymerization in emulsion

- 2.1 Introduction 8
- 2.2 Mechanism of Nitroxide-mediated CRP 8
- 2.3 Nitroxide-Mediated CRP in emulsion 10
 - 2.3.1 Requirements for rate coefficients 11
 - 2.3.2 Effect of heterogeneity and compartmentalization on NMCRP 17
- 2.4 Results and Discussion 22
 - 2.4.1 Bulk polymerizations 22
 - 2.4.2 Miniemulsion polymerizations 24
 - 2.4.3 Discussion 26
- 2.5 Conclusion 26
- 2.6 Experimental 26
- 2.7 References 28

Chapter 3

Homogeneous RAFT polymerizations 31

- 3.1 Introduction 32
- 3.2 The RAFT process 33
 - 3.2.1 Mechanism 33
 - 3.2.2 The transfer constant 37
- 3.3 Determination of the transfer constant 40
 - 3.3.1 The Mayo method 42
 - 3.3.2 The ln CLD method 48
 - 3.3.3 Mayo versus ln CLD method 49
 - 3.3.4 Results 53
- 3.4 Homopolymerizations of styrene and n-butyl acrylate 58
 - 3.4.1 The effect of RAFT on the rate of polymerization 58

- 3.4.2 Effect of the average termination rate, $\langle k_t \rangle$ on the 63
polymerization rate
- 3.4.3 Styrene polymerizations with a xanthate 65
- 3.4.4 n-Butyl acrylate polymerizations with xanthates 72
- 3.5 Conclusions 79
- 3.6 Experimental 80
- 3.7 References 82

Chapter 4

Seeded emulsion RAFT polymerizations 85

- 4.1 Introduction 86
- 4.2 Seeded emulsion polymerization for mechanistic studies 86
- 4.3 Zero-one seeded emulsion polymerization kinetics 87
 - 4.3.1 The rate of polymerization 87
 - 4.3.2 Model for entry 90
 - 4.3.3 Model for exit 95
 - 4.3.4 Literature overview of effect of RAFT agents and conventional 99
transfer agents on emulsion polymerization kinetics
 - 4.3.5 Retardation with RAFT in zero-one emulsion systems without 102
increased exit
- 4.4 Determination of the entry and exit rate by \odot -relaxation 104
 - 4.4.1 Determination of the exit rate coefficient, γ_{spont} and γ_{\odot} 104
 - 4.4.2 Determination of $\gamma_{\text{initiator}}$ 108
- 4.5 Experimental 108
- 4.6 Results and discussion 113
 - 4.6.1 The rate of polymerization without RAFT 114
 - 4.6.2 Influence of RAFT on the rate of polymerization 116
 - 4.6.3 Influence of RAFT on the molecular weight distribution 117
 - 4.6.4 Exit rate coefficients from \odot -relaxation experiments 120
 - 4.6.5 Dilatometry runs with chemical and \odot -initiation: determination 125
of entry rate coefficients
 - 4.6.6 Surface activity as the explanation for the decrease in entry rate 128
 - 4.6.7 Other explanations for the decrease in entry rate 131
- 4.7 Conclusions 133
- 4.8 References 133

Chapter 5

Block copolymer synthesis with RAFT 137

- 5.1 Introduction 138
- 5.2 Synthesis of polystyrene-block-poly(n-butyl acrylate) in solution 138
- 5.3 Synthesis of polystyrene-block-poly(n-butyl acrylate) in emulsion 148
- 5.4 Synthesis of polystyrene-block-poly(n-butyl acrylate) in emulsion 153

under semi-batch conditions
5.5 Polystyrene-block-poly(*n*-butyl acrylate) latex films 161
5.5.1 Introduction 161
5.5.2 The latexes and latex films 162
5.5.3 Discussion 165
5.6 Conclusions 166
5.7 Experimental 167
5.8 References 169

Appendices 171

Appendix 2.1 Calculation of M_n and M_w from two distributions 171
Appendix 3.1 Calculation of $\langle k_t \rangle$ 172
Appendix 3.2 Calculation of Q 172
Appendix 3.3 Simple model for RAFT 173
Appendix 3.4 Full model for RAFT 173
Appendix 4.1 Seeded emulsion polymerization rate 174
Appendix 4.2 Retardation by intermediate radical termination in emulsion 175
Appendix 5.1 PREDICI simulation of a block copolymerization 175

Summary 177

1. Introduction

1.1 *The history of polymers* [1,2]

The word polymer is derived from the Greek words *poly* and *mer*, meaning many and part, respectively, since a polymer consists of many repeating units. Natural polymers are as old as life. For instance DNA, wood and fur are all naturally occurring polymers. Many of these natural polymers were and still are used for clothing, building materials, weapons, *etc.*. Later on man started to modify these natural polymers in order to improve their properties. The first fully synthetic commercial polymer, Bakelite, appeared in 1910. At that time polymer structure was still a mystery, until Staudinger [3] suggested that polymers were large molecules containing long sequences of chemical units linked by covalent bonds. Nowadays synthetic polymers are part of everyday life and are used in cars, computers, packaging, paints, medicines, roads, houses, *etc.*

1.2 Free-radical polymerization

In order to produce a polymer, the repeating units of a polymer, the monomers, have to be linked by a chemical reaction. Free-radical polymerization is one of the most applied techniques to prepare synthetic polymers. A wide range of monomers of the general structure $\text{CH}_2=\text{CR}_1\text{R}_2$ can be polymerized via this method. Besides the wide range of monomers that can be used and thus the wide range of polymer properties that can be attained, the free-radical polymerization technique also is robust to higher impurity levels as compared to many other techniques, which make it a relatively cheap process.

Chapter 1

2. In a free-radical polymerization an initiator is used to initiate polymerization. The initiator generates radicals, active species that start the polymerization via monomer addition. Monomer addition continues until chain growth is stopped, either when two growing chains meet and terminate or when a growing chain abstracts a radical from another species, thereby transferring its activity towards this species. In both cases 'dead' polymer chains are formed, which cannot be re-initiated.

Generally, each chain grows very fast for a very limited time, in the order of nano Seconds or even less. Such a timescale is too short to vary polymerization conditions, e.g. the monomer composition, during chain growth. Moreover, the polymer chains do not grow simultaneously, on the contrary, initiation of new chains proceeds continuously throughout the polymerization during which polymerization conditions vary. These characteristics and the fact that 'dead' polymer chains are being formed, results in a very limited control over the molecular weight distribution, chemical composition distribution and polymer architecture. These drawbacks were removed by the development of new living polymerization techniques, like for instance anionic polymerization [4]. However, these techniques brought along other drawbacks. Monomer choice, for instance, is very limited and the reagents have to be extremely pure.

1.3 Controlled of free-radical polymerization

From the foregoing section one can deduce that ideally the versatility of free radical polymerization and the control over molecular weight, chemical composition and chain architecture, like in an anionic polymerization, are being combined in a single process. The last decade several of such techniques, that combine the advantages of free-radical polymerization and those of living polymerizations were invented[5]. These processes are being referred to as Controlled of free radical polymerizations and are based on two principles: reversible termination or reversible transfer. Examples of processes that rely on reversible termination are Nitroxide Mediated

Controlled free-Radical Polymerization (NMCRP)[6] and Atom Transfer Radical Polymerization (ATRP)[7]. In these processes species are added which prevent bimolecular termination by reversible coupling. In NMCRP this species is a nitroxide, whereas in ATRP this species is a halide atom, originating from a transition-metal complex to which it can be transferred reversibly. Processes that are based on reversible transfer include Degenerative Transfer (DT)[8] and Reversible Addition-Fragmentation chain Transfer (RAFT)[9]. In these processes there is a fast exchange between growing radicals and dormant species via transfer reactions, during which the RAFT-moiety (dithioester) or the DT-moiety (iodine atom) and radical activity are being exchanged. In RAFT this exchange proceeds via an intermediate radical, whereas in DT there is a direct exchange. In Scheme 1.1 a schematic representation is given of the key reactions in NMCRP, ATRP, DT and RAFT, respectively.

Scheme 1.1 Schematic representation of the exchange reactions in NMCRP (a), ATRP (b, M_n is a transition metal complex with a d_n electronic structure), DT (c) and RAFT (d).

1.4 Emulsion polymerization

Free-radical polymerizations can be carried out using different techniques, like bulk and solution polymerization. However, the tolerance towards all kind of impurities also allows free-radical polymerization to be performed in suspension or emulsion (*i.e.* carried out in an aqueous environment). In an emulsion polymerization, a water soluble initiator is added to an emulsion of monomer in water, stabilized with micelle forming surfactant. The aqueous phase radicals that are formed first initiate polymerization in monomer swollen micelles and later in monomer swollen polymer particles and finally a dispersion of polymer particles, typically 0.05-0.5 μm , is obtained. The emulsion polymers, which are being sold in water or in solid form, are

Chapter 1

4. being used in paints and coating, paper, adhesives, carpet backening, impact modification, *etc.*. Advantages of performing emulsion polymerization include:

- high polymerization rate and high conversions
- high heat transfer rates
- low viscosity at high solid contents and high molecular weights
- water-based rather than solvent-based and thus environmentally friendly and reduced safety hazards. The first patent on true emulsion polymerization appeared in 1929[10]. The first qualitative description of the characteristics of an emulsion polymerization were described by Harkins in 1945[11]. A quantitative description of Harkins model by Smith and Ewart [12] followed soon and the basics of this model are still widely used, although more and more detailed models have been published up to the present day. An excellent overview on emulsion polymerization kinetics is provided by Gilbert[13]. According to the theory provided by Harkins, Smith and Ewart

and others[13], an emulsion polymerization can be divided into 3 intervals. A short qualitative description is given below.

Interval I. In this stage soap micelles containing dissolved monomer are present, which serve as "generators" of the polymer particles. Entry of an aqueous phase radical, which has added enough aqueous phase monomer to become surface active, results in the formation of a monomer swollen polymer particle. The soap micelles continue to serve this function until all the soap becomes adsorbed on the polymer water interface of the monomer swollen polymer particles. At the end of Interval I only monomer swollen polymer particles and monomer droplets are present.

Interval II. Monomer is being transported from the monomer droplets through the aqueous phase to the polymer particles, where the polymerization takes place. At the end of Interval II all monomer droplets have disappeared and only monomer swollen polymer particles remain.

Interval III. In Interval III the remaining monomer present in the polymer particles is being polymerized.

A more detailed description of emulsion polymerization is provided in Chapter 4.

5.

1.5 Objective and outline

In the previous sections it was shown that emulsion polymerization presents many benefits over bulk or solution processes, whereas 'living' free-radical polymerization has expanded the possibilities of free-radical polymerization. Since the invention of 'living' free-radical polymerization processes the scope of the free-radical polymer chemist also includes controlled polymer architectures, a field that until recently was exclusively the domain of 'conventional' living polymerizations. The incentive to combine both the advantages of 'living' free-radical polymerization and emulsion polymerization in a single process is a logical one.

The main objective of this thesis is to investigate 'living' free-radical techniques in homogeneous media and in emulsion in order to obtain a thorough understanding of these systems. This knowledge will be applied to produce polymers with controlled architecture in emulsion. Two techniques will be investigated, NMCRP and RAFT.

In Chapter 2 kinetic and mechanistic aspects of NMCRP are discussed. The kinetic parameters, which are required for application in emulsion, *i.e.* at a temperature below the boiling point of water, are being evaluated using computer simulations. Furthermore, the effects of heterogeneity and compartmentalization on NMCRP are discussed. A series of nitroxides is screened for their applicability at reduced temperatures and in miniemulsion. In Chapter 3 homogeneous homo polymerizations of styrene and n-butyl acrylate using RAFT are described. The mechanism and the role of the transfer constant are discussed. Low conversion experiments were used to determine the transfer constants and the used methods and the reliability of these methods are discussed extensively.

High conversion homopolymerization using the same monomers are performed and the effect of RAFT on the rate of polymerization and on the molecular weight distribution is the subject of discussion. The results are compared with computer simulations.

Chapter 4 is dedicated to the kinetics and mechanism of RAFT in seeded emulsion polymerizations of styrene. The effect of RAFT on the polymerization rate, entry, exit and molecular weight distribution is studied using τ -relaxation experiments and dilatometry and the results are compared to theoretical models.

In Chapter 5 the RAFT technology is exploited for the synthesis of block copolymers of styrene and n-butyl acrylate. Both homogeneous systems and emulsion systems are considered. The synthesis of block copolymer latexes is further optimized by performing the polymerizations under semi-batch conditions. The film-forming properties of block copolymer latexes are being compared to random copolymer latexes and blended latexes of the same overall composition.

6.1.6 References

- [1] Stevens, M. P. **Polymer Chemistry; an introduction**; Oxford University Press: Oxford, (1999)
- [2] Young, R. J.; Lovell, P. A. **Introduction to polymers**; Chapman and Hall: London, (1991)
- [3] Staudinger, H. **From organic Chemistry to Macromolecules**; Wiley-Interscience: New York, (1970) / Originally published in: Chem. Ber. (1920), 53, 1073
- [4] Szwarc, M.. **"Living" polymers**. Nature (1956), 178 1168
- [5] Matyjaszewski, K. (Ed.) **Controlled Radical Polymerization**; ACS Symposium Series No. 685; Washington DC, 1997
- [6] Georges, M. K.; Moffat, K. A.; Veregin, R. P. N.; Kazmaier, P. M.; Hamer, G. K. **Narrow molecular weight resins by a free radical polymerization process; the effect of nitroxides and organic acids on the polymerization**. Polym. Mater. Sci. Eng. (1993) 69, 305
- [7] Wang, J. S.; Matyjaszewski, K. **"Living"/Controlled Radical Polymerization. Transition-Metal-Catalyzed Atom Transfer Radical Polymerization in the Presence of a Conventional Radical Initiator**. Macromolecules (1995) 28(22), 7572
- [8] Matyjaszewski, K.; Gaynor, S.; Wang, J. S. **Controlled Radical Polymerizations: The Use of Alkyl Iodides in Degenerative Transfer**. Macromolecules (1995), 28(6), 2093
- [9] Chiefari, J.; Chong, Y. K.; Ercole, F.; Krstina, J.; Jeffery, J.; Le, T. P. T.; Mayadunne, R. T. A.; Meijs, Gordon F.; Moad, C. L.; Moad, G.; Rizzardo, E.; Thang, S. H. **Living Free-Radical Polymerization by Reversible Addition-Fragmentation Chain Transfer: The RAFT Process**. Macromolecules (1998), 31(16), 5559
- [10] Dinsmore, R.P., US 1,1732,795 (1929)
- [11] Harkins, W. D. **A general theory of the reaction loci in emulsion polymerization**. J. Chem. Phys. (1945), 13(9), 381
- [12] Smith, W. V.; Ewart, R. H. **Kinetics of emulsion polymerization**. J. Chem. Phys. (1948), 16(6), 592
- [13] Gilbert, R. G. **Emulsion Polymerization: A Mechanistic approach**; Academic: London, (1995)

7.2 Nitroxide-mediated controlled radical polymerization in emulsion

Abstract

In this chapter the approach towards obtaining macromolecular architectures in emulsion via nitroxide-mediated controlled free-radical polymerization (NMCRP) is investigated. First, the kinetics of NMCRP are discussed. Subsequently, computer simulations are used to evaluate the parameters that control this process at 90 °C (below the boiling point of water), which is normally performed at temperatures above 110 °C. Hereafter the effect of heterogeneity and compartmentalization on NMCRP is the subject of discussion. Finally a series of nitroxides was screened for their applicability at 90 °C in bulk polymerization conditions and in miniemulsion.

Chapter 2

8

2.1 Introduction

Nitroxide-Mediated Controlled Radical Polymerization (NMCRP) was first discovered by Solomon *et al.*, who patented their discovery in 1985[1]. This opened new ways in the field of free-radical polymerization. Polymer architectures, which were the domain of the anionic polymer chemist, became accessible to the free-radical polymer chemist. Moreover, the robustness of the free-radical process allowed the use of a much wider range of monomers. However, not until the work of Georges *et al.* was published in 1993[2], the world of polymer chemistry became aware of the possibilities of this new class of free-radical polymerization. This was the beginning of what is nowadays one of the leading topics in free-radical polymer chemistry: Controlled or 'Living' Free Radical Polymerization. This initiated the search for new Controlled or 'Living' Free Radical Polymerization techniques, and soon afterwards other methods like Degenerative Transfer (DT)[3], Atom Transfer Radical Polymerization (ATRP)[4] and Reversible Addition-Fragmentation chain Transfer (RAFT)[5,6] were developed.

2.2 Mechanism of Nitroxide-mediated CRP

The mechanism of nitroxide-mediated CRP is based on the reversible activation of dormant polymer chains (P_n-T) shown in Scheme 2.1. This additional reaction step in the free-radical polymerization provides the living character and controls the molecular weight distribution.

Scheme 2.1 Reversible activation of dormant polymer chains.

When a dormant species or alkoxyamine dissociates homolytically, a carbon centered radical and a stable nitroxide radical are formed (Scheme 2.2). This is a reversible process and the reversible reaction is close to diffusion control, but at high enough temperatures where dissociation is competitive, the polymeric radicals ($P_n\cdot$) can add to monomer, which allows step wise growth of the polymer chains. The nitroxide is an ideal candidate for this process since it only reacts with carbon- P_n k_{act} k_{deact} $P_n + T$ centered radicals, is stable and does not dimerize, and in general couples nonspecifically with all types of carbon-centered radicals (close to diffusion controlled rates).

Scheme 2.2 Dissociation of a typical alkoxyamine into a carbon-centered radical (ethylbenzene radical) and a nitroxide (TEMPO).

In an ideal NMCRP, polymerization is started using an alkoxyamine as initiator such that no other reactions than reversible activation of dormant species and addition of monomer to carbon-centered radicals take place. The alkoxyamine consist of a small radical species, capable of reacting with monomer, trapped by a nitroxide.

Upon decomposition of the alkoxyamine in the presence of monomer, polymeric dormant species will form and grow in chain length over time. However, this is not a clean reaction and side products can form.

Since the nitroxide and the carbon-centered radical diffuse away from each other, termination by combination or disproportionation of two carbon centered radicals cannot be excluded. This will lead to the formation of 'dead' polymer chains and an excess of free nitroxide. The built-up of free nitroxide is referred to as the Persistent Radical Effect[7] and slows down the polymerization, since it will favor trapping (radical-radical coupling) over propagation. Besides termination, other side reactions play an important role in nitroxide-mediated CRP. One of the important side reactions is decomposition of dormant chains[8], yielding polymer chains with an unsaturated end-group and a hydroxyamine, TH (Scheme 2.3, reaction 6). Another side reaction is thermal self-initiation[9], which is observed in styrene polymerizations at high temperatures. Here two styrene monomers can form a dimer, which after reaction with another styrene monomer, results in the formation of 2 radicals (Scheme 2.3, reaction 7). This additional radical flux can make up the loss of radicals due to irreversible termination and allows the polymerization to proceed successfully, providing that the number of initiating radicals is small compared to the number of nitroxide-trapped polymer chains [10]. Also systems that do not show thermal self-O N O N initiation can be set under control by use of an additional initiator, which will provide the additional radical flux[10]. In addition, the dimer formed (Scheme 2.3, reaction 7) can react with a nitroxide molecule to provide the dimer radical and a hydroxyamine. In Scheme 2.3, all reactions of importance in nitroxide-mediated CRP are shown.

Scheme 2.3 Mechanism of Nitroxide-Mediated CRP. R-T represents an alkoxyamine, T· represents a nitroxide.

2.3 Nitroxide-Mediated CRP in emulsion

Many successful applications of Nitroxide-Mediated CRP (NMCRP) in bulk or solution have been published and are still under investigation[e.g. 12,13].

This

success is a result of the high temperatures that can be achieved in bulk or solution, being an ideal reaction condition for NMCRP. However, the goal of the work in this chapter was to apply NMCRP in emulsion polymerization, so the temperature is limited to the boiling point of water, *i.e.* 100 °C, unless the polymerization is performed under high pressure, as shown by Bon[11,14] and others[15-21].

Low temperature R $T_{kactkdeact}$ R + T P_n T $kactkdeact$ P_n + T
 (de)activation of alkoxyamine (1) R + M k_p P₁ propagation (2) (de)activation of dormant chains
 3) P_n + M k_p P_{n+1} propagation (4) P_n + P_m k_t P_{n+m} termination (5) k_{dec} P_n + T-H
 decomposition (6) P_n T = 2 M k_{dim} thermal self-initiation(7) $k_{d, f}$ 2 P₁ initiation (8) DIMER
 DIMER + M k_{dimM} P₁ + R

Applications require different nitroxides, because the homolytic dissociation rate of the C-O bond decreases drastically with temperature. Besides the low temperatures, an emulsion system brings along other complications, like the heterogeneity and compartmentalization of the system. In the following part the kinetic parameters that are required for a successful application of NMCRP in emulsion at 90 °C will be discussed. In addition, some aspects of the heterogeneity and compartmentalization of the system will be subject of discussion.

2.3.1 Requirements for rate coefficients

Lowering the reaction temperature to 90 °C has a large impact on NMCRP. This will be shown on the basis of the reactions shown in Scheme 2.3. These were entered in the software simulation package PREDICI[22], so the influence of all parameters can be evaluated.

Two very simple model systems will be considered, in which only reactions 1 to 5 from Scheme 2.3 are involved. Reactions 6 and 7 are slow processes and can for our purposes be neglected. One system has a low propagation rate coefficient k_p and the other has a high k_p . For simplicity it is assumed

11.

that the termination rate constant is equal in both systems and not chain length dependent, although this assumption might lead to differences between simulation and experiments [23]. Because of the low temperature, thermal self-initiation does not play a role. Unless otherwise stated, the parameters and concentrations used in both systems are summarized in Table 2.1. The reaction time was limited to 10 hours.

For each kind of polymeric species, *i.e.* polymeric radicals, dead chains and nitroxide end-capped chains, the number average molecular weight, the weight average molecular weight and the number of chains are calculated. The amount of polymeric radicals can be neglected, so the overall molecular weights can be calculated from the sum of the dead chains and the nitroxide end-capped (dormant) chains. These calculations are shown in Appendix 2.1.

Table 2.1 Rate coefficients[36] and initial concentrations used in PREDICI simulations of a NMCRP for the low k_p and high k_p model systems.

low k_p high k_p k_p $1 \cdot 10^3 \text{ dm}^3 \text{ mol}^{-1} \text{ s}^{-1}$ $2 \cdot 10^4 \text{ dm}^3 \text{ mol}^{-1} \text{ s}^{-1}$ k_{p1} $4 \cdot 10^3 \text{ dm}^3 \text{ mol}^{-1} \text{ s}^{-1}$ $8 \cdot 10^4 \text{ dm}^3 \text{ mol}^{-1} \text{ s}^{-1}$ k_{act} $1 \cdot 10^{-3} \text{ s}^{-1}$ $1 \cdot 10^{-3} \text{ s}^{-1}$ k_{deact} $1 \cdot 10^8 \text{ dm}^3 \text{ mol}^{-1} \text{ s}^{-1}$ $1 \cdot 10^8 \text{ dm}^3 \text{ mol}^{-1} \text{ s}^{-1}$ k_t $1 \cdot 10^8 \text{ dm}^3 \text{ mol}^{-1} \text{ s}^{-1}$ $1 \cdot 10^8 \text{ dm}^3 \text{ mol}^{-1} \text{ s}^{-1}$ $[R-T]_0$ 0.10 mol dm^{-3} 0.10 mol dm^{-3} $[M]_0$ 10 mol dm^{-3} 10 mol dm^{-3} **Influence of k_{act}**

In Figure 2.1 the results of the simulations, in which k_{act} is varied between 10^{-5} and 10^{-1} s^{-1} , are shown. In all simulations the amount of dead polymer chains formed was limited to a maximum of about 5 w%. It can be seen that k_{act} has a large effect of the polymerization rate, for both the low and high k_p system. For the low k_p system one can see that the conversion after 10 hours is very limited (Figure 2.1a), unless k_{act} has a very high and unrealistic value of 10^{-1} s^{-1} . For the high k_p system a reasonable conversion is obtained at all activation rate coefficients (Figure 2.1b).

To check whether a polymerization is controlled, both the number average degree of polymerization and the polydispersity versus conversion are considered. In an ideal 'living' system the degree of polymerization shows a linear increase with conversion with slope $[M]_0/[R-T]_0$ and the polydispersity is close to 1. From Figure 2.1c it can be observed that these criteria are met for the two highest k_{act} values in the low k_p system. In the high k_p system (Figure 2.1d), on the other hand, these criteria are only met for the case that k_{act} is 10^{-1} s^{-1} . Because of the high k_p value in this system, the monomer consumption is fast compared to the half-life time of the alkoxyamine R-T in the case that k_{act} is 10^{-5} s^{-1} or 10^{-3} s^{-1} . This means that each time an alkoxyamine dissociates, a lot of monomer is inserted before deactivation takes place. In the case that k_{act} is 10^{-5} s^{-1} this leads to very high degrees of polymerization, which therefore are not plotted in Figure 2.1d. It can also be observed that for the intermediate k_{act} , 10^{-3} s^{-1} , the degree of polymerization is high at lower conversions, but follows the ideal linear increase above ca. 65% conversion. This means that at a monomer conversion of about 65% all the initially present alkoxyamine has been consumed. However, for low polydispersities it is required that all chains grow more or less simultaneously. Therefore, the polydispersity in this case does not go below 1.5. Although in

12.

the end the polydispersity in this case is high it still means that (almost) all chains have a nitroxide end-group and therefore can be used for chain extension.

Figure 2.1 PREDICI simulations of the influence of k_{act} on conversion, degree of polymerization and polydispersity (PD) for model systems described in Table 2.1 with a low k_p (a and c) and a high k_p (b and d).

In conclusion one can say that for a reasonable polymerization rate in the low k_p system one needs a k_{act} of about 10^{-1} s^{-1} and for a low polydispersity a value of about 10^{-3} is required. For the high k_p system the rate of polymerization is no problem, however, for good control k_{act} values of about 10^{-1} are required. A k_{act} of 10^{-3} results in functional polymers with an

intermediate polydispersity. Since activation rate coefficients in the order of 10^{-1} s^{-1} are not realistic for a C-O bond dissociation rate at $90 \text{ }^\circ\text{C}$, one has to focus on values in the order of 10^{-3} s^{-1} .

This value is close to the highest k_{act} at $90 \text{ }^\circ\text{C}$ found in literature[24]. For the low k_p

a (low k_p)

0 7200 14400 21600 28800 36000

0.0

0.1

0.2

0.3

0.4

0.5

0.6

0.7

0.8

0.9

1.0

conversion [-]

time [s]

kact = 10^{-5} s^{-1}

kact = 10^{-3} s^{-1}

kact = 10^{-1} s^{-1}

0.1 0.2 0.3 0.4 0.5 0.6 0.7 0.8 0.9 1.0

0

10

20

30

40

50

60

70

80

90

100

Degree of polymerization [-]

conversion [-]

kact = 10^{-5}

kact = 10^{-3}

kact = 10^{-1}

1.2

1.6

2.0

2.4

2.8

3.2

3.6

4.0

PD [-]

kact = 10^{-5}

kact = 10^{-3}

kact = 10^{-1}

0 7200 14400 21600 28800 36000

0.0

0.1

0.2

0.3

0.4

0.5
 0.6
 0.7
 0.8
 0.9
 1.0
 conversion [-]
 time [s]
 b (high k_p)
 d (high k_p) c (low k_p)
 0.1 0.2 0.3 0.4 0.5 0.6 0.7 0.8 0.9 1.0
 0
 20
 40
 60
 80
 100
 Degree of polymerization [-]
 conversion [-]
 1.2
 1.6
 2.0
 2.4
 2.8
 3.2
 3.6
 4.0
 PD [-]

system control is possible using this value, however, the polymerization rate is very slow in that case.

In the next part the effect of the deactivation rate coefficient, k_{deact} , will be considered. A lower deactivation coefficient will increase the polymerization rate. The question is to which extent the rate will be increased and will it be without loss of control. After that the effect of an additional radical flux by use of an additional initiator will be discussed, which will also increase the polymerization rate.

For the high k_p system, no improvement is to be expected, because in this case the only way to improve the control of the polymerization would be a higher value of k_{act} . Since a value in the order of 10^{-1} is not realistic, this system will not be considered anymore in the following. However, it has to be kept in mind that a k_{act} in the order of 10^{-3} s^{-1} results in nitroxide end-capped polymers of intermediate polydispersity, which can be used for block copolymerizations.

Effect of k_{deact}

Figure 2.2 shows the results of simulations for the low k_p system from Table 2.1, in which the value for the deactivation rate coefficient, k_{deact} , has been varied between 10^4 and $10^8 \text{ dm}^3 \text{ mol}^{-1} \text{ s}^{-1}$.

As expected, a decrease in the deactivation rate coefficient results in a higher polymerization rate, as shown in Figure 2.2a. If the deactivation rate coefficient is low, bimolecular termination becomes competitive with trapping reactions. This leads to the formation of dead chains. In Figure 2.2a it is shown that a low value of k_{deact} of $10^4 \text{ dm}^3 \text{ mol}^{-1} \text{ s}^{-1}$ leads to a considerable weight fraction of dead chains. Figure 2.2b shows that for the two highest

values of k_{deact} the system is under control, although at low conversions the polydispersity is rather high. In the case that k_{deact} is $10^4 \text{ dm}^3 \text{ mol}^{-1} \text{ s}^{-1}$ it is shown that the number average degree of polymerization does not increase linearly with conversion and that the polydispersities are high throughout the reaction.

These are the consequences of the large amount of dead chains that are produced during this reaction.

Figure 2.2 PREDICI simulation of the influence of k_{deact} on conversion (a), weight fraction dead chains

(a), degree of polymerization (b) and polydispersity (b) for the low k_p system from Table 2.1. The deactivation rate coefficient $k_{\text{deact}} = 1 \cdot 10^8 \text{ dm}^3 \text{ mol}^{-1} \text{ s}^{-1}$, $1 \cdot 10^6 \text{ dm}^3 \text{ mol}^{-1} \text{ s}^{-1}$ and $1 \cdot 10^4 \text{ dm}^3 \text{ mol}^{-1} \text{ s}^{-1}$, respectively.

These results show that the rate of polymerization can be increased by using nitroxides with a lower rate coefficient of deactivation than the conventional ones, often having a k_{deact} of 10^8 - $10^9 \text{ dm}^3 \text{ mol}^{-1} \text{ s}^{-1}$ [37]. The rate coefficient of a fast reaction between two species can be calculated from the rate coefficient of diffusion and from the rate coefficient of the chemical reaction[11]:

$$k_{\text{chem}} D_{\text{deact}} k_1 k_2 = (2.1)$$

This means that one can lower the deactivation rate constant by synthesizing nitroxides with bulky groups attached to it. This will reduce both the diffusion rate and the chemical reaction rate due to steric hindrance

Effect of an additional radical flux

The additional radical flux in styrene polymerization at high temperatures is a result of thermal self-initiation of styrene. It determines the polymerization rate and is the key behind the success of these polymerizations[25]. At $90 \text{ }^\circ\text{C}$ and with other monomers thermal self-initiation plays no role. In order to produce an additional radical flux in these systems one can add an initiator[26]. In order to keep the amount of dead chains low, the amount of initiator consumed at the end of the reaction has to be small compared to the amount of nitroxide present.

a b
 0.1 0.2 0.3 0.4 0.5 0.6 0.7 0.8 0.9 1.0
 0
 25
 50
 75
 100
 125
 150
 $k_{\text{deact}} = 10^8$
 $k_{\text{deact}} = 10^6$
 $k_{\text{deact}} = 10^4$
 Degree of polymerization [-]
 conversion [-]
 1.0
 1.2
 1.4
 1.6
 1.8
 2.0
 2.2

2.4
 2.6
 2.8
 3.0
 k_{deact} = 108
 k
 deact
 = 106
 k_{deact} = 104
 PD [-]
 0 7200 14400 21600 28800 36000
 0.0
 0.1
 0.2
 0.3
 0.4
 0.5
 0.6
 0.7
 0.8
 0.9
 1.0
 conversion [-]
 time [s]
 k_{deact} = 108
 k_{deact} = 106
 k_{deact} = 104
 0.0
 0.1
 0.2
 0.3
 0.4
 0.5
 0.6
 0.7
 0.8
 0.9
 1.0
 k_{deact} = 108
 k_{deact} = 106
 k_{deact} = 104
 w dead chains [-]
Chapter 2

Chapter2

16

In Figure 2.3 the results of simulations in which additional initiator is present are shown. In these simulations the model is extended with the initiation reaction from Scheme 2.3 (reaction 8). It is assumed that the initiator efficiency, f , is equal to 1.

Further, the values for the low k_p system from Table 2.1 have been used.

Figure 2.3 PREDICI simulation of the influence of additional initiator on conversion (a), weight fraction dead chains (a), degree of polymerization (b) and polydispersity (b) for the low k_p system from Table 2.1.

A system without additional initiator, and systems with 0.01 and 0.1 M initiator having a k_d of 10^{-6} s^{-1} and 10^{-5} s^{-1} are being compared.

Figure 2.3 shows that, by using additional initiator, one can increase the polymerization rate considerably, without losing control. Both the weight fraction of dead chains and the polydispersity remain low, unless the amount of initiator is high and the decomposition is fast on the reaction timescale.

Influence of k_{dec}

When a carbon-centered radical is trapped by a nitroxide via disproportionation, which means that the nitroxide abstracts a β -hydrogen atom, a hydroxyamine and a polymer chain with an unsaturated chain-end are formed. In reaction 6 of Scheme 2.3 this decomposition of alkoxyamines or dormant chains is considered as an unimolecular process, with rate coefficient k_{dec} .

In order to play a negligible role, the half-life time of a dormant chain with respect to decomposition has to be large compared to the reaction time. This half-life time is equal to $\ln(2)/k_{dec}$. This means that the maximum value of k_{dec} has to be in the order of 10^{-6} s^{-1} when the reaction time is 10 hours. Such a value leads to about 4%

```

a b
0 7200 14400 21600 28800 36000
0.0
0.1
0.2
0.3
0.4
0.5
0.6
0.7
0.8
0.9
1.0
conversion [-]
time [s]
0.0
0.1
0.2
0.3
0.4
0.5
0.6
0.7
0.8
0.9
1.0
no initiator
[I]=10-2 M, kd=10-6
[I]=10-1 M, kd=10-6
[I]=10-2 M, kd=10-5
[I]=10-1 M, kd=10-5
w dead chains [-]
0.1 0.2 0.3 0.4 0.5 0.6 0.7 0.8 0.9 1.0
0
10
20
30
40
50

```

60
70
80
90
100

Degree of polymerization [-]
conversion [-]

1.0
1.2
1.4
1.6
1.8
2.0
2.2
2.4
2.6
2.8
3.0

no initiator

[I]=10⁻² M, kd=10⁻⁶

[I]=10⁻¹ M, kd=10⁻⁶

[I]=10⁻² M, kd=10⁻⁵

[I]=10⁻¹ M, kd=10⁻⁵

PD [-] dead chains, whereas a value one order of magnitude higher results in 30% dead chains.

2.3.2 Effect of heterogeneity and compartmentalization on NMCRP

In an emulsion polymerization the monomer-swollen polymer particles and monomer droplets are dispersed in the aqueous phase. Due to the heterogeneity of the system the kinetics are much more complex. In a bulk polymerization, all species present are distributed homogeneously over the reaction volume, whereas in an emulsion polymerization these species are distributed over the different phases with different concentrations. Some species are compartmentalized, since they cannot be transported from one phase to another, while other species can.

In 1998 Morbidelli *et al.*[27] carried out simulations on nitroxide-mediated polymerizations in miniemulsion systems. A miniemulsion consists of small metastable monomer droplets dispersed in an aqueous phase. In these monomer droplets the polymerization takes place. The advantage of miniemulsions is that no transport of species from the monomer droplets through the aqueous phase to the polymer particles is required, which enables one to use extremely water insoluble monomers or other water insoluble species, like *e.g.* transfer agents or alkoxyamines. Morbidelli *et al.* considered reaction 3, 4, 5 and 7 from Scheme 2.3. They started with very low molecular weight dormant chains and took thermal initiation into account. Further they assumed that not only polymer chains, but also the nitroxide molecules were completely compartmentalized. What they found was that the polymerization rate decreased with increasing segregation, *i.e.* decreasing particle size, and that the polydispersity also decreased with increasing segregation.

Opposite results were published by Charleux[28], who did simulations on a similar system. However, she did not take thermal initiation into account because a polymerization temperature below 100 °C was considered. More

importantly, Charleux assumed that the nitroxide molecules were not completely compartmentalized so exchange between the particles via diffusion through the aqueous phase is possible.

She found that both the polymerization rate and the polydispersity of the polymer increased with increasing segregation.

To check whether or not a nitroxide molecule is compartmentalized, the probability that a nitroxide will exit a particle can be calculated. It is assumed that a particle contains 1 nitroxide molecule and 1 carbon-centered radical. A nitroxide inside a particle can have two possible fates. It can either diffuse away into the aqueous phase or it can trap a carbon-centered radical. For the diffusional escape rate of a nitroxide a similar approach can be used as for a monomeric radical in an emulsion polymerization[29]. Therefore the following expression can be used for the diffusional escape rate coefficient of a nitroxide:

$$k_{\text{escape}} = \frac{D_w}{r_s} \left(\frac{k_p [P_n^\cdot]_p}{k_t [T^\cdot]_p + k_{\text{deact}}} \right) \quad (2.2)$$

in which D_w is the diffusion coefficient of the nitroxide in water, q is the partitioning coefficient of the nitroxide between the particle phase and the aqueous phase and r_s is the particle radius. Thus the probability that a nitroxide will escape from a particle is:

$$p_{\text{escape}} = \frac{k_{\text{escape}}}{k_{\text{escape}} + k_{\text{deact}} + k_p \frac{[P_n^\cdot]_p}{[T^\cdot]_p}} \quad (2.3)$$

in which $[T^\cdot]_p$ is the concentration of 1 nitroxide molecule in a particle and $[P_n^\cdot]_p$ is the concentration of 1 carbon centered radical in a particle. In Table 2.2 the values used in the calculations of p_{escape} versus particle diameter are shown. The result is shown in Figure 2.4a.

Table 2.2 Parameters used to calculate p_{escape} and $r_{p/d}$ versus particle diameter (Eqs. 2.3 and 2.4).

D_w $1.5 \cdot 10^{-9} \text{ m}^2 \text{ s}^{-1}$ Diffusion coefficient of styrene [29]. It is assumed that the diffusion coefficient of a nitroxide comparable.

q 900 Partitioning coefficient of TEMPO at 90 °C[30]

k_{deact} $1 \cdot 10^8 \text{ dm}^3 \text{ mol}^{-1} \text{ s}^{-1}$

$[P_n^\cdot]_p$ $1/N_{AV} \text{ mol dm}^{-3}$ Concentration is calculated using the Avogadro number and the volume of 1 particle in dm^3

k_p 900 $\text{dm}^3 \text{ mol}^{-1} \text{ s}^{-1}$ Propagation rate constant of styrene at 90 °C [31]

$[M]_p$ 8 mol dm^{-3} Concentration of styrene in a miniemulsion at

about 8% conversion $[T^\cdot]_p$ $1/N_{AV} \text{ mol dm}^{-3}$ Concentration is calculated using the Avogadro number and the volume of 1 particle in dm^3

Figure 2.4 (a) Probability that a nitroxide will escape from a particle that contains 1 carbon centered radical and 1 nitroxide molecule versus particle diameter. (b) Ratio of propagation over deactivation of a carbon-centered radical in a particle that contains 1 carbon centered radical and 1 nitroxide molecule versus particle diameter.

Figure 2.4a shows that a nitroxide, in this case TEMPO, has a large probability of escaping from a particle, unless a particle has an unrealistically small diameter for a miniemulsion. Moreover, as a result of the Persistent Radical Effect the number of nitroxide molecules per particle will generally be more than 1, which will even increase the probability of escape. For other nitroxides, similar results will be obtained, unless the nitroxide is extremely water-insoluble. These results indicate that the simulations done by Morbidelli *et al.* are not based on a realistic situation because they assumed that the nitroxide is strictly compartmentalized. The simulations of Charleux are therefore more realistic. However, if the nitroxide used is very water-insoluble, so it cannot escape, another aspect of compartmentalization has to be taken into account.

One can imagine that after activation of a dormant chain inside a particle there is a competition between monomer and the nitroxide to react with the carbon-centered radical. Increasing the particle size will favor propagation, since this will lower the nitroxide concentration, while the monomer concentration remains the same, assuming each particle contains only 1 free nitroxide molecule. This is why Morbidelli found that the polymerization rate increased with increasing the particle size. One can calculate the ratio of propagation over deactivation, $r_{p/d}$, as follows:

$$r_{p/d} = \frac{k_p [M]_p}{k_t [T\cdot]_p} \quad (2.4)$$

a b

Chapter 2

20

in which $[M]_p$ is the concentration of monomer in the polymer particle and $[T\cdot]_p$ the concentration of nitroxide in the polymer particle. In Table 2.2 the

monomer will lead to less nitroxide in the aqueous phase and thus better control.

If we consider, with respect to partitioning of the nitroxide, a conventional *ab initio* or seeded emulsion polymerization then a third phase is present, *i.e.* the monomer droplet phase. This phase can act as a huge reservoir for free nitroxide and alkoxyamine and therefore take away the controlled character of the NMCRP. For good control it is required that all the alkoxyamine is present in the polymer particles from the start of the reaction. Besides, the alkoxyamine in the monomer droplets will lead to polymerization inside the droplets, causing colloidal instability. This can be avoided by using water-soluble alkoxyamines, which after propagation in the aqueous phase, will become water insoluble and enter the particles because these have a much larger surface area than the monomer droplets. However, even if all the alkoxyamine were present in the particles from the start, the problem that the monomer droplet phase serves as a large reservoir for free nitroxide still exists. Although it is more likely that a nitroxide that has escaped from a particle will re-enter another particle rather than a monomer droplet, most of the nitroxide will still end up in the monomer droplets. This is because after re-entry in another particle, the nitroxide will re-escape again because most particles contain an excess of free nitroxide due to the Persistent Radical Effect. Therefore the distribution of the nitroxide over the different phases will be determined by partitioning behavior, which is dependent on volume ratios, and not on the ratios of surface area, which would be the case if re-entry were irreversible.

This means that most of the free nitroxide will end up in the monomer droplets, leading to loss of control. Therefore, the miniemulsion approach will be better than conventional emulsion polymerization techniques.

2.4 Results and Discussion

In the previous section it has been shown that in theory controlled polymerizations with nitroxides at 90 °C are possible. It requires that the activation rate coefficient of the dormant chains is high enough. The polymerization rate can be increased by using an additional radical flux and by using nitroxides with lower deactivation rate coefficients. Another important kinetic parameter is the decomposition rate coefficient of the dormant chains, which should be low since the amount of decomposition is determined by the reaction time.

Chapter 2

22

It was also shown that in emulsion polymerizations a nitroxide is expected not to be strictly compartmentalized. Therefore, increasing segregation will lead to increased polymerization rates and broader molecular weight distributions. Further, it has been discussed that partitioning of the nitroxide will lead to problems in conventional emulsion polymerizations and therefore miniemulsion is a better option.

The most commonly used nitroxide is TEMPO (Scheme 2.2). The polystyrene

adduct of this nitroxide has a k_{act} of $4 \cdot 10^{-5} \text{ s}^{-1}$ at $90 \text{ }^\circ\text{C}$ [32,14]. It has been shown in section 2.2.1 that this is too low for a successful application in emulsion at $90 \text{ }^\circ\text{C}$.

In the next sections the results which were obtained in bulk polymerizations of styrene at $90 \text{ }^\circ\text{C}$ and in miniemulsion polymerizations of styrene at $90 \text{ }^\circ\text{C}$ with different alkoxyamines will be discussed. The alkoxyamines differ from each other with respect to the nitroxide moiety and are shown in Scheme 2.4.

Scheme 2.4 Alkoxyamines used for bulk and miniemulsion polymerizations of styrene at $90 \text{ }^\circ\text{C}$.

2.4.1 Bulk polymerizations

Four different alkoxyamines have been synthesized in order to evaluate their usefulness at lower temperatures. Based on molecular orbital calculations, alkoxyamine **2** is supposed to have a lower activation enthalpy than **1**[33] and, therefore, should be more suitable for polymerizations at lower temperatures.



Alkoxyamine **3** is supposed to have a lower activation enthalpy based on interaction of the hydroxyl group. **4** has been patented[34] and has proven to be a suitable alkoxyamine for polymerizations at temperatures below $100 \text{ }^\circ\text{C}$ [24 and refs. herein].

In Table 2.3 the results of bulk polymerizations of styrene at $90 \text{ }^\circ\text{C}$ with a monomer to alkoxyamine mole ratio of 200 are shown.

Table 2.3 Results of bulk polymerizations of styrene at $90 \text{ }^\circ\text{C}$ with different alkoxyamines. The molar ratio of monomer to alkoxyamine is 200 (na means not analysed).

time [h] conversion [%] M_n [g/mol] experimental M_n [g/mol]
theoretical polydispersity M_w/M_n

(1)

7.5 0.03 na na
24.25 5.5 1427 1109 1.33
48.5 16.7 2774 3340 1.35
55 19.9 3167 3978 1.34
127.5 54.3 5720 10856 1.31
146.5 59.9 6197 11986 1.27

(2)

19.25 11.9 2552 2372 1.16

26.75 16.4 2515 3280 1.21
43.25 20.7 4242 4139 1.3
50.25 21.4 na na
67.25 20.5 3976 4101 1.36

(3)

17.25 18.6 3148 3717 1.55
24.25 27.5 4189 5492 1.48
41.5 42.0 5679 8400 1.41
48.75 47.9 6153 9574 1.38
65.75 51.2 na na
72.5 52.9 6322 10586 1.42
91.25 53.9 na na
161.3 73.9 6560 14781 1.34
185.5 84.2 6846 16835 1.34

(4)

2 23.0 4226 4594 1.57
6.17 40.2 6772 8045 1.36
22.5 81.7 13150 16337 1.22
29.25 96.9 14518 19388 1.25

Table 2.3 shows that indeed higher conversions are obtained for **2**, **3** and **4** than for **1** at comparable reaction times. When considering conversions at the polymerization times closest to 24 hours for each alkoxyamine, 5.5%, 16.4%, 27.5% and 81.7% conversion is found for **1**, **2**, **3** and **4**, respectively. The polydispersities are between 1.2 and 1.4 at almost all datapoints and the molecular weights are lower than theoretically expected. Since the theoretically expected value is deduced from moles of alkoxyamine that are put in the system and the moles of monomer that are consumed, this means that the number of polymer chains is higher than the number of alkoxyamine molecules that were put in the system, and thus side reaction like *e.g.*

transfer to monomer and thermal self-initiation play a role.

2.4.2 Miniemulsion polymerizations

The same experiments were repeated in a miniemulsion system for alkoxyamines

1, **3** and **4**. Alkoxyamine **2** was not used anymore because of the low conversion that

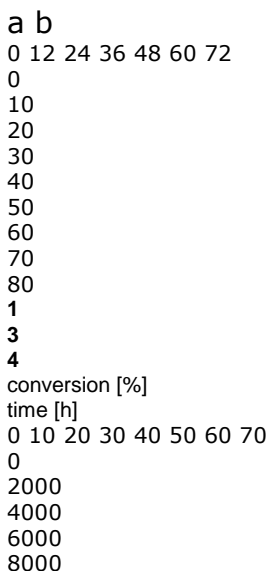
was obtained in the bulk experiment with this species. Miniemulsions are aqueous dispersions of relatively stable oil droplets within a size range of 50 to 500 nm containing monomer, water, surfactant and a so-called cosurfactant or hydrophobe, which hinders the Oswald ripening effect[36]. Ideally, these monomer droplets remain intact throughout the polymerization, while they gradually transform into polymer particles. However in practice not all monomer droplets are initiated and the final particle size distribution is not an exact copy of the initial monomer droplets size distribution. Because the reaction is so slow, the main problem here was to create a miniemulsion that is stable at 90 °C for a long time. After all, a miniemulsion is not thermodynamically stable. Conventional miniemulsion recipes with sodium

dodecyl sulfate did not result in stable miniemulsions. Moreover, dozens of other recipes, surfactants and hydrophobes have been tried, however non of these resulted in miniemulsion that were stable for more than 24 hours at 90 °C. Ultimately Dowfax 8390 in combination with hexadecane gave satisfying results, *i.e.* a stable miniemulsion with a z-average diameter in the order of 300-400 nm. This combination was used by El-Aasser *et al.* for miniemulsions at 125 °C under high pressure[18,19]. In Figure 2.5 the results of the miniemulsion polymerizations with **1**, **3** and **4** are shown.

Figure 2.5 Results of miniemulsion polymerizations of styrene at 90 °C with different alkoxyamines: (a) conversion versus time and (b) M_n and polydispersity versus conversion. The solid line represents the theoretically predicted M_n .

These results show that the reaction is controlled, *i.e.* a linear increase of M_n with conversion is observed and polydispersities are below 1.5, in the case of **4** even below 1.3. Moreover, M_n is close to the theoretical values, although at low conversions M_n is higher than the theoretical value and at higher conversions M_n is somewhat lower. The latter is probably the result of thermal initiation, which leads to an extra amount of polymer chains and thus a lower M_n .

According to the simulations performed by Charleux [28], segregation will lead to an increase in polymerization rate for small particles, whereas the simulation of Morbidelli *et al.*[27] predict the opposite. This difference is a result of a difference in the assumed fate of a free nitroxide. Charleux assumed that a nitroxide molecule is not completely compartmentalized while Morbidelli *et al.* assumed it is. If the polymerization rates of the miniemulsion polymerizations are compared to the bulk polymerizations, it can be seen that for **3** and **4** the polymerization rate in the bulk polymerization is higher and for **1** the polymerization in the miniemulsion polymerization is higher. However, in these experiments the particle size was in the order of 400 nm and in that case both Charleux and Morbidelli predict a polymerization rate similar to the polymerization rate in bulk. The differences in rate between bulk and miniemulsion will therefore have other causes and might be the result of side-reactions or differences in oxygen levels.



10000
12000
1
3
4
theory
Mn [g/mol]
conversion [%]
1.0
1.2
1.4
1.6
1.8
2.0
1
2
3
polydispersity [-]

2.4.3 Discussion

It has been shown that both in bulk and in miniemulsion controlled polymerization at 90 °C is possible, although the polymerization rate, except for **4** is very low. This low polymerization rate is probably a consequence of the low activation rate parameters of the nitroxides used. Due to the Persistent Radical Effect the polymerization rate is slowed down even more. As a consequence of the long polymerization times also side reactions like decomposition and thermal self-initiation become important, resulting in dead chains and lower molecular weights than desired.

Because of these drawbacks, NMCRP in emulsion at 90 °C does not seem very promising for most nitroxides. However, if nitroxides with properties like **4** or better are developed, NMCRP in miniemulsion can be a promising technique for creating complex architectures in emulsion, as has already been shown in literature[21].

In the following chapters another promising technique, Reversible Addition-Fragmentation chain Transfer (RAFT) will be investigated.

2.5 Conclusion

It was found that the use of alkoxyamines results in controlled polymerizations at 90 °C, both in bulk and in miniemulsion. However, extremely long polymerization times are required in order to obtain a reasonable conversion at this temperature and full conversion will even be harder to obtain. Therefore, industrial application of this method at temperatures below 100 °C does seem not promising with the nitroxides **1**, **2** and **3**. There are, however, novel nitroxides being prepared that allow controlled polymerizations at lower temperatures (**4**), but these still suffer from limited monomer choice and experimental conditions.

2.6 Experimental

Materials

Styrene was purchased from Aldrich and purified by distillation under reduced pressure. All other materials were from Aldrich (unless stated otherwise) and used as received.

2.6.1 Synthesis of alkoxyamines

1 and **2** were synthesized from ((-bromoethyl)benzene and the corresponding nitroxides, which were purchased, in the presence of 2,2'-bipyridine-complexed copper(I) bromide. THF was used as solvent. For the synthesis of **3** and **4**, the 2,2'-bipyridine ligands were replaced by pentamethyldiethylenetriamine ligands.

For **1** and **2** a yield above 90% was obtained, while for **3** and **4** the yields were 75% and 42% respectively. The nitroxide used for the synthesis of **3** was obtained using the classical synthesis of pyrrolidin-1-oxyl type nitroxides and is described elsewhere[11, p.14]. The synthesis of the nitroxide for **4** has been described by Tordo *et al.*[34].

2.6.2 Homogeneous polymerizations

Appropriate amounts of monomer and alkoxyamine were mixed in a round-bottom flask equipped with a magnetic stirrer and reflux condenser, all under an argon atmosphere. Oxygen was removed from the mixture by bubbling through nitrogen.

After that the flask was submerged in an oil bath which was at reaction temperature.

Conversion was determined gravimetrically.

2.6.3 Miniemulsion polymerizations

The miniemulsion was prepared as follows: a mixture of styrene, alkoxyamine and hexadecane was added to a mixture of water and Dowfax 8390 surfactant (supplied by Rhodia) and mixed at room temperature using a high shear mixer (Ystral X1020).

The emulsion was further homogenized using a sonifier (Dr. Hielscher UP 400S) for 3 minutes (50% duty, pulsed, power 5). A typical recipe contained 80 g water, 0.6 g Dowfax 8390, 1.0 g hexadecane, 20 g styrene and 0.4 g alkoxyamine. The miniemulsion was poured into a jacketed glass reactor, equipped with a reflux condenser and magnetic stirrer. Oxygen was removed by bubbling through nitrogen and keeping the reactor under argon atmosphere and stirring for 18 hours. Then the temperature was elevated to reaction temperature. Conversion was determined gravimetrically.

2.6.4 GPC Analysis

The dried polymer was dissolved in tetrahydrofuran (THF, Biosolve) to a concentration of 1 mg/mL. The solution was filtered over a 0.2 mm PTFE syringe-filter. Analyses were carried out using two PLGel (Mixed-C) columns (Polymer Laboratories) at 40 °C.

A Waters 486 UV-detector, operated at 254 nm, was used for detection. THF was used as eluent at a flow-rate of 1 mL/min. Narrow-distribution polystyrene standards (Polymer Laboratories) with molecular weights ranging from 580 to $7.1 \cdot 10^6$ g/mol were used to calibrate the GPC set-up.

2.7 References

[1] Solomon, D. H.; Rizzardo, E.; Cacioli, P. **Free radical polymerization and the produced polymers**. Eur. Pat. Appl. (1985), EP 135280

- [2] Georges, M. K.; Moffat, K. A.; Veregin, R. P. N.; Kazmaier, P. M.; Hamer, G. K. **Narrow molecular weight resins by a free radical polymerization process; the effect of nitroxides and organic acids on the polymerization.** Polym. Mater. Sci. Eng. (1993) 69, 305
- [3] Matyjaszewski, K.; Gaynor, S.; Wang, J.S. **Controlled Radical Polymerizations: The Use of Alkyl Iodides in Degenerative Transfer.** Macromolecules (1995), 28(6), 2093
- [4] Wang, J.S.; Matyjaszewski, K. **"Living"/Controlled Radical Polymerization. Transition-Metal-Catalyzed Atom Transfer Radical Polymerization in the Presence of a Conventional Radical Initiator.** Macromolecules (1995) 28(22), 7572
- [5] Le, T. P.; Moad, G.; Rizzardo, E.; Thang, S. H. **Polymerization with living characteristics with controlled dispersity, polymers prepared thereby, and chain-transfer agents used in the same.** PCT Int. Appl. (1998), WO 9801478
- [6] Rizzardo, E.; Thang, S. H.; Moad, G. **Synthesis of dithioester chain-transfer agents and use of bis(thioacyl) disulfides or dithioesters as chain-transfer agents in radical polymerization.** PCT Int. Appl. (1999), WO 9905099
- [7] Fischer, H. **The Persistent Radical Effect In "Living" Radical Polymerization.** Macromolecules (1997), 30(19), 5666
- [8] Gridnev, A. A. **Hydrogen Transfer Reactions of Nitroxides in Free Radical Polymerizations.** Macromolecules (1997), 30(25), 7651
- [9] Moad, G.; Solomon, D.H. **The chemistry of free radical polymerization**, 1st ed.; Elsevier Science Ltd.: Oxford, 1995
- [10] Fukuda, T.; Terauchi, T.; Goto, A.; Ohno, K.; Tsujii, Y.; Miyamoto, T.; Kobatake, S.; Yamada, B. **Mechanisms and Kinetics of Nitroxide-Controlled Free Radical Polymerization.** Macromolecules (1996), 29(20), 6393
- [11] Bon, S. A. F. **Debut. Collected Studies on Nitroxide-mediated Controlled Radical Polymerization.** Ph. D. thesis, Technische Universiteit Eindhoven, Eindhoven, 1998
- [12] Kobatake, S.; Harwood, H. J.; Quirk, R. P.; Priddy, D. B. **Block Copolymer Synthesis by Styrene Polymerization Initiated with Nitroxy-Functionalized Polybutadiene.** Macromolecules (1998), 31(11), 3735
- [13] Burguiere, C.; Dourges, M. A.; Charleux, B.; Vairon, J. P. **Synthesis and characterization of π -unsaturated poly(styrene-*b*-*n*-butyl methacrylate) block copolymers using TEMPO-mediated controlled radical polymerization.** Macromolecules (1999), 32(12), 3883
- [14] Bon, S. A. F.; Bosveld, M.; Klumperman, B.; German, A. L. **Controlled Radical Polymerization in Emulsion.** Macromolecules (1997), 30(2), 324
- [15] Lansalot, M.; Charleux, B.; Vairon, J.-P.; Pirri, R.; Tordo, P. **Nitroxide-mediated controlled free radical emulsion polymerization of styrene.** Polymer Preprints (1999), 40(2), 317
- [16] Marestin, C.; Noel, C.; Guyot, A.; Claverie, J. **Nitroxide Mediated Living Radical Polymerization of Styrene in Emulsion.** Macromolecules (1998), 31(12), 4041
- [17] MacLeod, P. J.; Barber, R.; Odell, P. G.; Keoshkerian, B.; Georges, M. K. **Stable free radical miniemulsion polymerization.** Macromol. Symposia (2000), 155 (Emulsion Polymers), 3
- [18] Prodpran, T.; Dimonie, V. L.; Sudol, E. D.; El-Aasser, M. S. **Nitroxide-mediated living free radical miniemulsion polymerization of styrene.** Macromol. Symposia (2000), 155(Emulsion Polymers), 1
- [19] Pan, G.; Sudol, E. D.; Dimonie, V. L.; El-Aasser, M. S. **Nitroxide-mediated living free radical miniemulsion polymerization of styrene.** Macromolecules (2001), 34(3), 481
- [20] Tortosa, K.; Smith, J. A.; Cunningham, M. F. **Synthesis of polystyrene-block-poly(butyl acrylate) copolymers using nitroxide-mediated living radical polymerization in miniemulsion.** Macromol. Rapid Comm. (2001), 22(12), 957
- [21] Farcet, C.; Charleux, B.; Pirri, R. **Poly(*n*-butyl acrylate) Homopolymer and Poly[*n*-butyl acrylate-*b*-(*n*-butyl acrylate-co-styrene)] Block Copolymer Prepared via Nitroxide-Mediated Living/Controlled Radical Polymerization in Miniemulsion.** Macromolecules (2001), 34(12), 3823
- [22] Wulkow, M. **The simulation of molecular weight distributions in polyreaction kinetics by discrete Galerkin methods.** Macromol. Theory Simul. (1996), 5(3), 393
- [23] Shipp, D. A.; Matyjaszewski, K. **Kinetic analysis of controlled/"living" radical**

polymerizations by simulations. 1. The importance of diffusion-controlled reactions.

Macromolecules (1999), 32(9), 2948

[24] Farcet, C.; Lansalot, M.; Charleux, B.; Pirri, R.; Vairon, J. P. **Mechanistic aspects of nitroxide-mediated controlled radical polymerization of styrene in miniemulsion, using a water-soluble radical initiator.** Macromolecules (2000), 33(23), 8559

[25] Fukuda, T.; Terauchi, T.; Goto, A.; Ohno, K.; Tsujii, Y.; Miyamoto, T.; Kobatake, S.; Yamada, B.

Mechanisms and Kinetics of Nitroxide-Controlled Free Radical Polymerization. Macromolecules (1996), 29(20), 6393

[26] Goto, A.; Fukuda, T. **Mechanism and Kinetics of Activation Processes in a Nitroxyl-Mediated Polymerization of Styrene.** Macromolecules (1997), 30(17), 5183

[27] Butte, A.; Storti, G.; Morbidelli, M. **Pseudo-living polymerization of styrene in miniemulsion.** DECHEMA Monographien (1998), 134, 497

[28] Charleux, B. **Theoretical Aspects of Controlled Radical Polymerization in a Dispersed Medium.** Macromolecules (2000), 33(15), 5358

[29] Gilbert, R. G. **Emulsion Polymerization: A Mechanistic approach;** Academic: London, (1995)

[30] Ma, J. W.; Cunningham, M. F.; McAuley, K. B.; Keoshkerian, B.; Georges, M. K. **Nitroxide partitioning between styrene and water.** J. Polym. Sci., Part A: Polym. Chem. (2001), 39(7), 1081

[31] Buback, M.; Gilbert, R. G.; Hutchinson, R. A.; Klumperman, B.; Kuchta, F. D.; Manders, B. G.;

O'Driscoll, K. F.; Russell, G. T.; Schweer, J. **Critically evaluated rate coefficients for free-radical polymerization. 1. Propagation rate coefficient for styrene.** Macromol. Chem. Phys. (1995), 196(10), 3267

[32] Goto, A.; Terauchi, T.; Fukuda, T.; Miyamoto, T. **Gel permeation chromatographic determination of activation rate constants in nitroxide-controlled free radical polymerization.**

Part 1. Direct analysis by peak resolution. Macromol. Rapid Comm. (1997), 18(8), 673

[33] Kazmaier, P. M.; Moffat, K. A.; Georges, M. K.; Veregin, R. P. N.; Hamer, G. K. **Free-Radical Polymerization for Narrow-Polydispersity Resins. Semiempirical Molecular Orbital Calculations as a Criterion for Selecting Stable Free-Radical Reversible Terminators.**

Macromolecules (1995),

28(6), 1841

[34] a) Couturier, J. L.; Henriët-Bernard, C.; Le Mercier, C.; Tordo, P.; Lutz, J.F. **Alkoxyamines derived from phosphorus-containing nitroxides and their use.** PCT Int. Appl. (2000), WO 0049027 b) Gillet, J. P.; Guerret, O.; Tordo, P. **Method for preparing @-phosphorus nitroxide radicals using nonhalogenated organic peracids in a biphasic medium.** PCT Int. Appl. (2000),

WO 0040526 c) Berchadsky, Y.; Kernevez, N.; Le Moigne, F.; Mercier, A.; Secourgeon, L.; Tordo, P.

Preparation of heterocyclic phosphono nitroxides. Brit. UK Pat. Appl. (1990), GB 2225015

[35] Landfester, K.; Bechthold, N.; Tiarks, F.; Antonietti, M. **Formulation and stability mechanisms of polymerizable miniemulsions.** Macromolecules (1999), 32(16), 5222

[36] The activation rate coefficient, k_{act} , is based on the highest value for this parameter at 90 °C found in literature, see [24]. The value of k_{deact} is based on the values found by Ingold *et al.* (J. Am. Chem. Soc.

(1992), 114, 4983) for trapping of TEMPO with a benzyl radical in various solvents. For simplicity it is assumed that the termination rate coefficient, k_t , is equal to k_{deact} .

[37] Schene, W.G.; Scaiano, J.C.; Listigovers, N. A.; Kazmaier, P. M.; Georges, M. K.. **Rate constants for the trapping of various carbon-centered radicals by nitroxides: unimolecular initiators for living free radical polymerization.** Macromolecules (2000), 33, 5065

Chapter 2

Homogeneous RAFT polymerizations

31

3

Homogeneous RAFT polymerizations

Abstract

In Chapter 2 it was shown that nitroxide-mediated controlled radical polymerization in emulsion is possible. However, the polymerization rate was extremely slow. Therefore, in this chapter another 'living' free-radical polymerization technique is being applied: Reversible Addition-Fragmentation chain Transfer (RAFT). First the mechanism and the role of the transfer rate is discussed. Subsequently, the transfer constants of the RAFT agents used in this work, xanthates, are determined for styrene and n-butyl acrylate and are found to be much lower than those of the conventionally used dithioesters. The applied methods, the Mayo method and In CLD method are discussed extensively. Hereafter, the effect of RAFT on the polymerization rate is the subject of discussion. The role of the intermediate radical and the effect of RAFT on the average termination rate coefficient are discussed theoretically. Finally RAFT homopolymerizations of styrene and n-butyl acrylate in homogeneous media under various conditions are investigated and compared with simulations. It is found that the xanthates used in this work have no effect on the polymerization rate of styrene and that for n-butyl acrylate retardation is observed for one of the xanthates. Simulations are used to explain the results.

3.1 Introduction

The discovery of free-radical polymerization processes showing characteristics of 'living' polymerization allowed new classes of polymer architectures to be synthesized.

The advantages of both 'living' polymerization (control over the polymer structure) and the robustness (wide choice of monomers and reaction conditions) of free-radical polymerization can now be combined in a single process. Different techniques have been developed, all based on alternating activation and deactivation of the polymer chains, allowing stepwise growth. ATRP[1] (Atom Transfer Radical Polymerization) and NMCRP[2] (Nitroxide Mediated Controlled Radical Polymerization, see Chapter 2) are based on the concept of reversible termination. In these processes a capped dormant chain is activated and the polymeric radical that is formed adds monomer until it is deactivated by the capping agent. In NMCRP, a nitroxide is used as the capping agent, whereas in ATRP a halogen atom is used. Both techniques have proven to be successful in the preparation of well-defined polymers, however, there are also some limitations. These include, for instance, monomer choice (especially in NMCRP), reaction conditions, heavy metals in the product (from the ATRP process) and poor applicability in conventional *ab initio* or seeded emulsion polymerization.

In 1997, two patents based on reversible chain transfer emerged, and opened up a new area of 'living' radical polymerization. First, RAFT (Reversible Addition-Fragmentation chain Transfer) was patented by DuPont[3,4] and somewhat later MADIX (Macromolecular Design via Interchange of Xanthates) by Rhodia[5]. These two processes only differ in the type of activating group of the transfer agents used, but are mechanistically identical. The main reason for this difference in nomenclature

is due to the different patent strategies set down by each company. The RAFT terminology holds for all agents undergoing addition of polymeric radicals to a compound, which can then fragment to produce the same or a different radical.

Therefore, the term RAFT will be used in this thesis since it is a mechanistic description of the process used in this work.

In this chapter the use of RAFT agents with a low transfer constant in homogeneous systems will be discussed. After all, in order to be able to understand the RAFT mechanism in emulsion polymerization, it is wise to first start to understand what happens in the more simple homogeneous systems. In Chapter 4 the basic understand gained from this chapter will be then applied to the kinetically more complex emulsion system.

First, the proposed mechanism of RAFT and the role of the transfer constant will be discussed. The next section will deal with the criteria that allow accurate determination of the transfer constants for low reactive RAFT agents. Then experiments that follow the above criteria will be used to determine the transfer constants for styrene and butyl acrylate polymerizations at different temperatures using a xanthate agent. These transfer constants will then be used to simulate the rate of polymerization and molecular weight distributions both in dilute and bulk conditions. Comments will be made on the effect of the average termination rate coefficient, $\langle k_t \rangle$, on the polymerization rate and its relationship to retardation in rate.

3.2 The RAFT process

3.2.1 Mechanism

In 1998 Rizzardo *et al.* published a novel 'living' free-radical polymerization technique, which they designated the RAFT process[6] because the mechanism involves Reversible Addition-Fragmentation chain Transfer. This technique allowed the production of polymer with a narrow molecular weight distribution. In fact this concept was not entirely new and stemmed from the same researchers previously published work to produce block copolymers using methacrylate macromonomers as reversible addition-fragmentation chain transfer agents in 1995[7]. However, these macromonomers were not very effective RAFT agents. The breakthrough came with the invention of a more reactive double bond species, $S=C(Z)SR$. In the case of styrene polymerizations the propagating radicals were very reactive to the dithioesters and to a much lesser extent to the xanthates (Scheme 3.4).

Chapter 3

34

Scheme 3.1 Schematic representation of the proposed RAFT mechanism. It should be noted that in these equilibria any radical can react with any dormant species or RAFT agent.

(1) Addition of a propagating polymeric radical to the initial RAFT agent **1**, forming the intermediate radical **2**. The intermediate radical can either fragment into the two species it was formed by or into a dormant polymeric RAFT agent **3** and a small radical $R\cdot$.

(2) The small radical initiates polymerization, forming a polymeric radical, rather than react with **3** forming back **1**. Therefore R should both be a good leaving group capable of addition to monomer so $k_{p1}[M] \gg k_{-3}$.

(3) Equilibrium between propagation polymeric radicals and dormant polymeric RAFT agents. A brief description of the RAFT process is given below, and a schematic representation is given in Scheme 3.1. A conventional free-radical initiator that is added (contrary to some other 'living' free-radical polymerization techniques) generates radicals, which can either add to monomer or the S=C moiety of the RAFT agent (**1**). In most cases the addition of small carbon-centered radicals to the RAFT agent is rapid and is not rate determining. Therefore, step (1) involves polymeric radical addition to **1** to form an intermediate radical species **2** that will fragment back to the original polymeric radical species or fragment to a dormant species **3** and a small radical, R·. R· can then further propagate to form a polymeric radical (step (2) in Scheme 3.1), rather than adding to **3** (ideally $k_{p1}[M] \gg k_{-3}$, so k_{-3} can be discarded from the kinetic equations). The dormant polymeric RAFT agent acts similar to a RAFT agent, so growing polymeric radicals can also add to the dithiocarbonyl double bond of the polymeric RAFT agent, thereby forming an intermediate radical **4**. This intermediate has equal probability to fragment back into its starting species

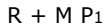
or



Z



Z



35

into a dormant polymeric RAFT agent and a polymeric radical, in which the dithiocarbonate moiety has been exchanged between the active and dormant polymer chains of the starting species. This equal probability to fragment to both sides of the equilibrium is a result of the symmetry of **4**. There might only be a difference in the chain length of both sides, but this will not have an effect, unless one of the two sides is extremely short. This mechanism of addition of radicals to the dithiocarbonyl double bond and fragmentation of the intermediate was shown by Moad *et al.*[8] who have observed the intermediate radical directly by ESR.

Overall, polymer chains with a dithiocarbonate end-group are formed. If addition to the dithiocarbonyl double bond is fast compared to propagation, and termination is suppressed by keeping the radical concentration low, all chains will grow in a stepwise process leading to a low polydispersity. The number of chains is determined by the amount of RAFT agent and initiator that has been consumed. Assuming termination by combination, the number of dead chains will be equal to the amount of initiator that is consumed. The number of chains with a dithiocarbonate end-group, the dormant chains, is equal to the amount of consumed RAFT agent. In order to obtain a high percentage of dormant chains the initiator to RAFT agent ratio should be kept low.

This criterion is especially important in the preparation of block copolymers such that low amounts of the two homopolymers are formed (by termination) [9,10,11]. In fact, the RAFT process resembles the degenerative transfer (DT) process [12]. In a polymerization in which an alkyl iodide is used as the degenerative transfer agent, the iodine atom is exchanged between a polymeric radical and a dormant chain, similar to the dithiocarbonate exchange in RAFT. However, in the case of degenerative transfer there is a direct equilibrium between the dormant and growing chains, without formation of an intermediate radical.

As mentioned before, the breakthrough of RAFT in the area of 'living' polymerization was a result of the discovery of effective reversible addition-fragmentation

transfer agents (*i.e.* $S=C(Z)SR$, see Scheme 3.2). A RAFT agent used to produce a polymer that shows a linear increase in M_n and has a narrow molecular weight distribution occurs when the dithiocarbonate moiety is exchanged rapidly between the polymer chains. In Scheme 3.2, a schematic representation of a RAFT agent is shown.

Chapter 3

36

Scheme 3.2 Reversible Addition-Fragmentation Transfer agent.

A rapid exchange is achieved when a propagating polymeric radical has a high reactivity towards the thiocarbonyl double bond compared to monomer.

The activating group Z in Scheme 3.2 determines the reactivity of this bond. If, for example, a phenyl group is used, the rate of addition for styrene will be high, but the same group will be less effective when vinyl acetate is used. If Z is either an oxygen or a nitrogen substituent the effect is essentially reversed [13].

Furthermore, the RAFT agent must have a good leaving group that is able to reinitiate polymerization. From step (1) in Scheme 3.1 it can easily be deduced that the transfer rate coefficient, k_{tr} , is equal to:

$$k_{tr} = \frac{k_{add}}{k_{\oplus}} \quad (3.1)$$

From this equation it is obvious that, in order to obtain a high transfer rate to the initial RAFT agent, k_{add} should not be orders of magnitude greater than k_{\oplus} , or in other words, R should be a good 'leaving' group, preferably better than the added polymeric radical. Once all initial RAFT agent has been consumed, step 1 in Scheme 3.1 does not play a role, but should be the dominant step at very low conversion, so that all polymer chains grow simultaneously throughout the polymerization. At the stage where all the initial RAFT agent has disappeared, there will only be transfer between polymeric radicals and polymeric dormant species (step (3) in Scheme 3.1), leading to a symmetrical intermediate, 4. Therefore, k_{add} is equal to k_{\oplus} and Eq. 3.1 reduces to:

$$k_{tr} = 1 \quad (3.2)$$

The aspect that R should be a good leaving group also plays an important role in the synthesis of block copolymers[9]. In order to synthesize block copolymers, the monomer resulting in propagating radicals with the better leaving group ability should be polymerized first. The leaving group ability decreases from tertiary to primary leaving groups and from poly(methacryl) to poly(styryl) to poly(acryl)[8].

3.2.2 The transfer constant

It will be clear that, in order to obtain a high transfer rate coefficient k_{tr} , both the addition rate to the RAFT agent should be high and the leaving group ability of the RAFT agent should be at least of the same order of magnitude as that of the propagating radical, otherwise the intermediate radical goes back to its originating species. Or in terms of Eq. 3.1, the addition rate coefficient k_{add} should be high and the fragmentation rate coefficient k_{\oplus} should be of the same order of magnitude as the reverse addition rate coefficient k_{-add} .

One can discriminate 3 kinds of transfer reactions:

1) Transfer to the initial RAFT agent (reaction (1) in Scheme 3.1)

2) Transfer to polymeric RAFT agent in a homopolymerization (reaction (3) in Scheme 3.1)

3) Transfer to polymeric RAFT agent in a block copolymerization

In the case of 1) and 3) the transfer rate coefficient is determined both by addition

and the fragmentation rates k_{tr} and k_{-add} (Eq 3.1) and in the case of 2) only by the addition rate (Eq. 3.2), since here $k_{-add} = k_{tr}$.

A low k_{tr} compared to k_{-add} can easily be avoided by choosing a good leaving group in case 1) and by carrying out the block copolymerization in the right order (first polymerize the monomer which forms a better leaving group) in case 3. So the limiting and determining factor in the transfer rate coefficient will be the addition rate coefficient, k_{add} , which is determined by Z (Scheme 3.2) and the nature of the propagating radical. The transfer constant, C_T , is defined as the ratio of the transfer rate coefficient k_{tr} and the propagation rate coefficient k_p :

$$C_T = \frac{k_{tr}}{k_p} \quad (3.3)$$

Chapter 3

38

Müller *et al.* [14,15] derived equations for group transfer processes, which can be applied to the RAFT process assuming negligible bimolecular termination, providing an estimation of the effect of the transfer constant C_T on the number average molecular weight M_n and the weight average molecular weight M_w :

$$M_n = M_0 \frac{1 - x}{1 + C_T x} \quad (3.4)$$

$$M_w = M_0 \frac{1 + C_T x}{1 + 2 C_T x} \quad (3.5)$$

in which x is the fractional monomer conversion, M_0 is the initial monomer over initial

RAFT agent ratio and M_0 is the monomer molar mass. In the present work, Müllers equations are further simplified by assuming that the ratio of growing radicals to RAFT agent is negligible. Since these equation are only used to

show the trends in molecular weights and polydispersity with varying transfer constants, these assumptions are justifiable, at least when the initiator concentration is low.

Figure 3.1 Effect of C_T on number average molecular weight M_n (a) and polydispersity M_w/M_n versus conversion (b) for a polymerization with $\phi=200$ and $M_0=104.15$ (styrene), calculated using Eqs. 3.4 and 3.5.

Figure 3.1 shows the number average molecular weight and the polydispersity, *i.e.* M_w/M_n versus conversion for various transfer constants. It is shown that, in order to obtain a linear increase in M_n , the transfer constant has to be at least 10. In order

0.0 0.1 0.2 0.3 0.4 0.5 0.6 0.7 0.8 0.9 1.0

0
10000
20000
30000
40000
50000
60000
70000
80000
 $C_T=100$
 $C_T=3$
 $C_T=10$
 $C_T=1$
 $C_T=0.5$
 $C_T=0.2$

M_n [g/mol]

x [-]

0.0 0.2 0.4 0.6 0.8 1.0

1.0

1.2

1.4

1.6

1.8

2.0

2.2

2.4

2.6

$C_T=100$

$C_T=3$

$C_T=10$

$C_T=1$

$C_T=0.5$

$C_T=0.2$

M_w/M_n [-]

x [-]

a b

to obtain a low polydispersity throughout the polymerization the transfer constant has to be even higher (approximately 100).

The first reported RAFT agents *i.e.* the methacrylate macromonomers have a chain transfer constant of about 0.3 in MMA polymerizations[16]. From Figure 3.1 it can be seen that the use of RAFT agents with transfer constants of this order of magnitude will not show the characteristics of a typical 'living' polymerization, *i.e.* narrow MWD and linear increase in M_n with conversion.

Moreover, at high conversions, a high amount of low molecular weight material will be formed, since at that stage M_n drops dramatically, leading to a large increase in the polydispersity. However, the inventors of these RAFT agents were able to apply these macromonomers for the synthesis of block copolymers successfully, by using starved feed conditions[17], leading to block copolymers with a polydispersity of 1.3. By applying starved feed conditions the monomer to RAFT agent ratio is kept low, and thus transfer is favored as compared with a batch polymerization. Although the transfer constant is low, a propagating radical is 'forced' to undergo transfer, since the ratio between transfer and propagation rate is determined by both the transfer constant and the concentration of RAFT agent and monomer.

Therefore, the average number of monomer units being added to a propagating radical, $\bar{\nu}$, assuming no bimolecular termination can be calculated as follows:

{

====

1

] M [

] RAFT [

C

·] P][M [k

·] P][RAFT [k

R

R

] M [d

] RAFT [d

T

p

tr

p

τ(3.6)

Eq. 3.6 shows that, if the monomer to RAFT agent ratio is low, τ is low.

Therefore stepwise growth leading to low polydispersities is also possible using RAFT agents with a low transfer constant, since in a monomer fed process all the polymer chains are established at the beginning of the polymerization.

A few years later, in 1998, these researchers published a new living free-radical polymerization of "exceptional effectiveness and versatility", which at that stage they designated the RAFT process[6]. Mechanistically the process was identical to that of their earlier macromonomers, however, now dithioesters were used as RAFT agents.

The effectiveness of these RAFT agents was attributed to the very high transfer constants of these new agents with some monomers. In batch polymerizations, polydispersities below 1.1 were obtained at low conversions. Figure 3.1 shows that this means that the transfer constant of this new class of RAFT agents has to be greater than 100. It has been reported that values exceeding 1000 have been found for dithioesters with a phenyl activating group in combination with styrene[18].

In the before mentioned 1998 paper[6], Moad *et al.* reported that RAFT agents, which have an alkoxy group or a dialkylamino group as Z, are ineffective in methyl methacrylate polymerizations. Transfer constants < 0.1 were reported. However, the same authors patented these xanthates and dithiocarbamates at about the same time, reporting transfer constants between 2 and 7 for the xanthates and low polydispersities for both with various other monomers[13]. At about the same time, the xanthates have also been patented by Rhodia[5] as agents for synthesizing block copolymers. In this investigation xanthates have been used as RAFT agents. Although these have lower transfer constants and therefore are less effective than dithioesters with most monomers, they also have some very important advantages: - easy to synthesize[5] - colorless or light yellow as compared with the deep purple of the dithioesters resulting in colorless polymer rather than pink polymer - much less odor as compared with dithioesters

- easy to apply in emulsion polymerization [11,19]

3.3 Determination of the transfer constant

From the foregoing discussion it appears that the transfer constant is an important parameter in RAFT polymerizations. Figure 3.1 shows that it is the transfer constant that determines the extent to which a RAFT polymerization shows the characteristics of a linear growth of M_n (high C_T of initial RAFT agent) with conversion and a narrow molecular weight distribution (also high C_T of polymeric RAFT).

In 1943, Frank Mayo developed a method for determining transfer constants to solvent from the number-average molecular weights by varying the solvent to monomer ratios[20]. Until recently the Mayo method was the most common and accepted method of determining transfer constants. More recently, Gilbert *et al.*[21,22] were able to extract transfer constants from entire instantaneous molar mass distributions by plotting the logarithmic number molecular weight distribution.

This method is now referred to as the ln CLD (Chain Length Distribution) method. For both the Mayo method and the ln CLD method it is required that the transfer agent to monomer ratio remains constant during the experiment and that the polymer formed has undergone not more than a single transfer event. Therefore, experimental data has to be obtained from low conversion experiments. However, the use of very reactive transfer agents results in a relatively fast consumption of the transfer agent compared to the monomer and therefore the transfer agent to monomer ratio will not be constant, even at very low conversions. In this case conventional methods cannot be used to determine the transfer constants of these agents. Moreover, since RAFT agents can transfer more than once, it cannot be guaranteed that the polymer formed using these agents has undergone one single transfer event. Therefore, other or new methods have been developed to determine the transfer constants of this class of highly reactive transfer agents.

One such method is the GPC peak resolution method of Goto *et al.*[18]. In this method the starting RAFT agent and new-formed polymer are separated by GPC and therefore monomer and RAFT agent conversion can be monitored. The RAFT agent in this case is a pre-polymer with a chain-end consisting of a $S=C(Z)S-$ moiety. In order to separate the new-formed polymer from the initially present dormant chains sufficient monomer units have to be inserted between activation and deactivation. Eq. 3.6 shows that in the case of a high transfer constant the concentration of RAFT has to be very low in order to add sufficient monomer units. However, this leads to complications with respect to the detection by GPC. Therefore, this method can only be used to determine intermediately high transfer constants, *i.e.* in the order of 10^2 , accurately.

De Brouwer monitored the consumption of RAFT agent and the evolution of the concentrations of oligomeric dormant chains throughout a polymerization with HPLC[23]. He was able to baseline separate the oligomers to a degree of polymerization of 15 to 20. The concentration evolution of these oligomers and the initial RAFT agent were compared with the results of simulations. However, also in this method the sensitivity is lost for very high transfer

constants. Both Goto's GPC peak resolution method and De Brouwer's oligomer profiles resulted in a transfer constant between 1000 and 10000 for a styrene polymerization in the presence of a dithiobenzoate RAFT agent. In this work, xanthates are used as RAFT agent. Preliminary polymerizations revealed a C_T close to 1 for styrene and butyl acrylate polymerizations [5, this work].

This means that in the present case conventional methods like the Mayo method and the ln CLD method can be used to determine the transfer constant since the monomer to transfer agent ratio will hardly change in a low conversion experiment. It also seems save to assume here that at low conversions there will be not more than one addition-fragmentation per polymer chain.

3.3.1 The Mayo method

Consider a simple bulk system, in which only initiation, propagation, termination, transfer to monomer and transfer to RAFT agent and dormant chains plays a role. The kinetic scheme is shown in Scheme 3.3.

In this scheme it is assumed that small radical species formed by initiator decomposition are reactive and quickly propagate to form a new polymer chain $P_1\cdot$.

Moreover, the role of the intermediate radical is neglected, since this will hardly affect the number average molecular weight for RAFT agents with a low transfer constant[25].

Scheme 3.3 Kinetic scheme of a bulk polymerization in the presence of a RAFT agent with rate coefficients. I is the initiator, $P_i\cdot$ is a radical with degree of polymerization i , M is the monomer, P_i a dead chain with degree of polymerization i , X-R the RAFT agent and P_i-X a dormant chain with degree of polymerization i .

I

$P_i\cdot + M$

$2 P_1\cdot$

$P_{i+1}\cdot$

$P_i\cdot + P_j\cdot \rightarrow P_{i+j}$

$P_i\cdot + P_j\cdot \rightarrow P_i + P_j$

$P_i\cdot + M \rightarrow P_i + P_1\cdot$

$P_i\cdot + X-R \rightarrow P_i-X + P_1\cdot$

$P_i\cdot + P_j-X \rightarrow P_i-X + P_j\cdot$

k_d

k_p

k_{tc}

k_{td}

k_{trM}

k_{trRAFT}

k_{trRAFT}

p

initiation (1)

propagation (2)

termination by combination (3)

termination by disproportionation (4)

Homogeneous RAFT polymerizations

- transfer to monomer (5)
- transfer to RAFT agent (6)
- transfer to polymeric RAFT agent (7)

The number average degree of polymerization \bar{DP}_n of the polymer produced in a unit of time is given by the ratio of the moles of monomer consumed to the moles of polymer formed in that unit of time. Based on Scheme 3.3 this means:

$$\bar{DP}_n = \frac{2k_p[M][P\cdot] + k_{trM}[M][P\cdot] + k_{trRAFT}[M][P\cdot]}{k_p[M][P\cdot] + k_{trM}[M][P\cdot] + k_{trRAFT}[M][P\cdot] + k_{tc}[P\cdot]^2} \quad (3.7)$$

The factor 2 in the 'termination by disproportionation' term takes into account that two polymer chains are formed in this termination reaction. Dividing numerator and denominator of Eq. 3.7 by $k_p[M][P\cdot]$ and taking the reciprocal, results in:

$$\frac{1}{\bar{DP}_n} = \frac{k_p[M][P\cdot] + k_{trM}[M][P\cdot] + k_{trRAFT}[M][P\cdot]}{2k_p[M][P\cdot] + k_{trM}[M][P\cdot] + k_{trRAFT}[M][P\cdot] + k_{tc}[P\cdot]^2} \quad (3.8)$$

Assuming that k_{trRAFT} is of the same order of magnitude as k_{trM} and $[P-X]$ is

negligible as compared with $[X-R]$, the transfer to polymeric RAFT term can be neglected. It can be seen from Scheme 3.3 that $[P-X]_x$, the concentration of polymeric RAFT at conversion x , which is initially zero, is equal to $[X-R]_0 - [X-R]_x$. It then can be derived [14,15] that:

$$[P-X]_x = [X-R]_0 x - [X-R]_x x \quad (3.9)$$

where x is the fractional monomer conversion. Eq. 3.9 shows that at low conversions in combination with a low transfer constant k_{trRAFT}/k_p , indeed $[P-X]_x \ll [X-R]_x$.

Therefore Eq. 3.8 can be reduced to:

$$\frac{1}{DP} = \frac{1}{DP_0} + \frac{k_{trM}}{k_p} \frac{[X-R]}{[M]} + \frac{C_T}{2} \frac{[X-R]}{[M]} \quad (3.10)$$

in which the transfer to monomer constant $C_M = k_{trM}/k_p$, the transfer to RAFT agent constant $C_T = k_{trRAFT}/k_p$, $\langle k_t \rangle$ is the average termination rate coefficient which is equal to $k_{td} + k_{tc}$ and q is the fraction of termination reactions that proceeds by disproportionation, *i.e.* $q = k_{td}/\langle k_t \rangle$. Eq. 3.10 is known as the Mayo equation and is normally written as:

$$\frac{1}{DP} = \frac{1}{DP_0} + \frac{C_T}{2} \frac{[X-R]}{[M]} \quad (3.11)$$

in which DP_0 is the degree of polymerization in the absence of chain transfer. By performing a series of experiments at low conversion, in which the RAFT agent to monomer ratio is varied, $1/DP$ can be plotted versus $[X-R]/[M]$. The slope of this plot is equal to C_T . Here it is assumed that DP_0 and thus $\langle k_t \rangle$ and $[P\cdot]$ are independent of the RAFT agent to monomer ratio. This is true only if:

ad 4) *The effect of [RAFT] on the average termination rate coefficient*

Any effect on the $\langle k_t \rangle$ will lead to changes in the chain transfer constant. It can be seen from Eq. 3.11 that for reliable C_T values to be obtained, $\langle k_t \rangle$ should be unaffected by the concentration of RAFT agent. However, since RAFT due to its very nature will significantly lower the chain length distribution it will in principle increase $\langle k_t \rangle$. This will be evident for RAFT agents with high C_T values. However, it is not certain whether similar effects will be observed for RAFT agents with low C_T values (e.g. xanthates where C_T is close to one). The effect of RAFT on the $\langle k_t \rangle$ and the effect of $\langle k_t \rangle$ on the transfer constant determination using the Mayo method will be illustrated on the basis of a detailed example. Therefore, the polymerization of styrene in the presence of a RAFT agent with a transfer constant of 1 is considered. A typical Mayo plot consists of 4 data-points at different monomer to RAFT concentrations (i.e., $[RAFT]/[M] = 0.005, 0.010, 0.015$ and 0.020) over a wide range.

From Eq. 3.10 and Eq. 3.11 and by calculating the radical concentration $[P\cdot]$ from $2k_d[I] = 2\langle k_t \rangle [P\cdot]^2$, the following expression can be obtained for \bar{DP}_0 :

$$\bar{DP}_0 = \frac{[I] k_p}{[M] k_t} \left(1 + \frac{[RAFT]}{[M]} \right) \quad (3.13)$$

If $\langle k_t \rangle$ is independent of $[RAFT]/[M]$, \bar{DP}_0 will be identical for all RAFT to monomer ratios and a Mayo plot will result in $C_T = 1.00$.

However, the termination rate is known to be chain-length dependent [26]. Since the chain-length distribution will depend on the RAFT to monomer ratio, also $\langle k_t \rangle$ will depend on the RAFT concentration. The $\langle k_t \rangle$ can be calculated from the radical chain length distribution and the microscopic termination coefficients $k_{t,ij}$ of two chains

having length i and j :

$$\langle k_t \rangle = \frac{1}{\bar{P}_n} \sum_{i,j} k_{t,ij} P_i P_j$$

= > <

.

..

(3.14)

The microscopic termination coefficients can be calculated using the Smoluchowski equation, which was corrected by Russel *et al.* [27-29] to take into account that only a fraction of all radical-radical encounters results in termination because only encounters of two compatible spin states results in termination:

$$k_{t,j,i} = p_{spin} \cdot 4\pi D_i D_j \cdot r \quad (3.15)$$

in which p_{spin} is the probability that a radical-radical encounter will result in termination, D_i and D_j are the diffusion coefficients of chains of length i and j , r is the reaction radius at which termination takes place, and N_A is Avogadro's constant.

Assuming that the radical chain length distribution (CLD) is dominated by chain transfer, which is true at low initiator concentrations, the chain length distribution can be expressed as a Flory-Schulz distribution[30]:

...

.

...

$\sum_{i=1}^{\infty} n_i = 1$

$\sum_{i=1}^{\infty} i n_i = \bar{n}$

$\sum_{i=1}^{\infty} i^2 n_i = \overline{i^2}$

$\sum_{i=1}^{\infty} i^3 n_i = \overline{i^3}$ (3.16)

The constant in Eq. 3.16 can be neglected since the distribution is essentially normalized. Therefore, in order to calculate $\langle kt \rangle$, only the diffusion coefficients as a function of chain length must to be known.

Piton *et al.*[31] measured diffusion coefficients of polystyrene oligomers in a polystyrene matrix as a function of chain length and weight fraction of polymer, w_p .

Homogeneous RAFT polymerizations

47

They found that for $w_p=0$, the diffusion coefficient of chains of length i corresponds to:

$D_{i,0}$

mon

i

D

$D = (3.17)$

in which D_{mon} is the monomer diffusion coefficient. Since experimental data for Mayo plots are obtained from low conversion experiments (typically <2%), here w_p is considered to be constant and equal to zero. Using the data in Table 3.1, $\langle k_t \rangle$ can be calculated (Appendix 3.1) using Eqs. 3.14 to 3.17 for the different RAFT to monomer ratios. Using Eq. 3.16, the radical CLD is calculated for $i=1$ to $10 \text{ } n \text{ DP}$, where $n \text{ DP}$ is equal to $[M]/C_T[R-X]$. Integration of Eq. 3.16 shows that this involves more than 99.99% of all chains. The results of the calculations of $\langle k_t \rangle$ and $1/ n \text{ DP}$ are shown in Table 3.1.

Table 3.1 Parameters used in $\langle k_t \rangle$ calculations of a styrene polymerization at 50 °C with AIBN and the results of these calculations for different $[R-X]/[M]$.

parameter	value	reference
p_{spin}	0.25	[28]
\hat{r}	$6.02 \cdot 10^{-9} \text{ dm}$	[28]
N_A	$6.02 \cdot 10^{23}$	
D_{mon}	$2.09 \cdot 10^{-7} \text{ dm}^2 \text{ s}^{-1}$	[32]
C_T	1.00	
k_d	$2.4 \cdot 10^{-6} \text{ s}^{-1}$	AIBN, extrapolated from [33]
$[I]$	$1 \cdot 10^{-3} \text{ mol dm}^{-3}$	
q	0	[34]
k_p	$237 \text{ dm}^3 \text{ mol}^{-1} \text{ s}^{-1}$	[35]
$[M]$	8.65 mol dm^{-3}	
$[R-X]/[M]$	$\langle k_t \rangle$	$1/ n \text{ DP}$ (using Eqs. 11 and 13)
0.005	$2.93 \cdot 10^8 \text{ dm}^3 \text{ mol}^{-1} \text{ s}^{-1}$	$5.409 \cdot 10^{-3}$
0.010	$4.03 \cdot 10^8 \text{ dm}^3 \text{ mol}^{-1} \text{ s}^{-1}$	$1.048 \cdot 10^{-2}$
0.015	$4.83 \cdot 10^8 \text{ dm}^3 \text{ mol}^{-1} \text{ s}^{-1}$	$1.553 \cdot 10^{-2}$
0.020	$5.49 \cdot 10^8 \text{ dm}^3 \text{ mol}^{-1} \text{ s}^{-1}$	$2.056 \cdot 10^{-2}$

A Mayo plot of the results in Table 3.1 results in a transfer constant of 1.01, an overestimation of 1%. So indeed the chain length dependent termination rate coefficient hardly has an effect on the observed C_T at 50 °C, which is presumably due to the low radical concentration. However, at higher temperatures the radical concentration will be much higher and, as can be seen from Eq. 3.10, in that case $\langle k_t \rangle$ will play a more important role. To illustrate this, the same example is

considered at 100 °C. In this case $k_p = 1200 \text{ dm}^3 \text{ mol}^{-1} \text{ s}^{-1}$ [35] and $k_d = 1.6 \cdot 10^{-3} \text{ s}^{-1}$ [33] for styrene and AIBN, respectively. It is assumed that $\langle k_t \rangle$ scales with D_{mon} . Griffiths *et al.* estimated the activation energy for monomer diffusion to be about 14.7 kJ mol⁻¹ at $w_p=0.1$ [32], which means an increase by a factor of 2 for the monomer

diffusion coefficient between 50 °C and 100 °C, and thus $\langle k_t \rangle$ is estimated to also increase by a factor of 2. Using Eqs. 3.11 and 3.13, a Mayo plot now results in $C_T = 1.07$, an overestimation of 7%. These calculations show that indeed at low radical concentrations chain length dependent termination can be ignored, but at higher concentrations it can become important. It is therefore recommended that the radical concentrations and the effect of $\langle k_t \rangle$ on the C_T values are being calculated before carrying out experiments. An important consideration is the influence of the GPC analysis on the determination of n DP and consequently C_T . However, the determination of n DP is very sensitive to baseline selection and selection of the start of a peak at the low molecular weight side, especially with low molecular weight polymer[36 and references herein].

This makes the M_n more susceptible to baseline errors. This can be overcome for transfer dominated systems where $M_w = 2 M_n$. n DP can now be obtained by dividing M_w by $2 \cdot M_0$. The reason that M_w is used instead of M_n is that it is less sensitive to baseline error. One must take care since this procedure may not be used if $M_w \neq 2 M_n$, which is the case for the high-reactive RAFT agents and for very low molecular weights.

3.3.2 The ln CLD method

In the ln CLD method[21,22] the number molecular weight distribution $P(M)$ or the chain length distribution $P(i)$ is plotted as $\ln(P(M))$ versus M or $\ln(P(i))$ versus i . It has been derived that the high molecular weight slope at low initiator concentrations of such a plot, α , can be written as:

$$\alpha = \frac{1}{M} \left(\frac{d \ln(P(M))}{dM} \right) \lim_{M \rightarrow \infty} \dots$$

+ - + - = = ϕ

. 8 .

(3.18)

or in term of chain length:

Homogeneous RAFT polymerizations

49

..

.

.

..

.

. > <

+ - + - = = ϕ

. 8 .] M [k

.] P [k

] M [

] R X [

C C

di

) i (P ln(d

lim

P

t

T M

0] I [, M

(3.19)

The slope of a ϕ versus $[X-R]/[M]$ plot will give C_T . The number molecular weight distribution can be obtained from a GPC distribution ($W(\log M)$ versus $\log M$) by dividing by $M_z[22]: \frac{1}{M} \int M W(\log M) d(\log M)$ tan cons arbitrary () M

(P · = (3.20)

In principle, the optimal way to obtain transfer constants using this method is by determining the transfer constant as a function of initiator concentration and extrapolating the results to zero initiator concentration.

However, when $M \rightarrow 0$, $W(\log M)$ approaches zero, and no reliable slope can be determined, since in this region the GPC molecular weight distribution strongly depends on baseline selection and detector noise. Moad *et al.*[37] proposed that the greatest accuracy will be obtained by analyzing the slope of the $\ln CLD$ plot that corresponds to the maximum in the GPC molecular weight distribution. They examined the $\ln CLD$ method and it appeared that in this method the transfer constant is insensitive to the mode of termination and chain length dependent termination, and therefore the most reliable results are obtained around the maximum of the GPC trace.

3.3.3 Mayo versus $\ln CLD$ method

When the Mayo method and the $\ln CLD$ method are compared[36] it stands out that Eqs. 3.10 and 3.19 are almost identical, except that in Eq. 3.19 a term for the mode of termination is missing. This term 'disappeared' by assuming that in the long chain limit, only short-long termination takes place, and thus both termination by combination and termination by

disproportionation result in approximately the same chain length. For the rest, both methods look identical and whether the Mayo method or the ln CLD method will give the most reliable results will depend on the accuracy of

Chapter 3

50

the determination of the number average molecular weight and the high molecular weight slope of the ln CLD plot, respectively. Moreover, it will depend on which method is most sensitive to the error introduced by assuming the same average termination rate coefficient for all RAFT agent to monomer ratios. In section 3.3.1 it was estimated that, using the Mayo method, the error introduced was about 1% at low radical concentrations increasing to 7% at high radical concentration.

In practice, not the long chain limit of a ln CLD plot but the area around the maximum of the GPC distribution is used to determine α . In this case Eq. 3.19 is no longer valid and the following equations should be applied[36]:

$$\dots\dots$$

$$\cdot$$

$$\cdot$$

$$\dots\dots$$

$$\cdot$$

$$\cdot$$

$$+ - + - = = \alpha$$

$$\cdot 8$$

$$=$$

$$\left[\frac{M}{P} \right] \left[\frac{k}{k^2} \right] \left[\frac{M}{R} \right] \left[\frac{X}{C} \right] \left[\frac{d}{C} \right]$$

$$\left(\frac{P}{d} \right) \ln \left(\frac{d}{P} \right)$$

$$\left(\frac{P}{d} \right) \ln \left(\frac{d}{P} \right)$$

$$\frac{P}{j} \frac{1}{j} \frac{j, i}{t}$$

$$T_M (3.21)$$

which assumes that the radical chain length distribution is equal to the chain length distribution of the dead and dormant chains. It is obvious that chain length dependent termination results in curvature in a ln CLD plot, especially when the radical concentration is high. To compare the ln CLD method with the Mayo method the same example as in section 3.3.1 is considered. $\alpha(i)$ is determined at the peak of the GPC distribution, which is assumed to be at $i=2 \cdot n \cdot DP$. It can be calculated that in the case that $i=2 \cdot n \cdot DP$ and $q=0$, i.e.

only termination by combination, $2 \cdot \left[\frac{P}{k_{jj, It}} \right] >$

$(1+q)\langle k_t \rangle [P\cdot]$ (compare Eqs. 3.10 and 3.21), whereas in the case that $q=1$, $2 \cdot [P\cdot] [k_{jj}, I] < (1+q)\langle k_t \rangle [P\cdot]$. This means that if $q=0$, the error in C_T introduced by chain length dependent termination is larger when the In CLD method is used, whereas if $q=1$ the error is larger with the Mayo method. However, it has to be remembered that these possible errors in C_T only show

51

up if both the radical concentrations is high and $\langle k_t \rangle$ shows a considerable dependence on the RAFT agent to monomer ratio. Theoretically the latter is expected, as shown in Table 3.1, however, in practice no effect of the RAFT concentration on the polymerization rate has been observed, as shown by the following experiments.

In a series of experiments the RAFT to monomer ratio has been varied and conversion versus time has been measured. In Figure 3.2 the results of three styrene polymerizations at 80 °C in toluene with varying concentrations of O-ethylxanthyl ethyl propionate (**I**, Scheme 3.4) are shown.

Scheme 3.4 O-ethylxantyl ethyl propionate and O-ethylxanthyl ethyl benzene.

The monomer concentration was kept low (2 M), to exclude the influence of changing medium viscosity, the concentration of **I** was 0, 0.01 and 0.02 M, respectively, while the initiator (AIBN) concentration was 5 mM.

Figure 3.2 Conversion versus time plot of 2 M styrene polymerizations in toluene with variable concentrations of **I**. Lines represent predictions according to Eq. 3.22 and $\langle k_t \rangle$ estimated by Eqs. 3.14 to 3.17. The solid line is for $n DP = 200$, dashed line for $n DP = 100$ and dotted line for $n DP = 67$.

The rate of polymerization, R_p , is given by:

$$R_p = \frac{d[M]}{dt} = k_p [P\cdot] [M] \quad (3.22)$$

0 1 2 3 4
 0
 5
 10
 15
 20
 25
 30
 conversion [%]
 time [h]
 no **I**
 0.01 M **I**
 0.02 M **I**
C
S
 C₂H₅O S

C
 CH₃
 C
 O
 OC₂H₅
(I) (II)
 C
 S
 C₂H₅O S
 C
 CH₃

in which f is the initiator efficiency. It can be seen that the rate of polymerization is independent of the concentration I . The results are compared with the predicted conversion-time plots, for which Eq. 3.22 can be used. Therefore $\langle k_t \rangle$ has to be estimated. Again Eqs. 3.14 to 3.17 can be applied. The molecular weight of the polymer formed in these experiments found by GPC was 20 kg/mol, 10 kg/mol and 7 kg/mol with increasing concentration of I , respectively. This corresponds exactly to the $\langle k_t \rangle$ values calculated in Table 3.1 for $[R-X]/[M]=0.005, 0.010$ and 0.015 , respectively. However, in these experiments the temperature was $80\text{ }^\circ\text{C}$, instead of $50\text{ }^\circ\text{C}$ in the calculations in Table 3.1. Since the activation energy for diffusion is about 14.7 kJ mol^{-1} [32], it can be calculated that the values of Table 3.1 have to be multiplied by a factor 1.6 in order to obtain the $\langle k_t \rangle$ at $80\text{ }^\circ\text{C}$. This results in $\langle k_t \rangle = 4.69, 6.45$ and $7.73 \cdot 10^8\text{ dm}^3\text{ mol}^{-1}\text{ s}^{-1}$, respectively. The predicted conversion-time plots using these values are shown in Figure 3.2. It can be seen that the predicted conversion-time plots lead to considerable differences in conversion over increasing time. However, the experimental data do not show this trend. The conversion-time plots overlap each other, indicating that $\langle k_t \rangle$ is approximately the same at these 3 n_{DP} 's. In these experiments, also samples were taken after 24 hours (not shown in Figure 3.2). In all cases the conversion was approximately 50%, confirming that the $\langle k_t \rangle$ is approximately the same in these experiments and is hardly dependent of the RAFT agent to monomer ratio at these concentrations. What does this mean for both the Mayo method and the In CLD method? If $\langle k_t \rangle$ is independent of the RAFT agent to monomer ratio, it means that both in the Mayo method and in the In CLD method also the term containing $\langle k_t \rangle$ (see Eqs. 3.10 and 3.19) is independent of the RAFT agent to monomer ratio. This means that no error will be introduced in the determination of C_T as a result of chain length dependent termination using the Mayo method and the long chain limit of the In CLD method. Normally, not the long chain limit of a In CLD plot is taken, but the slope in an area around the GPC peak molecular weight, for which Eq. 3.19 is replaced by Eq. 3.21. However, it is reasonable to assume that if the average termination rate coefficient over all chains is independent of the RAFT agent to monomer ratio, the average termination coefficient in the area around the GPC peak molecular weight will

also show little dependency. As a consequence, also using the ln CLD method around the GPC peak molecular weight will be free of errors introduced by chain length dependent termination.

Homogeneous RAFT polymerizations

53

3.3.4 Results

The results for the C_T values will be presented for low conversion experiments with styrene and n-butyl acrylate with I at various temperatures. From the aforementioned considerations about both the Mayo method and the ln CLD method, it can be assumed that both methods will give reliable results with respect to the influence of chain length dependent termination.

The C_T is obtained using 4 different procedures, which have been described in sections 3.3.1 to 3.3.3:

Procedure 1. The classical Mayo method, i.e. $1/n DP$ is plotted versus $[RAFT]/[M]$ in which $n DP = M_n/M_0$ obtained from GPC.

Procedure 2. The Mayo method in which $n DP = M_w/2M_0$

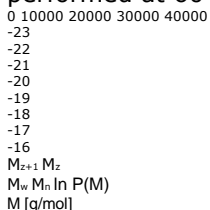
Procedure 3. The ln CLD method, i.e. φ is plotted versus $[RAFT]/[M]$, where φ is the peak molecular weight slope, which is defined as the slope between M_n and M_z and is referred to as φ_{peak} .

Procedure 4. The ln CLD method where φ is the slope between M_z and M_{z+1} , referred to as φ_{high} .

One of the requirements of the ln CLD method is that the region of the $\ln(P(M))$

versus M plot that is chosen has to be linear. However, if the peak region was chosen this was not always the case. This is shown in Figure 3.3 for the same experiment at 3 different temperatures.

Figure 3.3 ln CLD plots of low conversion experiments with a I to styrene ratio of 0.0145 performed at 60 °C (solid line), 80 °C (dashed line) and 120 °C (dotted line).



Beyond M_w all experiments showed a large linear region. The region between M_z and M_{z+1} was chosen because in this part of GPC trace there is a large detector signal, so GPC artifacts will be of minor importance.

Table 3.2 Results of transfer constant determinations of I with styrene at various temperatures using procedures 1 to 4. The 95% confidence interval of the reported C_T was about ± 0.03 .

	<i>Procedure 1</i>	<i>Procedure 2</i>	<i>Procedure 3</i>	<i>Procedure 4</i>	
	$[I]/[Styrene]$	$1/(M_n/M_0)$	$1/(M_w/2M_0)$	$-\varphi_{peak} \cdot M_0$	$-\varphi_{high} \cdot M_0$
60 °C					
	0.006178	0.00540	0.00543	0.005618	0.005482

0.010964 0.00910 0.00914 0.008939 0.009364
0.014790 0.01119 0.01159 0.011473 0.012099
0.026447 0.01905 0.02014 0.019591 0.019546
 $C_T=0.666$ $C_T=0.722$ $C_T=0.689$ $C_T=0.685$

80 °C

Chapter 3

54

0.007163 0.00665 0.00643 0.006492 0.006430
0.01092 0.00947 0.00946 0.009216 0.009839
0.01447 0.01256 0.01237 0.012136 0.012731
0.02152 0.01665 0.01752 0.017533 0.017252
 $C_T=0.699$ $C_T=0.772$ $C_T=0.773$ $C_T=0.747$

100 °C

0.004222 0.00546 0.005052 0.005177 0.005190
0.01524 0.01297 0.01330 0.013272 0.013628
0.01963 0.01632 0.01699 0.017171 0.016923
 $C_T=0.700$ $C_T=0.770$ $C_T=0.770$ $C_T=0.762$

120 °C

0.002314 0.00411 0.004240 0.004483 0.004394
0.005371 0.00773 0.007887 0.007900 0.007934
0.014452 0.01420 0.014337 0.014232 0.014544
0.030661 0.02420 0.026726 0.025545 0.027424
 $C_T=0.689$ $C_T=0.775$ $C_T=0.726$ $C_T=0.796$

Homogeneous RAFT polymerizations

55

The transfer constant for styrene in the presence of **I** has been determined at 60 °C, 80 °C, 100 °C and 120 °C and for n-butyl acrylate at 50 °C and 80 °C. All experiments were performed in bulk and the initiator concentration was 1 mM in all experiments. The results are shown in Table 3.2 and Table 3.3 for styrene and nbutyl acrylate, respectively.

Figure 3.4 (left) Transfer constants of **I** with styrene at various temperatures and determined by procedures 1 to 4.

Figure 3.5 (right) Molecular weight distributions of polystyrene produced using a low concentration of **I** (solid line) and a high concentration of **I** (dashed line). The arrow indicates that for the high RAFT concentration, the lowest molecular weight part is cut off the MWD. The transfer constants determined by the different procedures are plotted in Figure 3.4. It can be seen that the differences between the different procedures are small, however, the transfer constants determined by *procedure 1* systematically results in values lower than those in the other 3 procedures. This can be explained as follows.

In the experiments with the highest concentration of **I**, the measured polydispersity is below 2, which means that $1/(M_w/2M_0) > 1/(M_n/M_0)$, resulting in a lower C_T using *procedure 1*. This effect might be due to the

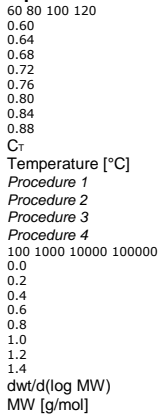
cutting off of the low molecular weight tail in the GPC chromatogram. Figure 3.5 illustrates this point clearly for experiments carried out at 120 °C with the lowest and highest concentration of I.

At the lowest concentration of I, the GPC trace returns to the baseline and is within the exclusion limit of the GPC columns. On the other hand, at the highest concentration of I, the detector trace on the low molecular weight side does not go back to the baseline completely and consequently is cut off

Chapter 3

56

from the Molecular Weight Distribution, and thus these low molecular weight species are not taken into account in the calculation of M_n .



The results obtained by *procedure 1* are therefore less reliable than those obtained by the other procedures. From Figure 3.3 it was clear the results obtained by *procedure 3* are not always derived from a linear region of the \ln CLD plot, and the results obtained by *procedure 4* are therefore more reliable. Distinction whether *procedure 2* or *procedure 4* is more reliable is hard to make and therefore the average value of these two procedures will be taken as the transfer constant of styrene to I at a certain temperature. This results in $C_T=0.704, 0.760, 0.766$ and 0.786 for $60\text{ }^\circ\text{C}, 80\text{ }^\circ\text{C}, 100\text{ }^\circ\text{C}$ and $120\text{ }^\circ\text{C}$, respectively, which indicates a trend towards higher transfer constants at higher temperatures. The 95% confidence interval of the reported C_T values is about ± 0.03 . The transfer constant, which is defined as k_{tr}/k_p , can be plotted in an Arrhenius plot:

$$\ln \left(\frac{k_{tr}}{k_p} \right) = C \ln \left(\frac{p}{T} \right) + \text{const} \quad (3.23)$$

in which A_{tr} and E_{tr} are the frequency factor and activation energy of the transfer reaction and A_p and E_p are the frequency factor and activation energy for propagation.

The Arrhenius plot is shown in Figure 3.6.

Figure 3.6 Arrhenius plot of the transfer constant of styrene to I.

From the slope and intercept of Figure 3.6 and Eq. 3.23 an estimation of the *Homogeneous RAFT polymerizations*

57

Homogeneous RAFT polymerizations

57

activation energy and frequency factor of the transfer reaction can be obtained. It was found that the slope is -225 ± 60 (95% confidence interval) and the intercept is

0.339 ± 0.17 . Using the Arrhenius parameters for styrene, $A_p=10^{7.63}$ and $E_p=32.5$

0.0025 0.0026 0.0027 0.0028 0.0029 0.0030
 -0.36
 -0.34
 -0.32
 -0.30
 -0.28
 -0.26
 -0.24

ln C_T [-]

1/T [1/K]

kJ/mol [35], it can be calculated that for the transfer reaction these parameters are

$A_{tr}=10^{7.78 \pm 0.07}$ and $E_{tr}=34.37 \pm 0.5$ kJ/mol, respectively.

Table 3.2 Results of transfer constant determinations of I with n-butyl acrylate (n-BA) at 50 °C and 80 °C using procedures 1 to 4. The 95% confidence interval of the reported C_T was about ± 0.10 .

Procedure 1 Procedure 2 Procedure 3 Procedure 4

[I]/[n-BA] $1/(M_n/M_0)$ $1/(M_w/2M_0)$ $-\phi_{peak} \cdot M_0$ $-\phi_{high} \cdot M_0$

50 °C

0.003139 0.00588 0.006422 0.006964 0.006388

0.005003 0.00951 0.009911 0.010234 0.009902

0.010708 0.01687 0.016951 0.018129 0.016940

0.017002 0.02747 0.029316 0.029979 0.029327

0.019592 0.03357 0.034968 0.036275 0.036275

$C_T=1.62$ $C_T=1.70$ $C_T=1.74$ $C_T=1.75$

80 °C

0.002709 0.00828 0.006066 0.006482 0.005599

0.005191 0.01049 0.010492 0.010842 0.010338

0.009522 0.01431 0.015301 0.016086 0.015568

0.020715 0.03243 0.037277 0.038559 0.038234

$C_T=1.37$ $C_T=1.73$ $C_T=1.78$ $C_T=1.81$

It was found that the transfer constant of n-butyl acrylate with I was higher than that of styrene. Again all procedures gave similar results, except *procedure 1* at 80 °C, which again was due to an error introduced by an early cut-off of the MWD, leading to an overestimation of M_n , as seen in the case of styrene. Again a trend towards higher transfer constants at higher

temperatures can be observed, indicating a somewhat higher activation energy for transfer than for propagation. Taking the average of the transfer constants determined by procedure 2 and 4 leads to transfer constants of 1.73 and 1.77 at 50 °C and 80 °C, respectively. The 95% confidence interval of the reported C_T values is about ± 0.10 .

Chapter 3

58

3.4 Homopolymerizations of styrene and n-butyl acrylate

3.4.1 The effect of RAFT on the rate of polymerization

If Scheme 3.3 is considered to be correct there is no reason to assume that addition of a RAFT agent to a conventional free radical polymerization will have an effect on the polymerization rate, unless the leaving group of the RAFT agent is slow to re-initiate or the fragmentation of the RAFT intermediate radical is also slow (the addition-fragmentation reaction, as shown in Scheme 3.1). The addition-fragmentation, which is not shown in Scheme 3.3, plays an important role in the polymerization mechanism. This reaction is simplistically considered as a single transfer reaction in Scheme 3.3, but in fact is more complex: addition of a radical to a dormant species leads to an intermediate radical **2** or **4** (Scheme 3.1), which can either fragment back to its originating species or form a new radical and dormant species. It has been found that this intermediate radical plays an important role in the retardation observed in RAFT polymerizations with dithioesters[24,25,38-40].

Another factor that might play a role in the polymerization rate in the presence of a RAFT agent is the fact that the radical chain length distribution is significantly lowered, thereby increasing the average rate of termination and thus decreasing the polymerization rate.

Both the role of the intermediate radical and the effect of RAFT on the average termination rate will be discussed below.

The intermediate radical.

The intermediate radical was postulated to be the reason for the significant retardation on the polymerization rate. Two explanations for retardation with respect to the intermediate radical have been put forward in literature:

A. slow fragmentation of the intermediate radical[38,39]

B. termination of the intermediate radical[24,25,40]

Neglecting chain length effects for the moment and assuming the reactivity of a dormant chain is equal to the reactivity of the initial RAFT agent, a RAFT polymerization can be represented by Scheme 3.5.

Scheme 3.5 Kinetic scheme of a RAFT polymerization. I is the initiator, R is a radical, M is the monomer, SR the RAFT agent or dormant chain, RSR is the intermediate radical and D is a dead polymer chain.

In explanation A reactions 1 to 6 from Scheme 3.5 are involved, whereas in explanation B additional reactions (reactions 7 and 8) play a role: termination of the intermediate radical, either by a 'normal' radical (7) or by another intermediate

Homogeneous RAFT polymerizations

59

radical (8). The rate of polymerization R_p is defined as the rate at which monomer is consumed:

$$- \frac{d[M]}{dt} = R_p = k_p [R] [M] - k_t [R]^2 - k_{ti} [R] [R] - k_{tii} [R] [R] - k_{add} [R] [M] \quad (3.24)$$

Assuming pseudo steady state for R and RSR and assuming that $k_{ti} = k_{add}$ the concentrations of these species are given by:

$$[RSR] = \frac{k_i [I]}{k_{add} [M]} \quad [SR] = \frac{k_{add} [R]}{k_{ti} [R]} \quad [R] = \frac{k_i [I]}{k_{add} [M]}$$

$$[RSR] = \frac{k_i [I]}{k_{add} [M]} \quad [SR] = \frac{k_{add} [R]}{k_{ti} [R]} \quad [R] = \frac{k_i [I]}{k_{add} [M]}$$

$$[R] = \frac{k_i [I]}{k_{add} [M]}$$

$$[SR] = \frac{k_{add} [R]}{k_{ti} [R]}$$

$$[RSR] = \frac{k_i [I]}{k_{add} [M]}$$

$$+$$

$$= - \quad (3.25)$$

$$[RSR] = \frac{k_i [I]}{k_{add} [M]} \quad [R] = \frac{k_i [I]}{k_{add} [M]}$$

$$[SR] = \frac{k_{add} [R]}{k_{ti} [R]}$$

$$[RSR] = \frac{k_i [I]}{k_{add} [M]}$$

$$[SR] = \frac{k_{add} [R]}{k_{ti} [R]}$$

$$[RSR] = \frac{k_i [I]}{k_{add} [M]}$$

$$=$$

$$-$$

$$(3.26)$$

in which $\langle k_{ti} \rangle$ is the termination rate coefficient for termination between an intermediate radical termination and a 'normal' radical and $\langle k_{tii} \rangle$ is the termination

I

R + M

R + SR

RSR

RSR

R + R

RSR + R

RSR + RSR

2 R (1)

R (2)

RSR (3)

R + SR (4)

R + SR (5)

D (6)

D (7)

D (8)

f k_d

k_p

k_{add}

k_{-add} <k_t> <k_{ti}>k₀<k_{tii}>

Chapter 3

60

rate coefficient for termination between two intermediate radicals. These equations can be solved numerically by estimating [RSR], calculating [R] with Eq. 3.26 and putting both values into Eq. 3.25. The obtained [R] is used to calculate [RSR] using Eq. 3.26. If the [RSR] then obtained is equal to the estimated [RSR] the problem is solved, otherwise the obtained [RSR] is used as the new estimation and the process is repeated.

If no RAFT agent is present, the rate of polymerization is given by:

> <

=

t

d

p

noRAFT

p k

] I [f k

] M [k R (3.27)

Now a retardation parameter, Q, can be defined:

noRAFT

p

p

R

R

Q = (3.28)

In explanation A, slow fragmentation of the intermediate radical is proposed as mechanism for retardation, thus without intermediate radical termination taking place.

Davis *et al.* had to use values for k_{-add} of 3.3·10⁻² s⁻¹ in order to fit their experimental data, which is 6-7 orders magnitude smaller than the values obtained by Fukuda[25] and Monteiro[24] for the same system. If <k_{ti}> and <k_{tii}> = 0, [R] can be calculated analytically by substitution of Eq. 3.26 into Eq. 3.25. This results in Q=1, since both k_{add} and k_{-add} cancel out and [R]=(k_d[I]/<k_t>)^{0.5} is obtained! This indicates that at steady state no retardation is expected in Davis' model and the observed retardation is the result of a slow build-up of the equilibrium in the approach to steady state.

However, after some time a pseudo steady state is reached, which will result in a polymerization rate independent of the RAFT concentration. It can be seen in their work that the simulated polymerization rates indeed become

independent of the RAFT concentration at longer polymerization times, however this does not correspond to their experimental conversion data. Comparing the highest and lowest RAFT concentration in Davis' work[38], it is observed that with the lowest RAFT concentration, conversion has increased 13.4% between 12 and 24 hours reaction time and with the highest concentration of RAFT the increase was only 5.5%. Based

Homogeneous RAFT polymerizations

61

on these considerations, slow fragmentation alone can be rejected as the reason for retardation in RAFT polymerizations.

Monteiro and De Brouwer proposed an additional termination reaction, *i.e.* intermediate radical termination (see Scheme 3.5 reactions 7 and 8)[24]. They were able to fit experimental data with rate parameters from literature using a fragmentation rate constant of 10^5 s^{-1} . Moreover, they obtained experimental evidence for the occurrence of this reaction. When dormant polymer chains, in the absence of monomer, were irradiated with UV light, which breaks the C-S bond between the polymer chain and RAFT moiety, polymer of double and triple molecular weight was formed as a result of bimolecular radical termination and intermediate radical termination, respectively.

The main problem with the intermediate termination mechanism is the type of radicals that can terminate with it. In the paper of Monterio and De Brouwer it was assumed that all radicals will terminate irreversibly even other intermediate radical species (although this was not specifically mentioned in their paper). Here we would like to investigate the effect of the type of radicals that terminate with the intermediate radical on the rate of polymerization, specifically on retardation. There has been some discussion that termination between two intermediate radicals could be a reversible process [40,48], and thereby this extra termination mechanism will have no effect on the rate. The plausibility of this statement will be tested below. If it is assumed that both $\langle k_{ti} \rangle [R]$ and $\langle k_{tii} \rangle [RSR]$ are very much less than

k_{-add} ,

Eqs. 25 and 26 can also be solved analytically, yielding:

$$] SR [k k k k 4$$

$$k] I [fk 4$$

$$] R [$$

$$\text{add ti add t}$$

$$\text{add d}$$

$$> < + > <$$

$$=$$

$$-$$

$$-(3.29)$$

Combination of Eqs. 3.24 and 3.27 to 3.29 will then yield estimated values for Q .

When the radical concentrations are being calculated by solving Eqs. 3.25 to 3.28 numerically, no such assumptions have to be made and, therefore, preference is given to numerical calculations (Appendix 3.2). In Table 3.3 Q values are summarized for a bulk polymerization of styrene at 80 °C with dithiobenzoate and O-ethyl xanthate as

Chapter 3

62

RAFT agent and for a bulk polymerization of n-butyl acrylate at 50 °C with O-ethyl xanthate.

Q_1 is the retardation factor for the system taking into account only termination of the intermediate radicals with all radicals that do not include other intermediate radicals.

Q_2 is the retardation factor taking into account intermediate radical termination with all radical species in the system (even other intermediate radicals).

Table 3.3 Retardation parameter Q for bulk polymerizations with 1% RAFT agent and 1 mM AIBN as

initiator. $\langle k_t \rangle$, $\langle k_{ti} \rangle$ and $\langle k_{tii} \rangle$ are $2 \cdot 10^8 \text{ dm}^3 \text{ mol}^{-1} \text{ s}^{-1}$, $f_{kd} = 1.1 \cdot 10^{-6}$ at 50 °C and $f_{kd} = 1.1 \cdot 10^{-4}$ at 80 °C. Q_1 is the retardation factor if $\langle k_{tii} \rangle = 0$, Q_2 is the retardation factor if $\langle k_{tii} \rangle = \langle k_{ti} \rangle = 2 \cdot 10^8 \text{ dm}^3 \text{ mol}^{-1} \text{ s}^{-1}$.

1. Q is calculated numerically using Eqs. 3.25 to 3.28.

$k_{\text{-add}} [\text{s}^{-1}]$ Q_1 Q_2

Styrene 80 °C, dithiobenzoate 10^7 0.983 0.983

k_p : $660 \text{ dm}^3 \text{ mol}^{-1} \text{ s}^{-1}$ [35] 10^6 0.863 0.828

C_T : 6000 [18] 10^5 0.473 0.249

10^4 0.168 0.029

10^3 0.054 0.003

Styrene 80 °C, xanthate 10^7 1.000 1.000

C_T : 0.8 [this work] 10^6 1.000 1.000

10^5 1.000 1.000

10^4 0.998 0.998

10^3 0.978 0.977

n-Butyl acrylate 50 °C, xanthate 10^7 1.000 1.000

k_p : $2.05 \cdot 10^4 \text{ dm}^3 \text{ mol}^{-1} \text{ s}^{-1}$ [44] 10^6 0.998 0.998

C_T : 1.73 [this work] 10^5 0.985 0.985

10^4 0.875 0.845

10^3 0.496 0.272

It can be seen that for the very reactive RAFT agents (e.g. dithiobenzoate),

retardation will be observed. Taking termination between two intermediates into account increases the retardation (Q_2 is lower than Q_1). Even if the termination product between two intermediate radicals is only partially reversible the retardation factor would lie between Q_1 and Q_2 . It can be seen that for the highly reactive RAFT agents the reversibility could have a large effect on retardation, depending upon the value for k_{-add} . The lower the value of k_{-add} the greater the extent of retardation. It should be noted that the amount of retardation observed is dependent upon the intermediate radical concentration. If this is high then the probability for intermediate termination will also be high and *vice versa*. The latter is the case for the less reactive xanthates used in this work.

Homogeneous RAFT polymerizations

63

It can be observed in Table 3.3 that retardation is not to be expected for the xanthates, unless very reactive monomers are being used in combination with a relatively slow fragmentation rate of the intermediate radical. The expectation that styrene with xanthates will not show retardation is confirmed by the results, which are shown in Figure 3.2, where styrene polymerizations with I did not show retardation. Experiments with n-butyl acrylate and a xanthate will give more insight in the order of magnitude of the fragmentation rate in polymerizations with xanthates. This will be discussed later in section 3.4.4.

3.4.2 Effect of the average termination rate, $\langle k_t \rangle$ on the polymerization rate

Besides the influence of the intermediate radical on the polymerization rate, also the average termination rate might play a role in RAFT polymerizations. After all, the radical chain length distribution will be affected and thus also the average termination rate coefficient.

In Table 3.1 the results of calculations of $\langle k_t \rangle$ for transfer dominated radical chain length distributions (Flory-Schulz), assuming a diffusion controlled termination rate, were shown. Polymerizations in which RAFT agents with a low transfer constant are used, like the xanthates, have a similar radical chain length distribution. Since the calculated $\langle k_t \rangle$ increased considerably with increasing concentration of RAFT agent, it was expected to see an effect of the concentration RAFT agent on the polymerization rate. However, in Figure 3.2 the effect of $\langle k_t \rangle$ on the rate of polymerization is shown, and it can be seen that the expected retardation in rate is not observed experimentally.

In polymerizations with RAFT agents with a high transfer constant retardation is observed [24,25,38-40], which was assigned to slow fragmentation or termination of the intermediate radical. However, also the average

termination rate will have an effect on the polymerization rates in these systems. This effect will be considered here.

The radical chain length distribution with very reactive RAFT agents will be completely different from a 'normal' transfer dominated radical chain length distribution, because now the reversibility of the transfer reaction becomes important.

Ideally, all growing chains will have the same length, which increases linearly with

conversion:

$$x = \frac{[R-X]_0}{[M]_0}$$

Chapter 3

64

= (3.30)

in which $[M]_0$ and $[R-X]_0$ are the initial monomer concentration and the initial RAFT agent concentration, respectively, and x is the fractional monomer conversion. In

Figure 3.7 calculated conversion time plots are shown for styrene polymerizations at 80 °C with RAFT agents of high reactivity and these are compared with conversion time plots of polymerizations with low reactivity RAFT agents. Details of the calculations with the low reactivity RAFT agents are given in section 3.3.3, whereas for the calculation of the termination rate of the high reactivity RAFT agent Eqs. 3.30, 3.15 and 3.17 were used. In the calculations the effect of the weight fraction polymer is neglected, because the example deals with a solution polymerization at relatively low conversions.

In Figure 3.8 the corresponding termination rate coefficients are shown. In the simulations with the low reactivity RAFT agents the average chain length remains the same from the beginning to the end, whereas with the high reactivity RAFT agents the chain length increases with conversion, resulting in a termination rate that decreases with conversion. Figures 3.7 and 3.8 further show that the overall effect on the polymerization rate is similar. Both with the low and high reactivity RAFT agents the increase in termination rate and reduction in polymerization rate with increasing concentration of RAFT agent is of the same order of magnitude. Although Figure 3.2 showed that there was no effect on the polymerization rate with the low reactivity RAFT agents, it cannot be concluded that there is no effect with the high reactivity RAFT agents. However, when highly reactive RAFT agents are used, also the intermediate radical causes retardation and one cannot discriminate between the separate contributions to the overall retardation, because real average

termination rate coefficients and fragmentation rate coefficients are not exactly known.

Figure 3.7 (left) Calculated conversion time plots of 2 M solution polymerizations in styrene with 5 mM

AIBN and $[M]/[R-X]=200$ or 100 for low reactivity RAFT agents (polydispersity = 2 and $\langle i \rangle = \text{constant} = [M]_0/[R-X]_0$) and high reactivity RAFT agents (polydispersity = 1 and $i = x[M]_0/[R-X]_0$).

(a) $[M]/[R-X]=200$, RAFT with low reactivity; (b) $[M]/[R-X]=100$, RAFT with low reactivity;

(c) $[M]/[R-X]=200$, RAFT with high reactivity; (d) $[M]/[R-X]=100$, RAFT with high reactivity.

Figure 3.8 (right) Calculated $\langle k_t \rangle$ versus conversion of 2 M solution polymerizations in styrene with 5 mM AIBN and $[M]/[R-X]=200$ or 100 for low (polydispersity = 2 and $\langle i \rangle = \text{constant} = [M]_0/[R-X]_0$) and high reactivity RAFT agents (polydispersity = 1 and $i = x[M]_0/[R-X]_0$).

(a) $[M]/[R-X]=200$, RAFT with low reactivity; (b) $[M]/[R-X]=100$, RAFT with low reactivity;

(c) $[M]/[R-X]=200$, RAFT with high reactivity; (d) $[M]/[R-X]=100$, RAFT with high reactivity.

Monteiro and De Brouwer [24] performed styrene solution polymerizations at 80 °C with a high reactivity RAFT agent. They observed that after 5 hours the conversion in the experiment with a monomer to RAFT agent ratio of 50 was 5% lower than with a ratio of 75 (15% vs. 10%). Using termination rates predicted by Eqs. 3.30, 3.15 and

65

a ratio of 75 (15% vs. 10%). Using termination rates predicted by Eqs. 3.30, 3.15 and 3.17, simulations in which only the effect of the termination rate is involved predict a difference in conversion of about 1% (13% vs. 12 %). This indicates that the retardation observed in their experiments cannot be the result of an increased termination rate alone, and that the effect of intermediate radicals on the polymerization rate dominates the effect of differences in the average termination rate.

3.4.3 Styrene polymerizations with a xanthate

It was shown that the intermediate radical does not play a role in the polymerization rate of styrene, when a xanthate is used as the RAFT agent. Therefore, the xanthates can only have an effect on the termination rate, since addition of xanthates leads to lower molecular weights and, therefore, higher termination rates.

```

0 3600 7200 10800 14400
0.00
0.05
0.10
0.15
0.20
0.25
conversion [-]
time [s]
0.2 0.4 0.6 0.8 1.0
1E8
1E9
<k_t> [dm3mol-1s-1]
conversion [-]
a
b
c
d
a
b
d
c

```

In Figure 3.2 it was shown that no effect of the xanthate concentration (I) on the polymerization rate was observed, and the polymerization rate could be calculated using the average termination rate calculated in section 3.3.1 for a styrene to RAFT agent ratio of 200. Similar experiments were performed with II, but also in this case no effect of the RAFT concentration on the polymerization rate was observed. In the experiments from Figure 3.2 both conversion and monomer concentration were low, so the weight fraction of polymer did not play an important role. In experiments in which the monomer concentration is higher and higher conversions are reached, not only the radical chain length distribution but also the weight fraction of polymer plays an important role in the average termination rate constant. This is shown in Figure 3.9. Figure 3.9 shows that for a 4 M styrene polymerization at 70 °C

Homogeneous RAFT polymerizations

with 0.5 mole% I, a constant average termination rate coefficient cannot predict the polymerization rate, although the radical chain length distribution is relatively constant. At higher conversions large deviations occur, indicating that the average termination rate decreases. This decrease is a result of a decreasing diffusion coefficient of polymer chains at higher weight fractions of polymer. In order to take this into account, Eq. 3.17 has to be replaced by [31,32]:

$$D_p = D_{p,0} \left(\frac{w_p}{w_{p,0}} \right)^{1.49} \quad (3.31)$$

where

w_p

is the weight fraction of polymer.

$$D_{p,0} = 1.79 \times 10^{-13} \text{ m}^2 \text{ s}^{-1} \quad (3.31)$$

in which w_p is the weight fraction of polymer. For the monomer diffusion coefficient in a polystyrene matrix at 50 °C the following empirical relation was determined experimentally [32]:

D_m

is given by

D_m

$$D_m = 1.79 \times 10^{-13} \left(\frac{w_p}{w_{p,0}} \right)^{1.49} \left(\frac{w_m}{w_{m,0}} \right)^{1.19} \quad (3.32)$$

Using the monomer diffusion coefficient from Eq. 3.32, the average termination rate $\langle k_t \rangle$ can be calculated at every w_p , using the same equations as in section 3.3.1. In order to obtain $\langle k_t \rangle$ at 70 °C, the value obtained for $\langle k_t \rangle$ at 50 °C has to be multiplied by 1.38, since the activation energy for diffusion is estimated at 14.7 kJ/mol [32].

Homogeneous RAFT polymerizations

Figure 3.9 Conversion time plot of a 4 M styrene solution polymerization in toluene at 70

°C. The styrene to I ratio is 200, and the I to AIBN ratio is 4.

The dashed line is the PREDICI[41] simulation using a constant $\langle k_t \rangle$ ($10^{8.606} \text{ dm}^3 \text{ mol}^{-1} \text{ s}^{-1}$), while the solid line is the PREDICI simulation using a w_p dependent $\langle k_t \rangle$. The w_p dependent $\langle k_t \rangle$ was calculated using Eqs 3.14 to 3.16, 3.31 and 3.32 at 6 points between $w_p=0$ and $w_p=0.3$ using $C_T=1$ and fitted to a polynomial:

$$10 \log(\langle k_t \rangle(w_p)) = 8.606 - 4.762w_p + 5.683w_p^2 - 7.089w_p^3 + 2.266w_p^4$$

Figure 3.9 shows that a w_p dependent termination rate coefficient fits the data

better than the constant termination rate coefficient, although at higher conversions

this leads to an overestimation of the polymerization rate. This effect is known as

transfer dominated termination. After all, addition of a transfer agent (in this case a

RAFT agent) strongly reduces the gel effect. However, this estimation of the w_p dependent

termination rate coefficient is assumed to be accurate enough for modeling molecular weights with PREDICI[41].

Homogeneous RAFT polymerizations

Homogeneous RAFT polymerizations

67

In Figure 3.1 the molecular weights and polydispersities for RAFT polymerizations as predicted by Müllers equations (Eqs. 3.4 and 3.5) were shown. However, when these equations are used to predict the molecular weights, large deviations can occur.

This is shown in Figure 3.10, in which the molecular weights of the experiment of Figure 3.9 are plotted versus conversion and compared with the predictions from Müllers equations.

0 600 1200 1800 2400
0
10
20
30
40
50
60
70
conversion [%]
time [min]

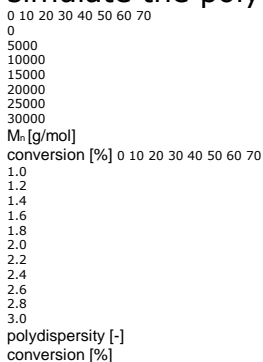
Figure 3.10 (a) M_n and (b) polydispersity versus conversion plot of a 4 M styrene solution polymerization in toluene at 70 °C. The styrene to I ratio is 200, and the I to AIBN ratio is 4. The dashed line is calculated using Eq. 3.4 with $C_T=0.73$, the solid lines are the PREDICI simulations.

Figure 3.10 shows that the use of Eq. 3.4 leads to a large overestimation of M_n .

The reason for this is that in Eq. 3.4 the influence of termination reactions (bimolecular and transfer to solvent or monomer) on M_n is neglected. It is obvious from Figure 3.10 that termination cannot always be neglected, especially when the transfer constant is low and the initiator concentration is high. More sophisticated methods have to be used to simulate these RAFT

polymerizations. Here the simulation package PREDICI is used for this purpose.

Since the intermediate radical plays no role in the kinetics of styrene with a xanthate, the model in Scheme 3.3, extended with transfer to solvent and initiator efficiency, is used in combination with the parameters of Table 3.5 to simulate the polymerization described in Figure 3.9.



a b

Table 3.5 Parameters used in PREDICI simulations of styrene polymerizations at 70 °C with I as the RAFT agent.

Parameter value reference

Homogeneous RAFT polymerizations

69

k_d $4 \cdot 10^{-5} \text{ s}^{-1}$ [33]

f (initiator efficiency) 0.6 [42]

k_p $480 \text{ dm}^3 \text{ mol}^{-1} \text{ s}^{-1}$ [35]

k_{tc} $10 \log(\langle k_t \rangle (w_p)) = 8.606$

- $4.762w_p + 5.683w_p$

2

- $7.089w_p$

3 + $2.266w_p$

4

[see Figure 3.9]

k_{td} 0 [34]

k_{trM} $0.054 \text{ dm}^3 \text{ mol}^{-1} \text{ s}^{-1}$ [43]

k_{trS} (transfer to solvent) $0.0096 \text{ dm}^3 \text{ mol}^{-1} \text{ s}^{-1}$ [33]

k_{trRAFT} ($=C_T \cdot k_p$) $350 \text{ dm}^3 \text{ mol}^{-1} \text{ s}^{-1}$ [This work]

k_{trRAFT}

P ($=C_T \cdot k_p$) $350 \text{ dm}^3 \text{ mol}^{-1} \text{ s}^{-1}$ Assumed: k_{trRAFT}

$P = k_{trRAFT}$

Figure 3.10 shows that the simulation fits the experimental data very well, although at higher conversions small deviations occur. The experimental number average molecular weights are lower, which indicates that the number of polymer chains is higher than expected from the simulation. Possibly this is a result of thermal self-initiation or transfer reactions to impurities or initiator (or initiator derived sideproducts).

Also the polydispersity shows small deviations at higher conversions. Most likely these deviations are related to the deviations observed in the number average molecular weights and have the same cause. Figures 3.9 and 3.10 show that the simulations agree with the experimental data. However, a robust model should also be able to predict experimental results at other conditions. Therefore two series of experiments were performed under different conditions. First a series in which the initiator concentration was varied. Moreover, also the monomer concentration was different from that in the experiment described before. In the second series a bulk experiment is compared with an experiment in which a solvent was added, so all concentrations were diluted by the same factor.

Effect of initiator concentration

Two 2 M styrene polymerizations in toluene were performed at 70 ° with a styrene to I ratio of 200. The I to initiator ratio was 1 or 20, respectively. The experimental conversion-time and M_n -conversion plots are compared with the results of the simulations using the parameters from Table 3.5 and are shown in Figure 3.11.

Figure 3.11 (a) Conversion versus time and (b) M_n versus conversion of 2 M styrene solution

Chapter 3

70

polymerizations in toluene at 70 °C. The styrene to I ratio is 200, and the I to AIBN ratios are 1 (high concentration) or 20 (low concentration), respectively. The solid and dashed lines are the simulations for the high and low initiator concentration, respectively, whereas the filled squares and the circles are the experimental data-points for the high and low initiator concentration, respectively.

Figure 3.11 shows that the simulations again fit the experimental data quite well, although at higher conversions small deviations occur. The polydispersities are not shown, but these also fit with simulations. It is obvious that the initiator concentration should be kept low, because it can have a huge effect on the molecular weight. A lower molecular weight means more chains and since the concentration of RAFT agent is equal in both experiments it means more dead chains. Since RAFT polymerizations are especially interesting because of the ability to allow for instance preparation of block copolymers, it is of vital importance that the initiator concentration is kept low.

However, more important in this context here is that again the model predicts the experimental data quite well.

0 240 480 720 960 1200 1440

0
10
20
30
40
50
60
70

conversion [%]
 time [min]
 10 20 30 40 50 60
 0
 5000
 10000
 15000
 20000
 25000
 30000
 M_n [g/mol]
 conversion [-]
 0 2 4 6 8 10 12 14 16 18 20 22

a b

Effect of solvent concentration

Two styrene polymerizations were performed at 70 ° with a styrene to I ratio of 200 and a I to initiator ratio of 10. One experiment was performed in bulk, in the other experiment the reaction mixture was diluted with toluene to a styrene concentration of 4 M. The experimental conversion-time and M_n-conversion plots are compared with the results of simulations using the parameters from Table 3.5 and are shown in Figure 3.12.

Figure 3.12 (a) Conversion versus time and (b) M_n versus conversion of styrene polymerizations at 70 °C. The styrene to I ratio is 200, and the I to AIBN ratio is 10. One experiment is in bulk, the other is diluted with toluene to a 4 M styrene concentration. The solid and dashed lines are the simulations for the bulk and solution experiment respectively, whereas the filled squares and the open circles are the experimental data-points for bulk and solution experiment, respectively.

Figure 3.12 shows that again the experimental data agree with the simulations, except for deviations in the conversion-time behavior occurring in the bulk experiment at higher conversions. There are two possible reasons for this deviation: Eq. 3.31 is not valid if $w_p > 0.4$ [32] and/or the initiator efficiency goes down at higher w_p values[42]. Both are not taken into account in the model. However, at conversions <35%, corresponding to $w_p < 0.35$, the simulations fit the experimental data.

It is interesting to see that the molecular weight in the bulk experiments is higher, although the monomer to RAFT and the RAFT to initiator ratios are exactly the same. This can easily be explained on the basis of Eq. 3.10. It can be derived that if the solution polymerization is diluted by a factor F, the ratio of the third term in Eq. 3.10 between the solution experiment and the bulk experiment is $F^{0.5}$. Since the first two terms in Eq. 3.10 are independent of the concentration, but only depend on the

0 480 960 1440 1920 2400 2880
 0
 20
 40
 60
 80
 100
 conversion [%]
 time [min]
 0 10 20 30 40 50 60 70
 10000
 15000
 20000
 25000
 30000
 M_n [g/mol]
 conversion [%]
 0 10 20 30 40 50

a b

monomer to RAFT agent ratio, it is obvious that n DP in the solution experiment is smaller than in the bulk experiment, as is confirmed experimentally.

It can be concluded that the model can be used to simulate polymerization rates and molecular weights under various reaction conditions, unless the weight fraction of polymer becomes too high.

3.4.4 n-Butyl acrylate polymerizations with xanthates

Polymerization rate

In section 3.4.1 and Table 3.3 it was already shown that no retardation as a result of slow fragmentation or termination of the intermediate radical has to be expected in styrene polymerizations with xanthates as RAFT agents. However, it was also argued that the use of monomers with a higher propagation rate, like n-butyl acrylate, might result in retardation when the fragmentation rate is 1 or 2 orders of magnitude smaller than the values of 10^4 - 10^5 s⁻¹ reported by Fukuda[25] and Monteiro[24]. Therefore, a series of n-butyl acrylate polymerizations was performed, in which the concentration of **I** and **II** was varied. The results are shown in Figure 3.13. It is found that no retardation takes place when **I** is used, whereas the use of **II** leads to considerable retardation. As can be seen in Table 3.3 and as discussed in section 3.4.1, these results suggest that for **I** the fragmentation rate = 10^4 s⁻¹ and that for **II** the fragmentation rate < 10^3 s⁻¹. This latter value is much lower than previously reported values of 10^4 s⁻¹- 10^5 s⁻¹[24,25] for dithiobenzoates with styrene.

The conversion-time data can be simulated using Scheme 3.5. This was done using MATLAB[appendix 3.3]. Since some time is required to reach reaction

Chapter 3

72

temperature, all experiments showed an inhibition time of about 10 minutes. In order to compare the results with simulations, 10 minutes were subtracted from all experimental time readings, since inhibition is not taken into account in the simulations.

Figure 3.13 Conversion time plots and simulations of 2 M solution polymerizations of n-butyl acrylate in toluene at 60 °C. The AIBN concentration is 1 mM and the concentration of **I** and **II** is 0, 1 or 2 mole% based on monomer.

(a) conversion-time plot with 0% **I** (closed squares), 1% **I** (open circles) and 2% **I** (open triangles) and simulation (solid line) with $\langle k_t \rangle = 4 \cdot 10^8$ dm³ mol⁻¹ s⁻¹, $k_p = 2.29 \cdot 10^4$ dm³ mol⁻¹ s⁻¹ and $k_{add} = 7.92 \cdot 10^4$ dm³ mol⁻¹ s⁻¹ and $k_{-add} > 10^4$ s⁻¹. From this simulation it was found that, since there is no retardation with RAFT, $k_{-add} > 10^4$ s⁻¹. The dashed line represents the simulation with a w_p dependent termination rate and $k_p = 1.8 \cdot 10^4$ dm³ mol⁻¹ s⁻¹.

(b) conversion-time plot with 0% **II** (closed squares), 1% **II** (open circles) and 2% **II** (open triangles) and simulations (solid lines) with $k_p = 2.29 \cdot 10^4$ dm³ mol⁻¹ s⁻¹, $k_{add} = 7.92 \cdot 10^4$ dm³ mol⁻¹ s⁻¹, $\langle k_t \rangle = \langle k_{ti} \rangle = 4 \cdot 10^8$ dm³ mol⁻¹ s⁻¹, $\langle k_{tII} \rangle = 0$ and k_{-add} values from Table 3.6 (second column). The dashed lines, which largely overlap the solid lines, represent the simulations with $\langle k_t \rangle = \langle k_{ti} \rangle = \langle k_{tII} \rangle = 4 \cdot 10^8$ dm³ mol⁻¹ s⁻¹ and k_{-add} values from Table 3.6 (third column).

Polymerization rate without RAFT

First the polymerization without RAFT agent is considered. At 60 °C $k_p = 2.29 \cdot 10^4$ dm³ mol⁻¹ s⁻¹[44], $k_d = 9.5 \cdot 10^{-6}$ s⁻¹[33] and the initiator efficiency f is

estimated to be 0.6[42]. The w_p -dependent termination rate coefficient (see Table

3.5) of styrene can be recalculated for 60 °C, resulting in $\log(\langle k_t \rangle) = 8.538 - 4.827w_p + 6.670w_p^2 - 12.166w_p^3 + 10.653w_p^4$.

4. Although this termination rate showed excellent agreement in styrene polymerizations, here it resulted in overestimation of the polymerization rate, possibly because the termination rate in butyl acrylate polymerizations is less dependent on the weight fraction polymer than for styrene polymerizations. Another explanation can be that the k_p , which is extrapolated from an Arrhenius equation determined in a range between 5 °C and 30 °C in bulk, is not correct[50]. Asua *et al.* recently reported that the k_p of acrylates is concentration dependent and is lower at lower concentrations [45]. Since these experiments were

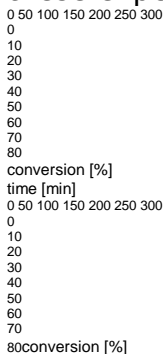


Figure 3.13a: Conversion [%] versus time [min] for two different conditions, labeled 'a' and 'b'.

74

performed in solution, also a lower k_p can be used in combination with the w_p -dependent termination rate. In that case the best fit was obtained with $k_p = 1.8 \cdot 10^4 \text{ dm}^3 \text{ mol}^{-1} \text{ s}^{-1}$. However, the curvature observed in the data-points from Figure 3.13 was not observed in the simulation and above 40% deviations started to occur (see dashed line in Figure 3.13a). This indicates that at higher conversions k_p decreases, which is in accord with a series of papers which report similar peculiarities with the polymerization rate of acrylates[50 and refs. herein]. Transfer to polymer followed by slow re-initiation and β -scission has been put forward as an explanation and is in accord with the here observed decrease of the apparent k_p . After all, with increasing conversion, the concentration of polymer increases and thus transfer to polymer increases, which lead to lower polymerization rates as a result of slow re-initiation of the transfer to polymer derived radical. On the other hand, when a constant and w_p -independent termination coefficient was used in combination with the literature value $k_p = 2.29 \cdot 10^4 \text{ dm}^3 \text{ mol}^{-1} \text{ s}^{-1}$, good agreement between simulation and experiment was obtained when $\langle k_t \rangle = 4 \cdot 10^8 \text{ dm}^3 \text{ mol}^{-1} \text{ s}^{-1}$ was used. This is probably the result of a decreasing termination rate which, by chance, seems to eliminate the effect of a decreasing k_p . The simulation using $k_p = 2.29 \cdot 10^4 \text{ dm}^3 \text{ mol}^{-1} \text{ s}^{-1}$ and $\langle k_t \rangle = 4 \cdot 10^8 \text{ dm}^3 \text{ mol}^{-1} \text{ s}^{-1}$ is shown in Figure 3.13a (solid line).

Polymerization rate with I

Since no retardation is observed when I is used, the fragmentation rate constant has to be of the order of 10^4 s^{-1} or higher. Moreover, these results indicate that the influence of chain length dependent termination on the polymerization rate is negligible, since the polymerization rate without RAFT is equal to the polymerization rate with 2 mole% I, while there is a considerable difference in molecular weight.

Without RAFT, M_w is of the order of $3 \cdot 10^5 \text{ g mol}^{-1}$, while with 2% I, M_w is of the order of $7 \cdot 10^3 \text{ g mol}^{-1}$.

Since the transfer constant of I with nBA is 1.71 at 50 °C and 1.77 at 80 °C (see section 3.2), $C_T=1.73$ at 60 °C is used. Eqs. 3.2 and 3.3 were used to calculate k_{add} although it has to be kept in mind that this is not always correct. However, here both the leaving group of the RAFT agent and the polymeric radical are secondary radicals and, therefore, k_{-add} will be close to k_{\oplus} . Therefore k_{add} is estimated to be $2 \cdot 1.73 \cdot 2.29 \cdot 10^4 = 7.92 \cdot 10^4 \text{ dm}^3 \text{ mol}^{-1} \text{ s}^{-1}$. Again a good agreement between simulation and experiment is obtained using k_p

$= 2.29 \cdot 10^4 \text{ dm}^3 \text{ mol}^{-1} \text{ s}^{-1}$ and $\langle k_t \rangle = 4 \cdot 10^8 \text{ dm}^3 \text{ mol}^{-1} \text{ s}^{-1}$ in combination with a fragmentation rate constant $> 10^4 \text{ s}^{-1}$. It has to be noted that in these simulations it is assumed that $\langle k_t \rangle = \langle k_{ti} \rangle = \langle k_{tii} \rangle$, and thus intermediate radical termination and intermediate-intermediate termination do not play a rate determining role.

Homogeneous RAFT polymerizations

75

Polymerization rate with II

Surprisingly, retardation is observed when II is used. Experiments have shown that the transfer constants of I and II are the same [this work, 47]. In order to fit the conversion-time data both cases, *viz.* the presence and absence of intermediate-intermediate termination, are considered.

Without intermediate-intermediate termination it is assumed that $\langle k_t \rangle = \langle k_{ti} \rangle$ and $\langle k_{tii} \rangle = 0$, similar to what was found by Fukuda ($\langle k_{ti} \rangle = 0.8 \langle k_t \rangle$) [25]. With intermediate-intermediate termination it is assumed that $\langle k_t \rangle = \langle k_{ti} \rangle = \langle k_{tii} \rangle$. For the termination rate coefficient and the propagation rate coefficient the same values as in the experiment without RAFT agent are used: $\langle k_t \rangle = 4 \cdot 10^8 \text{ dm}^3 \text{ mol}^{-1} \text{ s}^{-1}$ and $k_p = 2.29 \cdot 10^4 \text{ dm}^3 \text{ mol}^{-1} \text{ s}^{-1}$, so $k_{add} = 7.92 \cdot 10^4 \text{ dm}^3 \text{ mol}^{-1} \text{ s}^{-1}$. Simulations, in which k_{-add} is varied show that the best fit is obtained using the fragmentation rate constants shown in Table 3.6. The fits are shown in Figure 3.13b.

Table 3.6. Values for k_{-add} used to fit the conversion-time data in Figure 3.13. Both the situation in which intermediate-intermediate termination is neglected and the situation in which intermediate-intermediate termination is taken into account are considered.

k_{-add} without intermediate-intermediate termination

$k_{\text{-add}}$ with intermediate
intermediate
termination

1 mole% RAFT $6 \cdot 10^1 \text{ s}^{-1}$ $2.5 \cdot 10^2 \text{ s}^{-1}$

2 mole% RAFT $6 \cdot 10^1 \text{ s}^{-1}$ $3.5 \cdot 10^2 \text{ s}^{-1}$

The fragmentation rates found here are 2-4 orders of magnitude smaller than the fragmentation rate reported by Monteiro *et al.*[24] and Fukuda *et al.*[25] for the dithiobenzoate RAFT agent in combination with styrene and also at least two orders of magnitude smaller than for **I**, a RAFT agent similar to **II**. Although these unexpectedly low fragmentation rates fit the data quite well, they require a closer analysis and other possible reasons for the observed retardation have to be considered.

Chapter 3

76

Two other factors that might play a role are:

a. The RAFT agent has a poor leaving group

b. The RAFT leaving group adds slowly to monomer

In order to study these effects, the simple Scheme 3.5 cannot be used anymore,

and a more detailed reaction scheme, in which different radical species (growing

radicals and transfer to RAFT derived radicals), asymmetric intermediates and thus

mutually different addition and fragmentation rates have to be used (see Appendix

3.4).

a. A poor leaving group as a possible cause of the low fragmentation rate found with **II**

Chapter 3

76

If the RAFT agent has a poor leaving-group, a growing radical has to add more

often to a RAFT agent before an effective chain transfer event takes place because in

most cases the formed intermediate will fall back into its originating species.

In that

case the addition rate to an initial RAFT agent will be higher than expected from Eqs.

3.2 and 3.3, and is given by Eqs. 3.1 and 3.3.

As an example the situation where the fragmentation rate of R is 10 times lower

than the fragmentation rate of a polymer chain will be considered. This would mean

that $k_{\text{tr}} = 0.1 k_{\text{-add}}$, it follows from Eqs. 3.1 and 3.3 that $k_{\text{add}} \approx 9 k_{\text{tr}} \approx 3.6 \cdot 10^5$

$\text{dm}^3 \text{ mol}^{-1} \text{ s}^{-1}$ (see Scheme 3.6). Since both **I** and **II** have the same transfer constant and the

addition rate is mainly determined by Z, which is the same for both RAFT agents, this

explanation seems highly unlikely.

Scheme 3.6 Addition-fragmentation equilibrium of a growing poly(butyl acrylate) radical and a RAFT agent.

Using these values and assuming no intermediate-intermediate termination, it is

found that the conversion-time data is fitted best if $k_{-add} \approx 5.2 \cdot 10^2 \text{ s}^{-1}$ (and thus $k^{\circ} \approx$

$5.2 \cdot 10^1 \text{ s}^{-1}$). In the case that also intermediate-intermediate termination plays a role,

the data is fitted best using $k_{-add} \approx 2.5 \cdot 10^3 \text{ s}^{-1}$.

PBA + S S

Z

R PBA

S S

Z

R PBA

S

Z

S + R k_{add}

k_{-add}

k°

Homogeneous RAFT polymerizations

77

At first sight slow fragmentation of R can partly explain the low fragmentation rates that were found in Table 3.6 using the simple model (Scheme 3.5) in which it is assumed that $k_{-add} = k^{\circ}$. Since we assume here that $k_{-add} \gg k^{\circ}$, this also means that as soon as all initial RAFT agent is consumed, the transfer constant of dormant poly(butyl acrylate) chains is much higher than the transfer constant of the initial RAFT agent. This would mean that if dormant poly(butyl acrylate) chains are used as RAFT agents from the beginning, a linear increase in M_n with conversion and low polydispersities should be observed. Therefore, a solution polymerization of butyl acrylate was performed in which poly(butyl acrylate) dormant chains with an M_n of $7 \cdot 10^3 \text{ g/mol}$ and a polydispersity of 1.64 were used in a 4 to 1 weight ratio. This experiment resulted in a final polydispersity of 1.88, indicating that the transfer constant was not very high and in the order of 1-2, similar to the transfer constant of I and II. This again indicates that slow fragmentation of R cannot be the reason for the low fragmentation rates that were found.

b. Slow re-initiation as a possible cause of retardation.

Another aspect that might lead to an underestimation of the fragmentation rate in the simple model shown in Scheme 3.5 is that the RAFT leaving group has a low propagation rate as compared with a polymeric radical. The propagation rate of the leaving group of **II** can be estimated from the k_p of styrene[35] (see Scheme 4.3) and the styrene-butyl acrylate reactivity ratios[48]. This leads to a propagation rate constant of styrene to butyl acrylate of $411 \text{ dm}^3 \text{ mol}^{-1} \text{ s}^{-1}$ at $60 \text{ }^\circ\text{C}$. Assuming that k_{p1}

$\square 4k_p$ this leads to a propagation rate of $1.64 \cdot 10^3 \text{ dm}^3 \text{ mol}^{-1} \text{ s}^{-1}$ for the leaving group of **II**. However, if this value is used for k_{p1} , hardly any retardation is observed in the simulations in which $\langle k_t \rangle = 4 \cdot 10^8 \text{ dm}^3 \text{ mol}^{-1} \text{ s}^{-1}$, $k_p = 2.29 \cdot 10^4 \text{ dm}^3 \text{ mol}^{-1} \text{ s}^{-1}$, $k_{\text{add}} = 7.92 \cdot 10^4 \text{ dm}^3 \text{ mol}^{-1} \text{ s}^{-1}$, and $k_{\text{-add}} = 1 \cdot 10^5 \text{ s}^{-1}$. This is shown in Figure 3.14. The dashed lines almost fit the conversion-time data of the system without RAFT.

In order to be able to fit the data, a k_{p1} of about $80 \text{ dm}^3 \text{ mol}^{-1} \text{ s}^{-1}$ was used to provide agreement between simulation and experiment, as shown in Figure 3.14.

However, it can be seen that the solid lines tend to underestimate the low conversion data and overestimate the data at high conversions. No other value for k_{p1} is able to fit all the data and thus $80 \text{ dm}^3 \text{ mol}^{-1} \text{ s}^{-1}$ is probably a good estimate for k_{p1} . This strongly suggests that slow re-initiation is the cause of the retardation found in this system, although other effects concerning the not yet fully understood complex acrylate kinetics[50] also might play a role.

Figure 3.14 Conversion-time data and simulations of 2 M solution polymerizations of nBA

Chapter 3

76

with 0% **II** (closed squares), 1% **II** (open circles) and 2% **II** (open triangles), in which slow re-initiation is assumed to be the cause of retardation. The dashed lines represent the simulations with $k_{p1} = 1.64 \cdot 10^3 \text{ dm}^3 \text{ mol}^{-1} \text{ s}^{-1}$, whereas the solid lines represent the simulations with $k_{p1} = 80 \text{ dm}^3 \text{ mol}^{-1} \text{ s}^{-1}$.

Molecular weights

In order to simulate molecular weights of nBA RAFT polymerizations, the whole kinetic scheme should be taken into account, including the intermediate radical and intermediate radical termination, which brings along computational problems[23].

However, in polymerizations with **I** the influence of the intermediate radical and termination of this radical can safely be neglected. The following approach was used.

Scheme 3.3 was loaded into PREDICI, extended with transfer to solvent. The $\langle k_t \rangle$ was varied until the PREDICI simulation fitted the conversion time data. A $\langle k_t \rangle$ of $8 \cdot 10^8 \text{ dm}^3 \text{ mol}^{-1} \text{ s}^{-1}$ fitted the data. This is twice as large as in the

Matlab simulations in the previous sections, because in PREDICI another notation for termination is used.

In Figure 3.15 the results of a 2 M solution polymerization of nBA with I in toluene at 60 °C are shown and compared with the results of a PREDICI simulation.

0 50 100 150 200 250 300
 0
 10
 20
 30
 40
 2%
 1%
 1%
 conversion [%]
 time [min]

Figure 3.15 Simulation of M_n and polydispersity of a 2 M solution polymerization of n-butyl acrylate with 0.012 M I and 0.0025 M AIBN at 60 °C. Parameters used: $\langle k_t \rangle = 8 \cdot 10^8 \text{ dm}^3 \text{ mol}^{-1} \text{ s}^{-1}$ (both $k_{tc} = \langle k_t \rangle$ and $k_{td} = \langle k_t \rangle$ are shown), $k_p = 2.29 \cdot 10^4 \text{ dm}^3 \text{ mol}^{-1} \text{ s}^{-1}$, $C_T = 1.73$, $k_d = 9.5 \cdot 10^{-6} \text{ s}^{-1}$, $f = 0.6$, $k_{trM} = 1.5 \text{ dm}^3 \text{ mol}^{-1} \text{ s}^{-1}$ [46] and $k_{trS} =$ transfer to toluene rate coefficient = $2.1 \text{ dm}^3 \text{ mol}^{-1} \text{ s}^{-1}$ [33, value of ethyl acrylate]. The closed squares are the experimental M_n 's, the open circles are the experimental polydispersities and the lines are the PREDICI simulations, performed both for complete termination by combination and for complete termination by disproportionation.

Figure 3.15 shows that the agreement for the number average molecular weight is good, whereas the experimental polydispersities are in general somewhat lower than predicted by the simulations, but within experimental error. The transfer constant determined by low conversion experiments in bulk thus seems to be valid in a solution polymerization over the whole conversion range, indicating that the transfer constant of a dormant polymeric RAFT agent is similar to the transfer constant of the initial RAFT agent.

Homogeneous RAFT polymerizations

79

3.5 Conclusions

The transfer constants of O-ethylxanthyl ethyl propionate with styrene and with n-butyl acrylate have been determined. It has been shown that differences in the average termination rate as a consequence of differences in molecular weights with

0 20 40 60 80 100
 0
 5000
 10000
 15000
 20000
 25000
 M_n [g/mol]
 conversion [%]
 1.0
 1.5
 2.0
 2.5
 3.0
 3.5

varying the RAFT concentration did not introduce errors in the transfer constant determination.

Using the transfer constants that have been determined from low conversion experiments, it was possible to predict molecular weights versus conversion in high conversion experiments at various conditions. In the experiments with styrene no retardation was observed both with O-ethylxanthyl ethyl propionate and with Oethylxanthyl ethyl benzene. The n-butyl acrylate polymerization showed considerable retardation with increasing amounts of O-ethylxanthyl ethyl benzene, whereas no retardation was observed with O-ethylxanthyl ethyl propionate. This retardation was most likely not the result of intermediate radical termination, but a result of slow reinitiation of the ethylbenzene radical.

3.6 Experimental

3.6.1 Materials

Styrene (STY) and n-butyl acrylate (nBA) were purchased from Aldrich and purified of inhibitor by passing through an inhibitor-removal column (Aldrich). All other materials were from Aldrich (unless otherwise stated) and used as received.

3.6.2 Synthesis of RAFT agents

The following RAFT agents were synthesized according to the literature procedure[5].

Scheme 3.7 O-ethylxanthyl ethyl propionate (I) and O-ethylxanthyl ethyl benzene (II).

C
S
C₂H₅O S
C
CH₃
C
O
OC₂H₅ C
S
C₂H₅O S
C
CH₃

(I) (II)

O-ethylxanthyl ethyl propionate (I)

I was synthesized by adding 101.4 g of potassium O-ethyldithiocarbonate (Merck) to a mixture of 102 g ethyl 2-bromopropionate (Merck) dissolved in 1 L of ethanol at 0 °C under a nitrogen atmosphere. The mixture was stirred for 4 hours at 0 °C in the absence of light. 1 L of water was added, and the product was extracted by a 1:2 mixture of diethyl ether and pentane. The solvent was removed and the remaining ethyl 2-bromopropionate distilled off under vacuum. I was obtained at >99% purity according to ¹H NMR.

O-ethylxanthyl ethyl benzene (II)

II was synthesized by adding 104 g of potassium O-ethyldithiocarbonate (Merck) to a mixture of ethanol (1 L) and 80 mL of 1-bromoethyl benzene at 0 °C under a nitrogen atmosphere. The same procedure was carried out as for I, and the product was >98% purity according to ¹H NMR.

3.6.3 Homogeneous polymerizations

Appropriate amounts of monomer, initiator (AIBN), RAFT agent and solvent were mixed in a round-bottom flask equipped with a magnetic stirrer and reflux condenser, all under an argon atmosphere. Oxygen was removed from the mixture by bubbling through nitrogen. After that the flask was submerged in an oil bath which was at reaction temperature. Conversion was determined gravimetrically. For the transfer constant determination conversion was kept below 3% in most cases.

Chapter 3

81

3.6.4 GPC

The dried polymer was dissolved in tetrahydrofuran (THF, Biosolve) to a concentration of 1 mg/mL. The solution was filtered over a 0.2 mm PTFE syringe-filter. Analyses were carried out using two PLGel (Mixed-C) columns (Polymer Laboratories) at 40 °C.

A Waters 486 UV-detector, operated at 254 nm, and a Waters 410 refractive index detector were used for detection. THF was used as eluent at a flow-rate of 1 ml/min.

Narrow-distribution polystyrene standards (Polymer Laboratories) with molecular weights ranging from 580 to 7.1·10⁶ g/mol were used to calibrate the GPC set-up.

The molecular weights of the BA polymers were corrected with Mark-Houwink

parameters given in literature[44]: $a=0.716$ and $K=11.4 \cdot 10^{-5} \text{ dL} \cdot \text{g}^{-1}$ for polystyrene and $a=0.700$ and $K=12.2 \cdot 10^{-5} \text{ dL} \cdot \text{g}^{-1}$ for poly(n-butyl acrylate).

3.7 References

- [1] Wang, J. S.; Matyjaszewski, K. **"Living"/Controlled Radical Polymerization. Transition-Metal-Catalyzed Atom Transfer Radical Polymerization in the Presence of a Conventional Radical Initiator.** *Macromolecules* (1995) 28(22), 7572
- [2] Georges, M. K.; Moffat, K. A.; Veregin, R. P. N.; Kazmaier, P. M.; Hamer, G. K. **Narrow molecular weight resins by a free radical polymerization process; the effect of nitroxides and organic acids on the polymerization.** *Polym. Mater. Sci. Eng.* (1993) 69, 305
- [3] Le, T. P.; Moad, G.; Rizzardo, E.; Thang, S. H. **Polymerization with living characteristics with controlled dispersity, polymers prepared thereby, and chain-transfer agents used in the same.** *PCT Int. Appl.* (1998), WO 9801478
- [4] Rizzardo, E.; Thang, S. H.; Moad, G. **Synthesis of dithioester chain-transfer agents and use of bis(thioacyl) disulfides or dithioesters as chain-transfer agents in radical polymerization.** *PCT Int. Appl.* (1999), WO 9905099
- [5] Corpart, P.; Charmot, D.; Biadatti, T.; Zard, S.; Michelet, D. **Block polymer synthesis by controlled radical polymerization.** *PCT Int. Appl.* (1998), WO 9858974
- [6] Chiefari, J.; Chong, Y. K.; Ercole, F.; Krstina, J.; Jeffery, J.; Le, T. P. T.; Mayadunne, R. T. A.; Meijs, G. F.; Moad, C. L.; Moad, G.; Rizzardo, E.; Thang, S. H. **Living Free-Radical Polymerization by Reversible Addition-Fragmentation Chain Transfer: The RAFT Process.** *Macromolecules* (1998), 31(16), 5559
- [7] Krstina, J.; Moad, G.; Rizzardo, E.; Winzor, C. L.; Berge, C. T.; Fryd, M. **Narrow Polydispersity Block Copolymers by Free-Radical Polymerization in the Presence of Macromonomers.** *Macromolecules* (1995), 28(15), 5381
- [8] Hawthorne, D. G.; Moad, G.; Rizzardo, E.; Thang, S. H. **Living Radical Polymerization with Reversible Addition-Fragmentation Chain Transfer (RAFT): Direct ESR Observation of Intermediate Radicals.** *Macromolecules* (1999), 32(16), 5457
- [9] Chong, Y. K.; Le, T. P. T.; Moad, G.; Rizzardo, E.; Thang, S. H. **A More Versatile Route to Block Copolymers and Other Polymers of Complex Architecture by Living Radical Polymerization: The RAFT Process.** *Macromolecules* (1999), 32(6), 2071
- [10] De Brouwer, H.; Schellekens, M. A. J.; Klumperman, B.; Monteiro, M. J.; German, A. L. **Controlled radical copolymerization of styrene and maleic anhydride and the synthesis of novel polyolefin-based block copolymers by reversible addition-fragmentation chain-transfer (RAFT) polymerization.** *J. Polym. Sci., Part A: Polym. Chem.* (2000), 38(19), 3596

Chapter 3

82

- [11] Monteiro, M. J.; Sjoberg, M.; Van der Vlist, J.; Gottgens, C. M. **Synthesis of butyl acrylate-styrene block copolymers in emulsion by reversible addition-fragmentation chain transfer: effect of surfactant migration upon film formation.** *J. Polym. Sci., Part A: Polym. Chem.* (2000), 38(23), 4206
- [12] Matyjaszewski, K.; Gaynor, S.; Wang, J.S. **Controlled Radical Polymerizations: The Use of Alkyl Iodides in Degenerative Transfer.** *Macromolecules* (1995), 28(6), 2093
- [13] Chiefair, J.; Mayadunne, R. T.; Moad, G.; Rizzardo, E.; Thang, S.H. **Polymerization with living characteristics with controlled dispersity using chain transfer agents.** *PCT Int. Appl.* (1999), WO 9931144
- [14] Mueller, A. H. E.; Zhuang, R.; Yan, D.; Litvinenko, G. **Kinetic Analysis of "Living" Polymerization Processes Exhibiting Slow Equilibria. 1. Degenerative Transfer (Direct Activity Exchange between Active and "Dormant" Species). Application to Group Transfer Polymerization.** *Macromolecules* (1995), 28(12), 4326

- [15] Mueller, A. H. E.; Yan, D.; Litvinenko, G.; Zhuang, R.; Dong, H. **Kinetic Analysis of "Living" Polymerization Processes Exhibiting Slow Equilibria. 2. Molecular Weight Distribution for Degenerative Transfer (Direct Activity Exchange between Active and "Dormant" Species) at Constant Monomer Concentration.** *Macromolecules* (1995), 28(22), 7335
- [16] Moad, C. L.; Moad, G.; Rizzardo, E.; Thang, S. H. **Chain Transfer Activity of Γ -Unsaturated Methyl Methacrylate Oligomers.** *Macromolecules* (1996), 29(24), 7717
- [17] Krstina, J.; Moad, C. L.; Moad, G.; Rizzardo, E.; Berge, C. T.; Fryd, M. **A new form of controlled growth free radical polymerization.** *Macromol. Symp.* (1996), 111, 13
- [18] Goto, A.; Sato, K.; Tsujii, Y.; Fukuda, T.; Moad, G.; Rizzardo, E.; Thang, S. H. **Mechanism and kinetics of RAFT-based living radical polymerizations of styrene and methyl methacrylate.** *Macromolecules* (2001), 34(3), 402
- [19] Monteiro, M. J.; de Barbeyrac, J. **Free-Radical Polymerization of Styrene in Emulsion Using a Reversible Addition-Fragmentation Chain Transfer Agent with a Low Transfer Constant: Effect on Rate, Particle Size, and Molecular Weight.** *Macromolecules* (2001), 34(13), 4416
- [20] Mayo, F. R. **Chain transfer in the polymerization of styrene: the reaction of solvents with free radicals.** *J. Am. Chem. Soc.* (1943), 65 2324
- [21] Whang, B. C. Y.; Ballard, M. J.; Napper, D. H.; Gilbert, R. G. **Molecular weight distributions in emulsion polymerizations: evidence for coagulative nucleation.** *Aust. J. Chem.* (1991), 44(8), 1133
- [22] Clay, P. A.; Gilbert, R. G. **Molecular Weight Distributions in Free-Radical Polymerizations. 1. Model Development and Implications for Data Interpretation.** *Macromolecules* (1995), 28(2), 552
- [23] De Brouwer, H. **RAFT memorabilia : living radical polymerization in homogeneous and heterogeneous media.** Ph. D. thesis, Technische Universiteit Eindhoven, Eindhoven, 2001
- [24] Monteiro, M. J.; De Brouwer, H. **Intermediate Radical Termination as the Mechanism for Retardation in Reversible Addition-Fragmentation Chain Transfer Polymerization.** *Macromolecules* (2001) 34(3), 349
- [25] Kwak, Y.; Goto, A.; Tsujii, Y.; Murata, Y.; Komatsu, K.; Fukuda, T. **A Kinetic Study on the Rate Retardation in Radical Polymerization of Styrene with Addition-Fragmentation Chain Transfer** *Macromolecules* (2002) 35(8), 3026
- [26] Olaj, O. F.. **Radical termination processes. I. Extent of bimolecular termination between two radical chains originating from the same radical pair.** *Makromol. Chem.* (1970), 37 245
- [27] Russell, G. T.; Gilbert, R. G.; Napper, D. H. **Chain-length-dependent termination rate processes in free-radical polymerizations. 2. Modeling methodology and application to methyl methacrylate emulsion polymerizations.** *Macromolecules* (1993), 26(14), 3538
- [28] Russell, G. T.. **On exact and approximate methods of calculating an overall termination rate coefficient from chain length dependent termination rate coefficients.** *Macromol. Theory*

Homogeneous RAFT polymerizations

83

- Simul.* (1994), 3(2), 439 [29] Russell, G. T.. **The kinetics of free radical polymerizing systems at low conversion. 1. On the rate determining step of the bimolecular termination reaction.** *Macromol. Theory Simul.* (1995), 4(3), 497
- [30] Gilbert, R. G. **Emulsion Polymerization: A Mechanistic approach;** Academic: London, (1995)
- [31] Piton, M. C.; Gilbert, R. G.; Chapman, B. E.; Kuchel, P. W. **Diffusion of oligomeric species in polymer solutions.** *Macromolecules* (1993), 26(17), 4472
- [32] Griffiths, M. C.; Strauch, J.; Monteiro, M. J.; Gilbert, R. G. **Measurement of Diffusion Coefficients of Oligomeric Penetrants in Rubbery Polymer Matrixes.** *Macromolecules* (1998), 31(22), 7835
- [33] Brandrup, J.; Immergut, E. H.; Editors. **Polymer Handbook, Fourth Edition.** (1998)
- [34] Bovey, F. A.. **Polymer N.S.R. [nuclear spin resonance] spectroscopy. III. Rates of the propagation steps in the isotactic and syndiotactic polymerization of methyl methacrylate.** *J. Polymer Sci.* (1960), 46(No. 147), 59
- [35] Buback, M.; Gilbert, R. G.; Hutchinson, R. A.; Klumperman, B.; Kuchta, F. D.; Manders, B. G.; O'Driscoll, K. F.; Russell, G. T.; Schweer, J. **Critically evaluated rate coefficients for free-radical**

- polymerization. 1. Propagation rate coefficient for styrene.** *Macromol. Chem. Phys.* (1995), 196(10), 3267
- [36] Heuts, J. P. A.; Davis, T. P.; Russell, G. T. **Comparison of the Mayo and chain length distribution procedures for the measurement of chain transfer constants.** *Macromolecules* (1999), 32(19), 6019
- [37] Moad, G.; Moad, C. L. **Use of chain length distributions in determining chain transfer constants and termination mechanisms.** *Macromolecules* (1996), 29(24), 7727
- [38] Barner-Kowollik, C.; Quinn, J. F.; Morsley, D. R.; Davis, T. P. **Modeling the reversible addition-fragmentation chain transfer process in cumyl dithiobenzoate-mediated styrene homopolymerizations: assessing rate coefficients for the addition-fragmentation equilibrium.** *J. Polym. Sci., Part A: Polym. Chem.* (2001), 39(9), 1353
- [39] Barner-Kowollik, C.; Quinn, J. F.; Nguyen, T. L. U.; Heuts, J. P. A.; Davis, T. P.. **Kinetic Investigations of Reversible Addition Fragmentation Chain Transfer Polymerizations: Cumyl Phenylthioacetate Mediated Homopolymerizations of Styrene and Methyl Methacrylate.** *Macromolecules* (2001), 34(22), 7849
- [40] Barner-Kowollik, C.; Vana, P.; Quinn, J. F.; Davis, T. P. **Long-lived intermediates in reversible addition-fragmentation chain-transfer (RAFT) polymerization generated by γ radiation.** *J. Polym. Sci., Part A: Polym. Chem.* (2002), 40(8), 1058
- [41] Wulkow, M. **The simulation of molecular weight distributions in polyreaction kinetics by discrete Galerkin methods.** *Macromol. Theory Simul.* (1996), 5(3), 393
- [42] Buback, M.; Huckestein, B.; Kuchta, F. D.; Russell, G. T.; Schmid, E. **Initiator efficiencies in 2,2'-azoisobutyronitrile-initiated free-radical polymerizations of styrene.** *Macromol. Chem. Phys.* (1994), 195(6), 2117
- [43] Kapfenstein-Doak, H.; Barner-Kowollik, C.; Davis, T. P.; Schweer, J. **A Novel Method for the Measurement of Chain Transfer to Monomer Constants in Styrene Homopolymerizations: The Pulsed Laser Rotating Reactor Assembly.** *Macromolecules* (2001), 34(9), 2822
- [44] Beuermann, S.; Paquet, D. A., Jr.; McMinn, J. H.; Hutchinson, R. A. **Determination of freeradical propagation rate coefficients of butyl, 2-ethylhexyl, and dodecyl acrylates by pulsed laser polymerization.** *Macromolecules* (1996), 29(12), 4206
- [45] Plessis, C.; Arzamendi, G.; Leiza, J. R.; Schoonbrood, H. A. S.; Charmot, D.; Asua, J. M.. **A Decrease in Effective Acrylate Propagation Rate Constants Caused by Intramolecular Chain Transfer.** *Macromolecules* (2000), 33(1), 4
- [46] Maeder, S.; Gilbert, R. G.. **Measurement of Transfer Constant for Butyl Acrylate Free-**

Chapter 3

84

- Radical Polymerization.** *Macromolecules* (1998), 31(14), 4410[47] Private communication J.M. Catala[48] Chambard, G. **Control of monomer sequence distribution. Strategic approaches based on novel insights in atom transfer radical copolymerisation.** Ph. D. thesis, Technische Universiteit Eindhoven, Eindhoven, 2000
- [49] Monteiro, M.J.; Bussels, R.; Beuermann, S.; Buback, M. **High Pressure 'Living' Free-Radical Polymerization of Styrene in the presence of RAFT** *Aust. J. Chem. Special Polymer Edition*, Accepted [50] Van Herk, A.M. **Pulsed initiation polymerization applied to acrylate monomers: Sources for the failure of the experiment.** *Macromol. Rapid comm.* (2001), 22, 687

4

Seeded emulsion RAFT polymerizations

Abstract

In this chapter the application of xanthate-based RAFT agents, which were investigated under homogeneous conditions in Chapter 3, in seeded emulsion polymerizations of styrene is described. First the kinetics of zeroone seeded emulsion polymerizations are discussed. Based on existing theories, the role of a RAFT agent on entry and exit is evaluated. Furthermore, a literature overview of the effect of conventional transfer agents and RAFT agents on emulsion polymerization kinetics is provided. Subsequently, the effect of xanthate-based RAFT agents on the polymerization rate and molecular weight distribution is investigated. It is found that the polymerization rate decreases with increasing amount of RAFT and that the molecular weight distribution is close to what theoretically is to be expected from the transfer constants determined in Chapter 3. Next the effect of the amount of RAFT agent on the exit rate coefficient is determined using τ -relaxation experiments. It is found that, as expected, the exit rate increases with increasing amounts of RAFT. The entry rate coefficients are then determined from chemically initiated experiments and a dramatic decrease in the entry rate is observed when using RAFT. Surface-activity of the RAFT agent and other explanations are put forward to explain this theoretically unexpected decrease.

4.1 Introduction

Emulsion polymerization as a method to produce polymers has a lot of advantages. Nowadays especially its environmentally friendly character due to the absence of solvents is emphasized. However, also in times that this aspect was of minor importance, polymer producers were already aware of many other advantages.

Examples of these advantages are the high polymerization rate, which allows higher production rates, low viscosity at high solid contents, which makes the process as well as the product easy to handle, high conversions and

molecular weights can be reached and the polymerization heat can be exchanged easily. Moreover, control of the particle morphology like e.g. core-shell structures is possible.

The recent advent of 'living' radical polymerization has allowed the preparation of complex polymer architectures (e.g. block, hyper-branched, star) via free-radical polymerization. One such technique is the reversible addition-fragmentation chain transfer (RAFT) polymerization, in which

dithioester or xanthate compounds are used as the controlling agent. If RAFT
Seeded emulsion RAFT polymerizations

93

is applied in emulsion the advantages of emulsion polymerization can be combined with the extensive possibilities of living polymerizations. In the previous chapter the mechanism and kinetics of these agents in solution or bulk polymerization were discussed. This chapter will deal with the kinetics in emulsion polymerization. The optimal way to study the kinetics of emulsion polymerization is by seeded emulsion polymerization systems, whereby the presence of a pre-formed latex enables one to obviate the complexities of particle formation.

4.2 Seeded emulsion polymerization for mechanistic studies

Understanding and hence process optimization requires improved mechanistic understanding of the events peculiar in emulsion polymerization, such as the phasetransfer events of radical entry into, and exit (desorption) from, latex particles. The optimal way to obtain such information is by examination of the rates in a seeded emulsion polymerization system, whereby the presence of a pre-formed latex enables one to overcome the complexities of particle formation. Particle nucleation is poorly understood, especially from a quantitative point of view, and by performing seeded experiments, Interval I (see Chapter 1) is skipped because the loci of polymerization are already present from the start of the polymerization. Moreover, by skipping Interval I, the number of kinetic processes taking place is reduced, which simplifies the analysis of the data obtained. After illuminating the mechanism of particle growth by seeded experiments, *ab initio* experiments can be performed to study particle nucleation and its implications.

The aim of this work is to study the effect of xanthates on the entry and exit rate coefficients for styrene using a poly(methyl methacrylate) (PMMA) seeded system. A PMMA seed was used since PMMA is transparent to UV at 254 nm, and hence by using appropriate detectors in size exclusion chromatography the MWD of the newly formed polystyrene can be readily obtained. Growing a monomer in a seed containing a different polymer has been denoted "heteroseeded emulsion polymerization" in which one grows a seed of appropriate size and monodispersity using a convenient monomer such as MMA, where the second-stage monomer (in this case styrene) will swell the seed polymer (PMMA). Seeded studies are then carried out in the normal way. It is assumed that phase separation between the seed polymer and the new polymer is negligible due to the small size of the seed and the presence of excess monomer, which is soluble in both polymers. Moreover, one has to be sure that no secondary nucleation and coagulation take place, because a constant particle number is required.

4.3 Zero-one seeded emulsion polymerization kinetics

4.3.1 The rate of polymerization

Seeded emulsion polymerizations are carried out in order to avoid the complex nucleation period (Interval I). The polymerization, therefore, starts in Interval II where the number of particles and particle size are

predetermined. If conditions are chosen such that entry of a radical into a particle that already contains a growing polymeric radical results in *Seeded emulsion RAFT polymerizations*

89

instantaneous termination, the system is considered to be under zero-one conditions. Normally this means that the particle size has to be sufficiently small. Thus all particles will contain either zero radicals or only one, and termination is not rate determining. The following rate equation can be used for Interval II and Interval III seeded emulsion polymerization assuming a constant number of particles:

$$\frac{dx}{dt} = \frac{A}{N} \left(\frac{C_p}{C_m} - 1 \right) \quad (4.1)$$

where C_p is the concentration of monomer in the particles, n_{M0} is the initial number of moles of monomer, N_c the particle concentration, N_A is the Avogadro constant and A the so called conversion factor. The average number of radicals per particle, n , can thus be obtained from the polymerization rate. Because all quantities of Eq. 4.1 are fixed in a seeded emulsion polymerization during Interval II, the time variation of n is the appropriate quantity to deduce kinetic information. The most simple system that can be considered is a zero-one system, in which only entry and exit occur and the fate of exited radicals is ignored. The population balance equation for the particles containing 1 radical is as follows:

$$\frac{dN_1}{dt} = k_1 N_0 - k_2 N_1 \quad (4.2)$$

where N_0 and N_1 are the number of particles containing 0 and 1 radicals respectively, k_1 is the entry rate coefficient and gives the number of entry events per second into a particle and k_2 is the exit rate coefficient which gives the number of exit events per second. N_0 and N_1 can be normalized so that $N_0 + N_1 = 1$. Since n is the average number of radicals per particle, $N_1/(N_0+N_1)$, Eq. 4.2 can be rewritten as:

$$\frac{dn}{dt} = k_1 - 2kn \quad (4.3)$$

The evolution of n versus time, obtained by measuring the conversion versus time and using Eq. 4.1 can then be fitted to the integrated form of Eq. 4.3 and this will yield the entry and exit rate coefficients. However, this method is very sensitive to small errors both in the assumed values in the conversion

factor A and the measured conversion [1]. Moreover, the curvature in the early conversion-time data, which contains information about γ and k , is observed only in a few experimental points, which, in addition, cannot be measured very accurately. Therefore, the slope-and-intercept method has been

Chapter 4

90

developed [1], which relates the steady-state slope and the intercept of this steady-state slope at $t=0$ to values for γ and k . The advantage of this method is that the intercept incorporates all the information in the approach to steady state and is less sensitive to errors in the early conversion-time data. However, this method still requires that the conversion-time data at low conversion is accurate and that the number of data-points is sufficient to find the starting time of the polymerization. Conversion-time data obtained by gravimetry can normally not be used for the purpose of determining entry and exit rates. In the first place is the data not accurate, especially at low conversions. This inaccuracy is both a result of sampling and of the method of gravimetry itself. The sample that is taken has to be an exact representation of the reactor contents. Due to for instance monomer pooling or insufficient stirring this cannot always be guaranteed. Gravimetry itself is inaccurate at low conversions, because the amount of polymer formed is low, and small errors in weighing induce large errors in conversion. Moreover, one has to know exactly which compounds evaporate and which do not. A transfer agent for instance will evaporate, but will not evaporate if it has reacted. Also hydroquinone, which is normally added to the sample as inhibitor, can evaporate and lead to errors in the determined conversion. Besides that gravimetry is not accurate at low conversion there is also a second reason why this method is not appropriate and that is that normally not sufficient samples can be taken to determine the starting time, and thus the intercept. The injection time of the initiator is normally not equal to the starting time, because of inhibition. Therefore, other techniques should be applied, which allow more data-points and better accuracy. Examples of appropriate techniques include densitometry, Raman spectroscopy [2,3] and dilatometry [1]. However, even if a method is free of errors, it is still not guaranteed that it will result in the right entry and exit rate coefficients due to inhibitor artifacts. If not all inhibitor is consumed before any polymerization takes place, the approach to steady state will be different from that in a completely inhibitor-free system. Since in a chemically initiated system there is only one approach to steady state such systems cannot be used to determine the entry and exit rate coefficients. A way to overcome this problem is by combining the exit rate coefficients obtained from \odot -radiolysis relaxation data with the steady-state rate of chemically initiated systems [4,5,6]. From Eq. 4.3 one can derive that at steady state:

ss
ss

n₂ 1
 n_k
 –
 =) (4.4)

Chapter 4
 90

where n_{ss} is the steady-state value of n . As aforementioned, the exit rate coefficient is in this case obtained from \odot -radiolysis relaxation data. When \odot -radiolysis is used as initiation source, the initiation source can be switched on and off, and, after the first steady state, the following approaches to steady state will be free of inhibitor artifacts.

When the source is switched off at steady state, the system relaxes to a new steady state. Using the slope-and-intercept method or NLLS fitting, the exit rate coefficient and the spontaneous entry rate coefficient can be found for a certain system. This exit rate coefficient can then be used to find the entry rate coefficient for the same system, in which a chemical initiator is used.

4.3.2 Model for entry

The model proposed by Morrison *et al.*[7] is now widely accepted as the mechanism for describing the events that lead to entry, at least for systems with ionic stabilizer, or smaller amounts of polymeric or electrosteric stabilizer[8] and persulfate initiators. A growing oligomeric radical, initiated with a $SO_4\cdot$ radical, will enter a particle only if it reaches a critical degree of oligomerization, z . This z -mer is assumed to have no other fate except entry, and therefore, the entry rate is equal to the rate of formation of these z -mers. However, for a radical to reach a z -mer it must survive termination with other aqueous phase radicals. In the presence of a RAFT agent in the aqueous phase, an additional reaction step must be taken into account, namely the reaction of an aqueous phase radical with an aqueous phase RAFT agent. The leaving group R of the RAFT agent will also enter a particle, assuming it is not extremely water-soluble. If this occurs at a significant rate, this will lead to an increased rate of entry, and therefore the equations usually used to calculate the entry coefficients become more complex, as previously shown by Maxwell *et al.*[9], who took into account the effect of added chain transfer agents. The following reaction scheme can thus be proposed for the aqueous phase kinetics leading to entry:

Scheme 4.1 Aqueous phase kinetic scheme in the presence of a RAFT agent. $I-I$ (or I in Eq. 4.5) represents an initiator, $I\cdot$ represents an initiator derived radical, M a monomer, $IM_i\cdot$ an i -mer, $T\cdot$ any aqueous phase radical, $X-R$ a RAFT agent and $R\cdot$ a RAFT-derived radical. Reaction 2 in Scheme 4.1 is very fast compared with subsequent steps[ref. 20 in [7]], and also predominates reactions 3 and 4 because of the much higher monomer than radical and RAFT concentration. From Scheme 4.1, the following steady-state concentrations are derived:
 radical and RAFT concentration. From Scheme 4.1, the following steady-state concentrations are derived:

aq_{aq} , tr_{aq} , t_{aq}

$$[T]_{aq} = \frac{k_d [I]_{aq}}{k_t [M]_{aq} + k_{tr, aq} [M]_{aq}}$$
 Chapter 4
92
 = • (4.5)

$$[T]_{aq} = \frac{k_d [I]_{aq}}{k_t [M]_{aq} + k_{tr, aq} [M]_{aq}}$$
 Chapter 4
92
 = • (4.5)

in which $[M]_{aq}$ and $[RAFT]_{aq}$ are the aqueous phase concentrations of the monomer and the RAFT agent, respectively. The total aqueous phase radical concentration, $[T\cdot]$, is given by:

$$[T]_{aq} = \frac{k_d [I]_{aq}}{k_t [M]_{aq} + k_{tr, aq} [M]_{aq}}$$
 (4.7)

$I \rightarrow 2 I\cdot$ (1) initiator decomposition
 $I\cdot + M \rightarrow IM_1\cdot$ (2) initial propagation
 $I\cdot + T \rightarrow \text{inert product}$ (3) termination
 $I\cdot + X-R \rightarrow I-X + R\cdot$ (4) initial transfer to RAFT
 $IM_i\cdot + M \rightarrow IM_{i+1}\cdot$ (5) propagation
 $IM_i\cdot + T \rightarrow \text{inert product}$ (6) termination
 $IM_i\cdot + X-R \rightarrow IM_iX + R\cdot$ (7) transfer to RAFT
 $IM_z + \text{particle entry}$ (8) entry of initiator derived radical
 $R + \text{particle entry}$ (9) entry of transfer derived radical

k_d
 k_{pi}
 $k_{t, aq}$
 k_{tri}
 k_i
 $k_{p, aq}$
 $k_{t, aq}$
 k_i
 $k_{tr, aq}$
 k_{it}

The entry rate coefficients are found from the rate of formation of z-mers (\dot{M}_z) and the rate of formation of $R\cdot$ (\dot{M}_0):

$$\dot{M}_z = k_{t, z} M_z^2$$

N

N

$k_{t, z}$

$k_{t, z}$

$k_{t, z}$

c

A

Seeded emulsion RAFT polymerizations

93

$$\dot{M}_0 = k_{d, i} I$$

$$(4.8)$$

•-

=

$$= \dot{M}_z$$

$k_{t, z}$

$k_{t, z}$

$k_{t, z}$

c

A

$$\dot{M}_0 = k_{d, i} I + k_{t, z} M_z^2$$

N

N

$$(4.9)$$

and the total entry rate coefficient, \dot{M}_0 , is thus given by:

$$\dot{M}_0 = k_{d, i} I + k_{t, z} M_z^2 \quad (4.10)$$

Eqs. 4.5 to 4.10 can be solved numerically. The initiator efficiency f is given by

dividing \dot{M}_0 by the 100% efficiency entry rate coefficient:

$k_{d, i}$

$k_{d, i}$

$$f = \frac{\dot{M}_0}{k_{d, i} I}$$

N

N

$$f =$$

$$(4.11)$$

Now the influence of a RAFT agent on the aqueous phase kinetics and thus the entry rate and initiator efficiency can be considered.

Parameters for the calculation of the entry rate and the effect of a RAFT agent

In order to calculate whether or not the addition of a RAFT agent will have an effect on the entry rate, the initiator efficiency will be calculated as a function of $k_{tr, aq}$ and will be compared with a system without RAFT agent. The system considered is a seeded emulsion polymerization of styrene at 50 °C under the conditions as given in the experimental part later in this chapter. The parameters used are shown in Table 4.1 and some will be discussed in more detail.

Table 4.1 Parameters used to calculate the initiator efficiency of a seeded styrene emulsion polymerization at 50 °C. parameter value reference polymerization at 50 °C.

parameter value reference k_d $1 \cdot 10^{-6} \text{ s}^{-1}$ [10]
 [I] $0.0012 \text{ mol dm}^{-3}$ experimental condition z 3 [7] $k_{1,p, \text{aq}}$ $1000 \text{ dm}^3 \text{ mol}^{-1} \text{ s}^{-1}$
 [1,11] $k_{2,p, \text{aq}}$ $500 \text{ dm}^3 \text{ mol}^{-1} \text{ s}^{-1}$ [1] $[M]_{\text{aq}}$ $0.0043 \text{ mol dm}^{-3}$ [12]
 $k_{t, \text{aq}}$ $1.1 \cdot 10^9 \text{ dm}^3 \text{ mol}^{-1} \text{ s}^{-1}$ see below
 $k_{tr, \text{aq}}$ variable
 $[RAFT]_{\text{aq}}$ variable see below
 N_A $6.02 \cdot 10^{23} \text{ mol}^{-1}$
 N_c $1 \cdot 10^{17} \text{ dm}^{-3}$ experimental condition $k_{t, \text{aq}}$
 Chapter 4

94

The aqueous phase termination rate coefficient is estimated using:

$$k_{t, \text{aq}} = \sum_{j,i} k_{t, \text{aq}}^{j,i} = (4.12)$$

This equation has already been discussed in Chapter 3 (Eq. 3.15). Since $z=3$, only 2 types of aqueous phase radicals are present: $-\text{SO}_4-(\text{STY})_1 \cdot$ and $-\text{SO}_4-(\text{STY})_2 \cdot$, which correspond to sulfates ions with a C_8 and a C_{16} chain attached to it, respectively. So on average the diffusion coefficient will be close to the diffusion coefficient of a sulfate ion with a C_{12} chain, a very common surfactant (sodium dodecyl sulfate). The ionic diffusion coefficient of $-\text{SO}_4-C_{12}$ at $25 \text{ }^\circ\text{C}$ is $0.61 \cdot 10^{-7} \text{ dm}^2 \text{ s}^{-1}$ [13]. Using an activation energy of diffusion of 14.7 kJ mol^{-1} [14] this means that at $50 \text{ }^\circ\text{C}$ the average diffusion coefficient will be $0.95 \cdot 10^{-7} \text{ dm}^2 \text{ s}^{-1}$. This results in $k_{t, \text{aq}} = 1.1 \cdot 10^9 \text{ dm}^3 \text{ mol}^{-1} \text{ s}^{-1}$. The other parameters used for this calculation can be found in Table 3.1.

[RAFT]_{aq}

It is assumed that $[RAFT]_{\text{aq}}$, the aqueous phase RAFT concentration, can be calculated according to the following relationship [15]:

$$[RAFT]_{\text{aq}} = f \cdot [RAFT]_{\text{aq, sat}} \quad (4.13)$$

where f_{RAFTd} is the fraction of RAFT agent in the monomer droplets and $[RAFT]_{\text{aq, sat}}$ is the RAFT water saturation concentration. This assumes that the polymer in the particles has no influence on the free energy of the low molecular weight components, *i.e.* the RAFT agent and monomer, because only combinatorial entropy of mixing is important. The work of Maxwell *et al.* [16] showed that this assumption is valid for two low molecular weight species (two monomers being the usual case, but also applicable to monomer plus RAFT).

Here 2 RAFT agents with a different water-solubility will be evaluated. RAFT agent I is shown in Scheme 4.2 and has a water-solubility of $0.002 \text{ mol dm}^{-3}$. This value has been determined experimentally from UVVIS experiments. The molefraction of RAFT is varied between 0.0025 and 0.01, the same fractions will be used in the seeded emulsion polymerization described later in this chapter. Furthermore, an imaginary RAFT agent with a high water-solubility is considered.

The effect of RAFT on the initiator efficiency

Now a model for entry has been proposed and the parameters in this model have been evaluated, the effect of RAFT on the entry mechanism can be considered.

The results are shown in Figure 4.1.

Figure 4.1 The effect of RAFT on the initiator efficiency. The initiator efficiency is calculated using Eq. 4.11, in which η_{tot} is calculated numerically from Eqs. 4.5 to 4.10. Curves a to c represent the initiator efficiency versus C_T for a RAFT agent with a water-solubility of 0.002 M and a f_{RAFTd} of 0.01, 0.005 and 0.0025, respectively. Curve d represents

Seeded emulsion RAFT polymerizations

95

a RAFT agent with a watersolubility of 0.1 M and $f_{RAFTd} = 0.01$. Curve e is the initiator efficiency without RAFT.

0.1 1 10 100 1000 10000 100000
 0.4
 0.5
 0.6
 0.7
 0.8
 0.9
 1.0
 e
 d
 c b a
 initiator efficiency [-] C_T

Figure 4.1 shows that a RAFT agent with a water-solubility of 0.002 M will start to have an effect on initiator efficiency if $C_T > 10$. However, the RAFT agents used in this work have a C_T of about 0.7 with styrene (see Chapter 3). Therefore, it is expected that the initiator efficiency and thus the entry rate coefficients are not affected by the RAFT agents used in this work. What this figure also shows is that RAFT agents with a high water-solubility start to have an effect at very low transfer constants and that reactive RAFT agents will always have an effect, unless they have a very low water-solubility. In fact, an increased initiator-efficiency means that growing aqueous phase radicals react with RAFT in the aqueous phase before they reach a length z . So in this work, since it is expected that the initiator-efficiency is unaffected by the RAFT agent, the reaction of growing radicals with RAFT taking place in the aqueous phase is negligible. Thus, for the present system one can use the conventional rate equations used to describe n , and consequently evaluate the entry and exit rate coefficients for styrene emulsion polymerization in the presence of the RAFT agents by combination of chemical and gamma relaxation experiments.

In the calculations used to construct Figure 4.1 it is assumed that the leaving group of the RAFT agent enters a particle. However, it is imaginable that this leaving group is very water-soluble and has a very low propagation rate coefficient. In that case the initiator efficiency will decrease instead of increase because the only fate of such radical is to terminate in the aqueous phase. Nevertheless, this is not expected to be the case in the systems in this work, since the leaving groups of the RAFT agents do propagate readily. Moreover, it is expected that the RAFT agents used do not react in the aqueous phase as a result of their low reactivity and low aqueous phase concentration and, therefore, will not have an effect on entry, whatever properties the leaving group of the RAFT agent does have.

4.3.3 Model for exit

A monomeric radical inside a particle is formed by transfer to monomer or by an addition-fragmentation reaction with the RAFT agent. The rate coefficient for desorption, k_{dM} , of these radical species is given by [17,18]:

$$k_{dM} = \frac{D_w}{r_s^2} \left(\frac{q}{k_{dM} + k_p \frac{1}{C_p}} \right) \quad (4.14)$$

Chapter 4

96

in which q is the partitioning coefficient of the desorbing species, which is equal to C_p/C_w , the particle concentration of this species over the aqueous phase concentration, D_w the diffusion coefficient of this species in water, and r_s the swollen radius of the particle. Hence the probability that a monomeric radical will exit is $k_{dM}/(k_{dM} + k_p \frac{1}{C_p})$. This indicates that by increasing the radius, the probability of exit decreases. In the presence of the RAFT agent, the leaving radical, $R\cdot$, will exit if it has a favorable partitioning into the aqueous phase and/or a low reactivity to the monomer. In any case, exit invariably leads to a reduction in n and consequently a reduction in rate of polymerization. Taking into account the possible fates of exited radicals in the aqueous phase, the full set of rate equations can be derived and solved numerically. However, it is more useful to look at limits for these expressions, since these can be interpreted in terms of the dominating mechanisms and individual rate coefficients can also be obtained from these limits [1,18].

Limit 1: complete aqueous phase termination of exited radicals

In this limit the only fate of exited radicals is termination in the aqueous phase with either another exited radical or with an initiator-derived radical. In this case the overall kinetics are given by:

$$\frac{dn}{dt} = -k_{ct} n^2 - k_{ct} n \lambda_{spont} + \lambda_{initiator} \quad (4.15)$$

in which $\lambda_{initiator}$ is the entry rate parameter of initiator-derived radicals, λ_{spont} is the entry rate parameter derived from spontaneous-formed radicals and k_{ct} is the Limit 1 exit rate coefficient and is given by:

$$k_{ct} = \frac{k_{p,RAFT}}{k_{dM,RAFT}} \left(\frac{C_p}{C_w} \right) \left(\frac{k_{dM}}{k_{dM} + k_p \frac{1}{C_p}} \right) \quad (4.16)$$

$$\begin{aligned}
& C k k \\
& k \\
& C k k \\
& + \\
& + \\
& + \\
& = (4.16)
\end{aligned}$$

in which k_{dM} is the rate coefficient for desorption of a transfer to monomer derived radical and $k_{dM,RAFT}$ the rate coefficient for desorption of a transfer to

Seeded emulsion RAFT polymerizations

97

RAFT agent derived radical, k_{p1} is the rate coefficient of propagation of a transfer to monomer derived radical, $k_{p1,RAFT}$ the rate coefficient for propagation of a transfer to RAFT agent derived radical, k_{tr} is the transfer to monomer rate coefficient, $k_{tr,RAFT}$ is the transfer to RAFT rate coefficient and $C_{p,RAFT}$ is the concentration of RAFT in the particles.

Limit 2: Negligible aqueous phase termination of exited radicals

In this limit it is assumed that an exited radical re-enters another particle and never undergoes termination in the aqueous phase. A radical that re-enters can terminate if it re-enters a particle that already contains a radical and it can propagate or re-escape if it re-enters a particle that does not contain a growing radical. Limit 2 is applicable when:

$$\begin{aligned}
& \cdot] T [k \\
& N \\
& N \\
& r D N 4 \\
& N \\
& N \\
& k_{aq,t} \\
& A \\
& c \\
& s W A \\
& A \\
& c
\end{aligned}$$

$k_{re} \gg k_{t,1} = \text{Condition 1.}$

This limit can be divided in 2 sub-limits where either propagation or re-escape of a reentered radical is more likely.

Limit 2a: Complete re-entry and minimal re-escape.

In this limit a re-entered radical either terminates if the particle already contains a radical or propagates if it re-enters a particle that does not contain a growing radical. This limit is applicable if it meets, beside condition 1, also the following

condition:

$$\begin{aligned}
& p \\
& 1 \\
& k_{p,dM} C k n k \ll \text{Condition 2.}
\end{aligned}$$

In this case free-radical loss is second-order with respect to n. The overall kinetics are given by:

$\frac{dn}{dt} = -k_{tr} n^2 - k_{cr} n$ (4.17) in which the Limit 2a exit coefficient, k_{cr} , is given by:

$$k_{cr} = \frac{k_{tr} k_{p,RAFT,1}}{k_{p,RAFT,1} + k_{tr}}$$

Chapter 4

98

$$k_{cr} = \frac{k_{tr} k_{p,RAFT,1}}{k_{p,RAFT,1} + k_{tr}} \quad (4.18)$$

Limit 2b: Complete re-entry and re-escape.

In this limit it is assumed that a re-entering radical re-escapes unless it re-enters a particle that already contains a growing radical. In that case it terminates. This means that an exited radical always terminates. This limit is applicable if both condition 1 and the following condition are met:

$$k_{tr} n \gg k_{p,RAFT,1} \quad \text{Condition 3.}$$

This leads to:

$$\frac{dn}{dt} = -k_{tr} n^2 - k_{p,RAFT,1} n \quad (4.19)$$

with an exit rate coefficient:

$$k_{cr} = \frac{k_{p,RAFT,1}}{k_{tr} + k_{p,RAFT,1}} \quad (4.20)$$

If both condition 2 and condition 3 do not apply, which means that some of the reentered radicals start growing and some of them re-escape and if $k_{tr,RAFT} C_p \gg k_{tr} C_p$, the general limit 2 equation applies:

$$\frac{dn}{dt} = -k_{tr} n^2 - k_{p,RAFT,1} n \quad (4.21)$$

$$k_{cr} = \frac{k_{p,RAFT,1}}{k_{tr} + k_{p,RAFT,1}}$$

dM RAFT

p RAFT, tr spont initiator +

$$- - \rangle + \rangle = (4.21)$$

For simplicity it is assumed in Eq. 4.21 that the amount of transfer to monomer derived radicals is negligible compared with transfer to RAFT derived radicals.

It is obvious that in all limits described here, addition of a RAFT agent leads to an increase in the exit rate coefficient, as a result of an increase in intra-particle transfer to RAFT agent. When the entry rate is unaffected by the RAFT agent this will lead to a decrease in the polymerization rate, since n will decrease. However, also the opposite effect might happen. If for instance a

Seeded emulsion RAFT polymerizations

99

very reactive RAFT agent (a RAFT agent with a high C_T) is used, both the entry rate coefficient and the exit rate increase. In that case n can both increase or decrease, depending on which effect is most dominant. What also plays a role here is the time period that RAFT agents are present. A highly reactive RAFT agent will only be present in the first few percent of conversion, after which all RAFT agent will be transformed into dormant polymer chains. As a result of their water-insolubility these will not have an effect on entry, and as a result of the water-insolubility of its leaving group, these will not have an effect on exit either.

RAFT agents with a low C_T , on the other hand, will be present throughout the polymerization and therefore influence the zero-one kinetics throughout the polymerization.

4.3.4 Literature overview of effect of RAFT agents and conventional transfer agents on emulsion polymerization kinetics

Smith and Ewart[19] already took the effect of radical desorption into account in the emulsion polymerization kinetics and Romatowski *et al.*[20-22] experimentally showed that transfer to monomer derived radicals indeed escape from the particles.

Nomura *et al.*[23] and Lichti *et al.*[5] studied the effects of transfer agents on the kinetics of *ab initio* and seeded emulsion polymerization of styrene, respectively.

Nomura *et al.* found that the polymerization rate per particle decreased with increasing amounts of carbon tetrachloride, carbon tetra bromide and primary mercaptans and that the effects were stronger when the transfer constant or the water-solubility was higher. Lichti *et al.* observed the same in seeded experiments with carbon tetrachloride and carbon tetra bromide as chain transfer agents. They were the first to actually measure the exit rate coefficient, using \odot -radiolysis relaxation data, a method that will be discussed later. They found an increasing exit rate coefficient with increasing amounts of transfer agents and a higher exit rate coefficient when the transfer constant was higher. They also found that the entry rate

coefficient increased with increasing amounts of carbon tetra bromide, exactly what is predicted by Figure 4.1. Due to the counterbalancing effects of an increased exit rate and an increased entry rate the polymerization rate passed through a minimum.

Maxwell *et al.*[9] extended their own model for entry by taking the effect of transfer agent into account and used this model to explain the increase observed in emulsion polymerizations with monomers with a high critical chain length z and thiols of intermediate chain length. They also used this model to show that longer chain thiols are too water-insoluble to have an effect and that short chain thiols might suffer aqueous-phase termination and increase the exit rate, and, therefore, can reduce the

Chapter 4

100

polymerization rate in stead of increasing it. For styrene no effect was expected from Maxwell's model, which was confirmed by the work of Asua *et al.*[24]. They found that n-dodecyl mercaptan had no effect on the polymerization rate.

The work of Monteiro *et al.* [48] showed that when RAFT agents are applied in emulsion, the rate of polymerization was significantly retarded. This effect was stronger when a RAFT agent with a more water-soluble leaving group was used. Exit from the particles after fragmentation was proposed to be the main reason for the retardation observed. Because of the high reactivity of the RAFT agents used, it is expected that after a few percent conversion all RAFT agent is consumed, and no longer should have an effect. However it was observed that also in interval II the rate of polymerization was lower with increasing RAFT. Monteiro *et al.* claimed this was a result of transport limitation of RAFT from the monomer droplets to the particles. Due to transport limitation there is a constant flux of RAFT agent to the particles, even if in the particles all RAFT agent has been consumed. Therefore, not all chains start to grow simultaneously, resulting in broad polydispersities. However, also in Interval III retardation was observed, which cannot be ascribed to exit and transport limitation anymore. At that time, intermediate radical termination[25,26] had not yet been put forward by Monteiro *et al.* as a source of retardation. However, since in Interval III the system might not be under zero-one conditions anymore as a result of an increased particle size, intermediate radical termination might explain these results. Another observation Monteiro *et al.* made was that during interval II a red layer was observed, consisting of low molecular weight dormant chains, swollen with monomer. At the switch to Interval III this red layer coalesced, forming red coagulant.

The same red layer was also observed by De Brouwer *et al.*[27] in miniemulsions stabilized with ionic surfactants. When polymer was used as the so-called co surfactant, this polymer was not present in the red layer, indicating that this layer was not a result of droplet coalescence. Also the use of an oil-soluble initiator did not reduce the red layer formation. Experiments

with a higher radical flux, to enhance droplet nucleation did not have an effect. On the contrary, the formation of the red layer was correlated to the polymerization rate, which indicates that product formed during the polymerization plays a crucial role in the destabilization. However, when nonionic surfactants were used, the destabilization did not occur, and controlled miniemulsion polymerizations could be performed without destabilization. The precise reason for the red layer formation and why it does not show up when using nonionic surfactants is still not clear. Moad *et al.*[28] showed that the type of RAFT agent is important. Using a very reactive RAFT agent ($C_{T} \approx 6000$) similar to that in the work of De Brouwer and Monteiro indeed resulted in a broad polydispersity in *ab initio* styrene polymerizations

Seeded emulsion RAFT polymerizations

101

with ionic surfactant, which was ascribed to the fact that the RAFT agent was not uniformly dispersed in the polymerization medium. The use of less reactive RAFT agents ($C_{T} \approx 10-30$) did not result in destabilization and the final polymer had a polydispersity close to 1.4.

Prescott *et al.*[29] used acetone to transport a water insoluble RAFT agent to the seed particles. After removing the acetone the polymerization was started in Interval III. No destabilization was observed, which from the foregoing might indicate that the transfer constant of the RAFT agent used was not extremely high. However, it was high enough to result in a linear increase in molecular weight and polydispersities between 1.2 and 1.4. Although the RAFT agent is consumed at the beginning of the reaction (the molecular weight follows the theoretical linear increase), a reduction in rate is observed throughout the reaction. In these experiments a small seed was used and the amount of monomer was such that the particle size does not increase much, which means that the system is under zero-one conditions throughout the polymerization and intermediate radical termination, therefore, cannot explain the retardation observed.

Monteiro *et al.*[30] also studied the effect of xanthates, the same RAFT agents as will be used in this work, in *ab initio* styrene polymerizations. Again retardation in rate was observed throughout the polymerization. This is not surprising because due to their low transfer constant (see Chapter 3) these RAFT agents will be present during the whole polymerization, and, therefore, result in an increased exit rate throughout the reaction. They also found that in Interval I, the increase in exit results in more nucleation, since exiting radicals re-enter micelles, and thus more particles are formed with increasing amounts of RAFT and constant soap concentration.

Summarizing, it can be said that RAFT can be applied in emulsion, however the mechanism is not fully understood yet. Highly reactive RAFT agents can lead to destabilization, however, the use of nonionic surfactants seems to prevent this destabilization. In all cases retardation in rate is observed. This can be partly ascribed to increased exit, however, even if all RAFT agents has

been consumed, the retardation is still observed. In that case, intermediate radical termination might explain the reduction in rate. However, also when the system is under zero-one conditions and all RAFT is consumed, retardation still plays a role while it can neither be ascribed to intermediate radical termination nor to exit. The explanation for this might in fact be quite simple, as shown in the next section.

4.3.5 Retardation with RAFT in zero-one emulsion systems without increased exit

Retardation with RAFT in zero-one systems in which all RAFT has been consumed

Chapter 4

102

cannot be ascribed to increased exit anymore, as the leaving groups of dormant polymer chains can not exit. Intermediate radical termination is also not a dominant mechanism, since each particle contains only 1 radical. However, the fact that each particle contains only one radical explains why retardation is observed in these systems. This one radical is either present as a 'normal' radical, $R\cdot$, capable to propagate and thus to consume monomer, or as a 'intermediate' radical, $I\cdot$. The time that the radical is in the intermediate state it does not consume monomer, which will thus lead to retardation. Since the system is under zero-one conditions, the system does not reach a steady state on microscopic level, *i.e.* inside a particle, since a particle contains either no radical or 1 'normal' radical or 1 intermediate radical. The lifetimes of $R\cdot$ and $I\cdot$ are given by:

$\tau_{R\cdot} = \frac{1}{k_{add}}$
 $\tau_{I\cdot} = \frac{1}{k_{add}}$

$\tau_{R\cdot} = \frac{1}{k_{add}}$

$\tau_{I\cdot} = \frac{1}{k_{add}}$

$\tau_{I\cdot} = \frac{1}{k_{add}}$ chains dormant [k_{add}

$\tau_{I\cdot} = \frac{1}{k_{add}}$

$\tau_{I\cdot} = \frac{1}{k_{add}}$

$$\tau_{I\cdot} = \frac{1}{k_{add}} \quad (3.22)$$

Using the rate parameters for a dithiobenzoate RAFT polymerization of styrene at 70°C as reported by Monteiro *et al.*[25] ($k_{add}=4\cdot 10^6 \text{ dm}^3 \text{ mol}^{-1} \text{ s}^{-1}$, $k_{add}=1\cdot 10^5 \text{ s}^{-1}$) and a concentration of dormant chains of 0.06 M ($=C_p/100$) this result in a lifetime of $4.2\cdot 10^{-6} \text{ s}$ for a 'normal' radical and a lifetime of $5.0\cdot 10^{-6} \text{ s}$ for an intermediate radical.

This means that the fraction of time that a radical is present as a propagating radical in this system is $4.2\cdot 10^{-6}/(4.2\cdot 10^{-6}+5.0\cdot 10^{-6})=0.46$. This also means that the polymerization rate in this example is only 46% of the polymerization rate without RAFT. The mechanism proposed by Monteiro *et al.*, which included intermediate radical termination, was supported by

Fukuda *et al.* [26]. However, the latter authors proposed a value of $k_{\text{-add}}$ in the order of 10^4 s^{-1} . Following the same pathway this value means that the polymerization rate with RAFT is only 7.7 % of the rate without RAFT in a zero-one system. Since no good experimental data is available of zero-one emulsion systems with dithiobenzoate RAFT agents, at the moment no statement can be made which value of $k_{\text{-add}}$ describes a zero-one system better. However, these results indicate that zero-one experiments can be a useful tool to determine this rate parameter.

It should be noted that for the RAFT agents used in this work, xanthates, no retardation is expected in styrene polymerizations, since k_{add} is much smaller than for the dithiobenzoate RAFT agents and no retardation was observed in homogeneous polymerizations, as was shown in Chapter 3.

Seeded emulsion RAFT polymerizations

103

As already discussed in Chapter 3, Davis *et al.*[31] suggested that slow fragmentation was the main reason for retardation. In a latter paper[32] they adapted their hypothesis on the basis of experiments with \odot -initiation and included the possibility that the intermediate radicals can be terminated reversibly. After switching off the \odot -initiation source at room temperature, systems in which RAFT was present showed a significant increase in conversion when the system temperature was elevated to 60 °C, whereas in systems without RAFT the increase in conversion was much less. They interpreted these results as follows: in the presence of a RAFT agent a considerable amount of 'radical activity' is either stored in intermediate radicals or in reversibly terminated intermediate radicals, whereas without RAFT or with irreversible intermediate radical termination all radical activity quickly disappears as a result of termination. For a styrene polymerization with RAFT at 60 °C Davis *et al.* fitted conversion-time data with $k_{\text{add}} = 5.4 \cdot 10^5 \text{ dm}^3 \text{ mol}^{-1} \text{ s}^{-1}$ and $k_{\text{-add}}$ is $3.3 \cdot 10^{-2} \text{ s}^{-1}$. For a zero-one system with 1 mole% of RAFT and $C_D=6$ these values would lead to $|_R=3.1 \cdot 10^{-5} \text{ s}$ and $|_I=15.2 \text{ s}$. This means as much that a zero-one polymerization cannot proceed because the radicals are present as intermediate radicals for more than 99.99% of time. Since experimental evidence is there that RAFT systems under zero-one conditions do proceed [29], these rate parameters seem highly unlikely, although it has to be noted that in the experiments of Prescott a RAFT agent with a less stable intermediate was used. That the fragmentation rate reported by Davis must be wrong was also shown in the work of Monteiro[25] and Fukuda[26].

The observation by Davis *et al.* of proceeded polymerization with RAFT after \odot -initiation does not necessarily have to be a result of reversibly terminated

intermediates but can also be a result of other by-products of the aggressive γ -

radiation. For instance, compounds containing an unstable S-S bond might be formed in the presence of RAFT, whereas without RAFT such species will not be present.

These species decompose at higher temperatures, which might explain why, after raising temperature, conversion in systems with RAFT is higher than without RAFT.

Summarizing, it has been shown that in a zero-one system with 'reactive' RAFT agents, e.g. dithiobenzoate RAFT agents in combination with styrene, retardation will be observed, even if exit and intermediate radical termination do not play a role. In fact, zero-one emulsion polymerizations can be used to obtain kinetic parameters such

Chapter 4

104

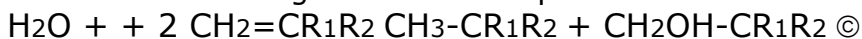
as k_{add} by measuring the polymerization rate versus the dormant chain concentration.

4.4 Determination of the entry and exit rate by γ -relaxation

4.4.1 Determination of the exit rate coefficient, λ_{spont} and λ_{γ}

In γ -relaxation experiments, γ -radiation from a ^{60}Co source is used as initiation source. The main advantage of this method of initiation is that it can be switched on and off by moving the reaction vessel into or out of the source. Both the approach to steady state and the relaxation from this steady state to a new steady state maintained by spontaneous initiation can be followed using dilatometry and can be repeated several times in order to be free of inhibitor artifacts. Of course also other initiation sources, like for instance UV photolysis or electron beam initiation[33], can be switched on and off. Compared to UV photolysis and electron beam initiation, γ -radiation has more penetration power, especially in emulsions. Moreover, no additional photosensitive initiator is required.

The main component in an emulsion system is water, so the γ photons will mainly break water into electrons, protons and hydroxyl radicals[34]. In the presence of aqueous phase monomer these will rapidly react with monomer. Overall the following reaction takes place:



The radicals formed will either enter a particle, terminate in the aqueous phase or propagate to a certain critical chain length after which they enter. Since these radicals do not possess a charged initiator fragment, this critical chain length is shorter than the critical chain length z for initiator-derived radicals. For styrene polymerizations this will probably mean that these radicals can enter without further propagation.

Figure 4.2 \odot -relaxation setup and a typical conversion-time plot of a \odot -relaxation experiment. The jacketed dilatometer with automated tracking device can be moved in and out the ^{60}Co source within 7 s by a moving platform.

In Figure 4.2 a \odot -relaxation setup is shown. The dilatometer can, after temperature equilibration, be lowered into the source, after which a steady-state polymerization rate will be reached, maintained by spontaneous and \odot -initiation. Spontaneous polymerization can for instance be thermal self-initiation of styrene. When the steady state is reached, the dilatometer can be removed from the source by moving the platform up. As a result of radical desorption from the particles and subsequent termination of exited radicals, either in the aqueous phase or, after reentry, in another particle, the polymerization rate will relax to a new steady state which is maintained by spontaneous polymerization. A typical conversion-time plot of 5 subsequent insertions is shown in Figure 4.2. From this conversion-time data the requested kinetic parameters can be derived: the exit rate coefficient k , the

Seeded emulsion RAFT polymerizations

105

moving platform
 ^{60}Co
 source
 lead shielding
 thermostated
 dilatometer
 meniscus tracking device
 stirrer
 0 2000 4000 6000 8000 10000 12000
 0.00
 0.05
 0.10
 0.15
 0.20
 conversion [-]
 time [s]

Chapter 4

106

spontaneous entry rate coefficient k_{spont} and the \odot -initiated entry rate coefficient, k_{\odot} .

Two methods can be used to obtain these parameters: the slope-and-intercept

method and non-linear least squares (NLLS) fitting of n versus time.

The slope-and-intercept method

Eqs. 4.15, 4.17 and 4.19 (in which $k_{\text{initiator}} = 0$) can be integrated to yield n versus time. This expression can be substituted into Eq. 4.1, which after integration

yields an expression for conversion versus time. The long time limit of this equation

reduces to the form:

$$) t t (x) t (x 0 0 - + = - \mathbf{b a} (4.23)$$

in which **a** is the intercept and **b** the steady-state slope after relaxation. This is shown graphically for a typical relaxation in Figure 4.3.

Figure 4.3 Conversion-time data of a typical relaxation experiment. At to the reaction vessel is removed from the source, after which the system relaxes from a steady state in the source with a certain slope to a new steady state with slope **b**. The intercept **a** is the conversion where the linear fit of the new steady-state data intercepts the t_0 axis, minus x_0 . In the long time limit $x(t)$ is described by Eq. 4.23. From these data values for k , γ_{spont} and γ_{\odot} can be derived.

For each limit the exit rate coefficient k and the spontaneous entry coefficient γ_{spont} can now be determined using the in-source slope, out of source slope **b** and the

7400 7600 7800 8000 8200 8400 8600
 0.116
 0.120
 0.124
 0.128
 0.132
 0.136
 $x(t)$
 slope out of the source (**b**)
 slope in the source
 intercept
 (**a**)
 (t_0, x_0)
 conversion [-]
 time [s]

Chapter 4
106

intercept **a**. The equations allowing to obtain k and γ_{spont} from these data have been described by Gilbert[1]. The steady-state forms of Eqs. 4.15, 4.17 or 4.19 (in which $\gamma_{initiator}$ is replaced by γ_{\odot}) can now be used to calculate γ_{\odot} using n_{ss} obtained from the in-source steady state and γ_{spont} and k from the relaxation data.

NLLS fitting of n

As with the slope-and-intercept method, Eqs. 4.15, 4.17 and 4.19 (in which $\gamma_{initiator} = 0$) can be integrated to yield n versus time for each limit. These equations can be found elsewhere[1, Eq. 3.3.52]. Conversion-time data can be transformed into n -time data using Eq. 4.1:

$$\frac{dx}{dt} = A - kx$$

$$x = \frac{A}{k} (1 - e^{-kt})$$

$$n = \frac{A}{k} (1 - e^{-kt}) - x_0 \quad (4.24)$$

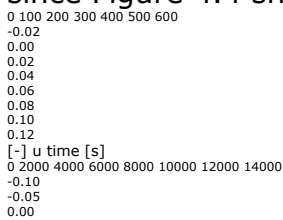
Differentiation of the conversion-time plot and division by the conversion factor will result in a n versus time plot.

Figure 4.4 n versus time data of a typical \odot -relaxation experiment with 6 insertions into the \odot -source.

The time that the reaction vessel is taken from the source is considered as $t=0$. The n versus time of all 6 relaxations from the left hand side figure, where the time that the vessel is removed from the source for each relaxation is set as $t=0$, are put together in the right hand side figure and fitted with the appropriate n versus time equation.

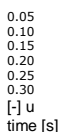
In Figure 4.4 a typical n versus time plot of a \odot -relaxation experiment is shown.

Putting all relaxations together, by taking the time of removal from the source as $t=0$ results in an n versus time plot with an increased number of data points, and thus more reliable fitting parameters. Here this can be done, since Figure 4.4 shows that



Seeded emulsion RAFT polymerizations

107



after each insertion the same steady-state value for n is obtained. Another method to

Seeded emulsion RAFT polymerizations

107

obtain more data points is by increasing the sampling time of the tracking device. However, this in general gives an increased scatter, and therefore will not result in more reliable fitting.

Again, the steady-state form of Eqs. 4.15, 4.17 or 4.19 (in which $\gamma_{\text{initiator}}$ is replaced by γ_{e}) can be used to calculate γ_{e} .

4.4.2 Determination of $\gamma_{\text{initiator}}$

Now values for the exit rate coefficient and γ_{spont} have been determined, $\gamma_{\text{initiator}}$ can be determined from chemically initiated polymerizations under the same conditions, *i.e.* the same temperature, particle size and monomer to RAFT agent ratio.

From these experiments n_{ss} is obtained from conversion-time data and the steady-state form of Eqs. 4.15, 4.17 or 4.19 is used to obtain $\gamma_{\text{initiator}}$ using the exit rate coefficient and γ_{spont} from the relaxation experiments.

4.5 Experimental

4.5.1 Materials

Styrene (STY) and methyl methacrylate (MMA) were purchased from Aldrich and purified of inhibitor by passing through an inhibitor-removal column (Aldrich). Sodium dodecyl sulfate (SDS, Merck), sodium persulfate (SPS, Merck), potassium persulfate (KPS, Merck), NaHCO_3 (Merck) and AMA 80 (Aerosol MA 80, disodium sulfosuccinate, National Starch and Chemicals) were used as received. All other materials were from Aldrich (unless otherwise stated) and used as received.

4.5.2 Synthesis of RAFT agents

The following RAFT agents were synthesized according to the literature procedure[35].

Scheme 4.2 O-ethylxanthyl ethyl propionate (I) and O-ethylxanthyl ethyl benzene (II).

O-ethylxanthyl ethyl propionate (I)

I was synthesized by adding 101.4 g of potassium O-ethyldithiocarbonate (Merck) to a mixture of 102 g ethyl 2-bromopropionate (Merck) dissolved in 1 L of ethanol at 0 °C under a nitrogen atmosphere. The mixture was stirred for 4 hours at 0 °C in the absence of light. 1 L of water was added, and the product was extracted by a 1:2 mixture of diethyl ether and pentane. The solvent was removed and the remaining ethyl 2-bromopropionate distilled off under vacuum. I was obtained at >99% purity according to ¹H NMR.

O-ethylxanthyl ethyl benzene (II)

II was synthesized by adding 104 g of potassium O-ethyldithiocarbonate (Merck) to a mixture of ethanol (1 L) and 80 mL of 1-bromoethyl benzene at 0 °C under a nitrogen atmosphere. The same procedure was carried out as for I, and the product was >98% purity according to ¹H NMR.

4.5.3 Determination of the water-solubility of I and II by UVVIS

The saturation concentration of I and II was determined by mixing an excess of the RAFT agent overnight using a magnetic stirrer. After that the mixture was left standing for a few hours. A sample was taken from the aqueous phase using a syringe, and mixed with a ninefold amount of ethanol. The RAFT concentration was then determined by UV absorption at a wavelength

Seeded emulsion RAFT polymerizations

108

of 278 nm (I) or 283 nm (II), using calibration samples of I and II in 9/1 ethanol-water mixtures.

C

S

C₂H₅O S

C

CH₃

C

O

OC₂H₅

(I) (II)

C

S

C₂H₅O S

C

CH₃

Chapter 4

110

4.5.4 Synthesis and characterization of PMMA seed latex

Design of seed

The design of the seed is crucial for understanding the events that control the

molecular weight distribution. The size of the seed must be small to explore the effects of exit, since under appropriate circumstances exit is proportional to the inverse of the particle radius squared (see Eq. 4.14 – however, note that if the particle is very small, then monomeric-radical desorption is so rapid that transfer to monomer becomes rate-determining for exit, and this size dependence is lost). The seed cannot be too small for this reason and because for extremely small particles the concentration of monomer will change significantly during particle growth. Moreover, the seed needs to be relatively monodisperse in size, which again means that the size cannot be too small (the fundamentals of nucleation theory show that large seeds are more monodisperse than smaller ones, all other things equal[1]). The Morton equation[36,37] describes this semi-quantitatively, and suggests that for particles with un-swollen radius greater than 20 nm the monomer concentration inside the particle remains relatively constant during Interval II. Therefore, the un-swollen PMMA seed radius for these styrene polymerizations was chosen to be approximately 20 nm.

Seeded emulsion RAFT polymerizations

109

An important design parameter is that the number of particles must be high in order to avoid secondary nucleation. N_c was chosen as approximately $1 \cdot 10^{17} \text{ dm}^{-3}$. In all cases the final latex was checked for secondary nucleation by capillary hydrodynamic fractionation (CHDF). New particles could not be observed in most cases and in those cases where it was observed the amount of new particles was always less than 5% based on particle number. Although CHDF may not reliably detect small particles among larger ones under some circumstances, the conclusion that secondary nucleation was negligible was confirmed by the observation that the final particle size was always close to the values expected at full conversion, and that the polymerization rate was constant. Both these observations indicate a constant particle number and thus no secondary nucleation.

The first PMMA seed latex (PMMA1) was prepared as follows: a 1.1 L stainless steel kettle was filled with 927 g water, 3.0 g SDS, 0.3 g NaHCO_3 and 90.8 g MMA, stirred at 350 rpm and heated to 80 °C under an argon atmosphere. A mixture of 0.3 g KPS and 15 g water was added and the reaction was continued for 4 hours. The resulting latex was dialyzed extensively. Solid contents after dialysis was 7.3%. The number-average diameter after measuring 284 particles by TEM was 38.8 nm and the polydispersity (D_w/D_n) was 1.13. This seed was used in experiments to obtain the MWD of polystyrene as a function of conversion.

The second PMMA seed latex (PMMA2) was produced as follows: a 1.5 L glass reactor was filled with 879.7 g water, 2.68 g SDS, 0.31 g NaHCO₃ and 95.2 g MMA, stirred at about 150 rpm and heated to 80 °C under a argon atmosphere. A mixture of 0.33 g SPS in 17.8 g water was added and the reaction was continued for 2.5 hours. The resulting latex was dialyzed extensively. Solid contents after dialysis was 7.1%. The number-average diameter after measuring 469 particles by TEM was 46.5 nm and the polydispersity was 1.09. This seed was used in the dilatometry and ©-source experiments.

The 94 nm diameter polystyrene seed was made as follows: 11.35 g of AMA 80 surfactant, 1 g NaHCO₃, 300 g styrene were added to 560 ml of water. The reaction temperature was raised to 85 °C and stirred. Once the reaction temperature was reached, 1 g of KPS in 45 g water was added to the mixture and polymerization commenced. The resulting latex was dialyzed extensively. The number average particle size was 94 nm and the polydispersity was 1.02.

4.5.5 Styrene seeded emulsion polymerizations

All ingredients except initiator solution were loaded in the 250 mL jacketed glass reactor, equipped with a reflux condenser, and stirred at 400 rpm for 1 hour at 50 °C under an argon atmosphere. After that, the initiator solution was added. A typical recipe contained 155.1 g of water, 0.339 g of SDS, 0.046 g of NaHCO₃, 8.1 g of seed latex (PMMA1), 0.0476 g of SPS, 40.27 g of styrene and variable amounts of RAFT

Seeded emulsion RAFT polymerizations

111

agents. Samples were taken using a syringe with a long needle through a rubber septum and conversion was determined by gravimetry. The same samples were used for GPC analysis afterwards. For the long swelling experiments the mixture was stirred at 300 rpm for about 65 hours at room temperature and at 400 rpm for 1 hour at 50 °C. After that the initiator solution was added.

Chapter 4

112

4.5.6 Styrene seeded emulsion polymerization measured by dilatometry

Dilatometry was performed in a jacketed dilatometer, using a temperature-controlled water bath. The ingredients except initiator solution were, after degassing under vacuum, mixed together and stirred for 1 hour. A typical recipe contained 43.37 g of water, 0.102 g of SDS, 0.014 g of NaHCO₃, 4.25 g of seed latex (PMMA2), 0.0134 g of SPS, 11.90 g of styrene and variable amounts of RAFT agents. The dilatometer was heated at reaction temperature and 1 mL initiator solution was added. The capillary was installed and filled with dodecane. The volume contraction was followed by an automatic tracking-device. The final conversion was measured by gravimetry after each experiment, and the conversion for each time was calculated using

the final conversion and the contraction data assuming ideal mixing based on the final conversion.

4.5.7 Co -radiolysis and relaxation experiments

A jacketed Perspex dilatometer was filled with all degassed ingredients at least 16 hours before the start of the experiment. A typical recipe contained 27.57 g of water, 0.064 g of SDS, 0.009 g of NaHCO_3 , 2.703 g of seed latex (PMMA2), 3.57 g of styrene and variable amounts of RAFT agents. A typical recipe for the experiments performed using a 94 nm polystyrene seed latex contained 15.8 g of water, 0.054 g of SDS, 0.008 g of NaHCO_3 , 11.20 g of seed latex (polystyrene, 21.47% solid contents, 94 nm diameter), 3.57 g of styrene and variable amounts of RAFT agents.

The dilatometer was heated to reaction temperature and degassed again using a syringe and a rubber stopper. The capillary was installed and filled with dodecane. The volume contraction was followed with an automatic tracking device. After a constant temperature was reached the dilatometer was lowered into the Co -source (^{60}Co). When the reaction had reached a steady state, the dilatometer was removed from the source. After a new steady state was reached the dilatometer was lowered back into the source. This was repeated several times. The final conversion was measured by gravimetry after each experiment, and the conversions at intermediate times was calculated using the final conversion and the contraction data. Confirmation that the relaxation kinetics were free of inhibitor artifacts was obtained by the observation that relaxations obtained by successive insertions into and removals from the source showed the same relaxation behavior (within experimental scatter).

Seeded emulsion RAFT polymerizations

113

4.5.8 GPC

The dried polymer was dissolved in tetrahydrofuran (THF, Biosolve) to a concentration of 1 mg/mL. The solution was filtered over a 0.2 mm PTFE syringe-filter. Analyses were carried out using two PLGel (Mixed-C) columns (Polymer Laboratories) at 40 °C.

A Waters 486 UV-detector, operated at 254 nm, was used for detection. THF was used as eluent at a flow-rate of 1 ml/min. Narrow-distribution polystyrene standards (Polymer Laboratories) with molecular weights ranging from 580 to $7.1 \cdot 10^6$ g/mol were used to calibrate the GPC set-up.

4.5.9 ζ -potential measurements and conductivity measurements

ζ -potentials were measured using a Malvern Zetasizer III and conductivities were measured using a Radiometer Copenhagen CDM80 conductivity meter. The samples were prepared by stirring the PMMA1 seed latex (number-average diameter = 38.8 nm), styrene and RAFT agent for at least 24 hours. The N_c was $1 \cdot 10^{17} \text{ L}^{-1}$, $[\text{SDS}] = 7.4 \text{ mM}$, $[\text{NaHCO}_3] = 3.3 \text{ mM}$, $C_p = 5.0 \text{ M}$, and the amount of RAFT agents was varied.

All samples had a pH of approximately 7 measured using Merck Universalindikator. ζ -potentials for each sample were measured typically 10

times in the absence of electro-osmotic flow. In order to check for any aging of the latex, this was repeated 1 day later. No effect of aging was observed. The quoted ζ -potential values for each concentration of RAFT agent are average values of these measurements. The conductivity of each sample was measured and this was repeated 1 day later, giving similar results. The reported value is the average value of these two measurements.

4.6 Results and discussion

Seeded experiments with styrene were carried out to determine the effects of the RAFT agents I and II on the rates of polymerization, molecular weight distribution, and (using τ -relaxation) the entry and exit rate coefficients. The seed is designed (see experimental section) being small enough to be considered under zero-one condition in conventional styrene polymerizations, which allows the effects of entry and exit to dominate the kinetics. As already stated above, the formation of new polystyrene particles must be avoided and, in addition, the concentration of monomer inside the particles must be kept constant throughout Interval II. Eq. 4.1 can then be used to determine n for all experiments.

4.6.1 The rate of polymerization without RAFT

The models for entry and exit described in sections 4.3.2 and 4.3.3 will be used to see whether the rate of polymerization can be described using these models. Therefore, the parameters for a seeded emulsion polymerization of styrene at 50 °C without RAFT agent were put into these models. In order to calculate the entry rate, the parameters from Table 4.1 were used.

Chapter 4

114

Numerical iteration of Eqs. 4.5 to 4.10 yields that $\lambda_{\text{tot}} = 7.5 \cdot 10^{-3} \text{ s}^{-1}$ and the total aqueous phase radical concentration $[T\cdot] = 1.0 \cdot 10^{-9} \text{ M}$.

Table 4.2 Parameters used to describe the polymerization rate of a seeded emulsion polymerization of styrene at 50 °C. Additional parameters can be found in Table 4.1.

parameter value ref

D_w $1.5 \cdot 10^{-7} \text{ dm}^2 \text{ s}^{-1}$ [1]

k_p

$1 \text{ 1000 dm}^3 \text{ mol}^{-1} \text{ s}^{-1}$ [1]

C_p $6 \text{ mol dm}^{-3} \text{ det. Experimentally } k_p$ $237 \text{ dm}^3 \text{ mol}^{-1} \text{ s}^{-1}$ [38]

A $9.6 \cdot 10^{-5} \text{ s}^{-1}$ recipe and value from this table and Table 4.1

$k_{\text{tr}} \text{ (a)}$ $0.0125 \text{ dm}^3 \text{ mol}^{-1} \text{ s}^{-1}$ [39]

$k_{\text{tr}} \text{ (b)}$ $0.0167 \text{ dm}^3 \text{ mol}^{-1} \text{ s}^{-1}$ [40]

The recipe of the polymerization can be found in section 4.5.6. In order to calculate the exit rate, first the limit, which holds for this system has to be determined. Therefore, the 'Conditions' 1 and 2 from section 4.3.3 are used.

Condition 1.

Filling in the parameters from Tables 4.1 and 4.2 and using the $[T\cdot]$ from the

calculations of the entry rate yields that Condition 1 holds. This means that the system is under limit 2 conditions and thus aqueous phase termination of exited radicals can be neglected. The swollen particle radius, r_s , used in Condition 1 is calculated as follows:

$$r_s = r_u \left(\frac{M_0}{M} \right)^{1/3} \left(\frac{C_d}{C_m} \right)^{1/3} \quad (4.24)$$

in which r_u is the unswollen radius, d_M is the monomer density and M_0 the monomer molar mass.

Condition 2.

At the start of a polymerization, Condition 2 always will hold, since n is zero. Filling in the parameters from Tables 4.1 and 4.2 shows that also under steady-state zero-one conditions ($n < 0.5$) this Condition holds, and thus the system is in Limit 2a all the time, which means complete re-entry of exited radicals and minimal re-escape.

Seeded emulsion RAFT polymerizations

115

Since k_{dM} decreases with conversion as a result of an increasing particle size, this means that the system under investigation will stay in Limit 2a.

Since the system is at Limit 2a conditions, Eqs. 4.17 and 4.1 enable one to describe the polymerization rate of this system. This is done numerically using a simple computer program (Appendix 4.1). After each time step, the increase in conversion is calculated, from which the new particle size, and thus new exit rate coefficient is calculated (the exit rate coefficient of a transfer to monomer derived radical). The calculation is stopped when 30% conversion is reached, since at about that point the system reaches Interval III.

Figure 4.5 (a) Calculated versus experimental conversion time profile of a seeded styrene polymerization at 50 °C, using the parameters from Tables 4.1 and 4.2. Two different transfer to monomer rate coefficients were used for the calculations. (b) Calculated swollen radius and n versus conversion.

Figure 4.5 shows the results of these calculations for two transfer to monomer rate coefficients. What first strikes the eye is the excellent

agreement between the calculated and experimental conversion profiles. However, this may be partly

```

0 2000 4000 6000 8000 10000
0.00
0.05
0.10
0.15
0.20
0.25
0.30
experimental
k
tr
=0.0125
ktr=0.0167
conversion [-]
time [s]
0.00 0.05 0.10 0.15 0.20 0.25 0.30
30
40
50
60
70
80
90
ktr = 0.0125
ktr = 0.0167
rs [nm]
conversion [-]
0.00
0.05
0.10
0.15
0.20
0.25
0.30
0.35
0.40
0.45
0.50
[-] u

```

a b

coincidental since both the calculation and the experimental data contain errors. The conversion factor A for instance contains the particle number, which is determined from the particle size of the seed latex. A 5% error in particle size for instance, results in about 15% error in N_c and thus in A. Moreover, in these calculations partitioning coefficients and k_{p1} values of transfer to monomer derived radicals are estimated, which can also contain large errors. However, these results indicate that the models for entry and exits from sections 4.3.2 and 4.3.3 can at least be used to give a rough estimate of the polymerization rate.

Another observation that can be made from Figure 4.5 is the considerable

Chapter 4

116

increase in particle size and corresponding decrease in the exit rate coefficient. This means that the exit rate coefficient is far from constant at low conversions (in the example above the exit rate decreases by more than a factor of 2 between 0 and 5% conversion) and, therefore, the approach to steady state of a chemically initiated experiment at these conditions cannot be used to determine entry and exit rates.

After all, the curvature in the approach to steady state is partly the result of a changing exit rate coefficient. Moreover, a real steady state is not reached at low conversions due to this fast changing exit rate coefficient. Therefore, it seems essential to use ∞ -relaxation experiments to determine entry and exit rate coefficients, since in these experiments the exit rate can be obtained at conversions where the exit rate coefficient is relatively constant.

4.6.2 Influence of RAFT on the rate of polymerization

The conversion-time profiles of seeded styrene polymerizations at 50 °C, in the presence of the RAFT agents I or II over a range of monomer to RAFT ratios (*i.e.* 50 to 400), are given in Figure 4.6. It can clearly be seen that both the type and amount of RAFT agent affect the rate. Since the amount of RAFT agent is increased in the recipes so too is the retardation in rate, which is more pronounced for II as compared with I. From Eq 4.1, the steady-state value of n_{ss} , for all experiments can be determined (see Table 4.3). Without RAFT agent, the polymerization rate compares favorably with the rate calculated for these conditions from theory (see previous section) using the full expression for the entry rate coefficient (including chain-length-dependent propagation rate coefficients) and the Limit 2a exit rate coefficient. The addition of a small amount of RAFT (ratio to monomer 1:400) results in reduction in n by a factor of 3, and increasing the ratio of RAFT further (1:50), n was reduced by at least a factor of 6. The reduction in n was greater for II than I, which suggests that retardation is controlled by the type of leaving group R.

Figure 4.6 Conversion-time profiles of seeded styrene polymerizations at 50 °C in the presence of variable amounts I or II. The solid lines represent the dilatometry runs with I (or no RAFT), the dashed lines represent the dilatometry runs with II. The closed symbols and open symbols are gravimetric data from for I (or no RAFT) and II, respectively.

Table 4.3 The steady-state average number of radicals per particle, n_{ss} , for seeded emulsion polymerizations of styrene at 50 °C with various amounts of RAFT agents I or II.

n_{ss}	[STY]/[RAFT]
(I)	(II)
400	0.109 0.098
200	0.093 0.074
100	0.065 0.056
50	0.049 0.039
no RAFT	0.326

Seeded emulsion RAFT polymerizations

117

4.6.3 Influence of RAFT on the molecular weight distribution

Also shown in Figure 4.6 is the comparison between the dilatometric and gravimetric data. The agreement is good and suggests that we can use with confidence the polymer obtained from gravimetry to obtain the molecular weight distribution as a function of conversion. The polydispersities for all these experiments

0 18000 36000 54000 72000 90000
 0.0
 0.2
 0.4
 0.6
 0.8
 1.0
 2% (II)
 1% (II)
 0.50% (II)
 0.25% (II)
 2% (I)
 1% (I)

0.50% (I)
 0.25% (I)
 no RAFT
 conversion [-]
 time [s]

were close to two, which is in accord with ideal RAFT behavior (Eqs. 3.4 and 3.5), using a value for C_T of 0.7 for both RAFT agents. However, it is also close to the value expected for the RAFT agent acting solely as a 'normal' chain-transfer agent.

Figure 4.7 $M_w/2$ of seeded emulsion styrene polymerizations at 50 °C as a function of conversion for a range of monomer to RAFT agent ratios (I or II; 400:1, 200:1, 100:1) with a swelling time of 1 hour. For RAFT agent I also the results of experiments with a swelling time of 3 days are shown. The solid lines represent the theoretical molecular weights using Eq. 3.4 and $C_T=0.7$.

Figure 4.7 shows M_n (in fact $M_w/2$ is shown, however the polydispersity was close to 2 for all data points, so $M_n \approx M_w/2$) as a function of conversion for a range of monomer to RAFT ratios (*i.e.* 100 to 400). The time allowed for the monomer and RAFT agents to swell into the latex was 1 hr. Since the ratio of both RAFT agents increased, M_n decreased, and the trends with conversion were the same for both I and II. The solid lines are theoretically determined from Eq. 3.4, using $C_T = 0.7$. It should be kept in mind that Eq. 3.4 holds for homogeneous polymerizations (first order kinetics with respect to monomer and to RAFT agent); in emulsion where the order with respect to monomer is 0 in interval II, it does not strictly hold. However, because the transfer constant is close to 1, the induced error is small. At low conversions theory predicts an M_n slightly below the experimental values, but as the conversion increased the experimental points fit better with ideal RAFT behavior. This might be because in the initial stages of polymerization the rate of transportation of RAFT from the droplets into the particles is slow on the propagation time-scale.

Chapter 4

118

0 20 40 60 80 100
 0
 10000
 20000
 30000
 40000
 50000
 60000
 70000
 200:1
 100:1
 400:1
 $M_w/2$ [g/mol]
 conversion [%]
 I, 1 h swelling
 I, 3 days swelling
 II, 1 h swelling
 Eq. 3.4

Seeded emulsion RAFT polymerizations

119

Transport limitation

Simple calculations based on the aqueous phase concentration and the diffusion rate of the RAFT agent will reveal whether or not the transportation rate of the RAFT agent is faster than that of its consumption.

Rate of transportation

The rate of transportation is equal to the rate at which particles can capture aqueous phase RAFT agents. For an emulsion system at equilibrium, the rate of RAFT agents being captured by a particle can be derived from the Smolukowski equation and is given by:

$$r_{RAFT, sat} = \frac{4 \pi r_p D_{RAFT} C_w}{1 + k_{trRAFT} r_p / D_{RAFT}} \quad (4.26)$$

in which D_{RAFT} is the diffusion coefficient of a RAFT agent in water and the aqueous phase RAFT concentration, C_w

r_{RAFT} , is calculated using Eq. 4.13.

Rate of consumption

In a zero-one system, a particle contains either one or zero radicals. To calculate whether transport limitation plays a role, one has to consider transport limitation on a microscopic level, viz. on the level of one particle. If a particle does not contain a radical, no RAFT agent will be consumed, so only particles with one radical are considered. The consumption rate of RAFT agent in such a particle is given by:

$$r_{RAFT, cons} = k_{trRAFT} [R\cdot]_p \frac{1}{N_A} \frac{1}{v_p} \quad (4.27)$$

in which $[R\cdot]_p$ is the radical concentration in a particle containing 1 radical and is given

by $(1/N_A)/v_p$, v_p is the volume of a particle.

Using $D_{RAFT}=2 \cdot 10^{-7} \text{ dm}^2 \text{ s}^{-1}$ (rough estimation, based on diffusion coefficient of a monomer, see Table 4.2), $k_{trRAFT}=0.7 \cdot 237=166 \text{ dm}^3 \text{ mol}^{-1} \text{ s}^{-1}$ [Chapter 3, 38], $r_s=50 \cdot 10^{-8} \text{ dm}$ and $C_p=6 \text{ mol dm}^{-3}$, the rate of consumption and transportation can be plotted versus the RAFT aqueous phase saturation concentration for different fractions of RAFT agent. In Figure 4.8 this is shown for $f_{RAFT}=0.0025$ (1/400) and $f_{RAFT}=0.01$ (1/100).

Chapter 4

120

This figure shows that above a saturation concentration of $1 \cdot 10^{-8} \text{ M}$ no transport limitation is expected. The saturation concentrations of I and II have been determined experimentally by UVVIS experiments. I and II have aqueous phase saturation concentrations of $2 \cdot 10^{-3} \text{ M}$ and $4 \cdot 10^{-4} \text{ M}$, respectively. It can therefore be assumed that transport limitation is not an issue in these experiments, provided that the system is sufficiently stirred, such that the aqueous phase RAFT concentration does not reach the an extremely low value.

Figure 4.8 Rate of RAFT consumption in a particle containing 1 radical, and RAFT capture rate of a particle versus the aqueous phase saturation concentration of the RAFT agent for $f_{RAFT}=0.0025$ and $f_{RAFT}=0.01$.

Further experiments using only **I** were carried out with longer swelling times for over three days. In these polymerizations (Figure 4.7, open symbols) the trends were similar for all ratios of **I**. The M_n values fit well with ideal RAFT behavior for the whole conversion range. In order to avoid scatter due to inaccurate determination of M_n , M_n was calculated by dividing the weight average molecular weight by 2, which is more accurate [41]. From these data it can be inferred that equilibrium of the RAFT agent between the droplets and the particles is indeed established with a swelling time of just 1 hr, which is in agreement with the aforementioned calculations.

4.6.4 Exit rate coefficients from \odot -relaxation experiments

In order to determine values for the exit rate coefficient (k), \odot -relaxation experiments were performed. Once k is known for a certain system, the entry rate coefficient γ can be calculated from $\gamma_{ss} n$ (chemical experiments) for the limit that is applicable to the system.

1E-11 1E-10 1E-9 1E-8 1E-7 1E-6 1E-5
 0.01
 0.1
 1
 10
 100
 1000
 $R_{cap} (1/400)$ $R_{cap} (1/100)$
 $R_{cons} (1/100)$
 $R_{cons} (1/400)$
 $R_{cons}, R_{cap} [s^{-1}]$
 C_w
 $sat_{RAFT} [M]$

Seeded emulsion RAFT polymerizations

121

Finding the right Limit

In section 4.6.1 it was found that the system is in Limit 2a conditions if no RAFT agent is present. Condition 1 is still applicable if RAFT is present, assuming that the diffusion coefficient in water of a transfer to monomer derived radical is comparable with that of a transfer to RAFT derived radical and assuming that the total aqueous phase radical concentration does not change dramatically by the addition of a RAFT agent. In order to test Condition 2, a closer look at the leaving groups of the two RAFT agents is required. These are shown in Scheme 4.3 together with their polymeric analogues.

Scheme 4.3 Leaving groups of **I** and **II** and their polymeric analogues.

For the desorption rate coefficient of a monomeric radical, which is in this case the leaving group **R(I)** or **R(II)**, Eq. 4.14 can be used. Therefore, values for q and D_w of **R(I)** and **R(II)** have to be estimated. The aqueous phase diffusion coefficient will be comparable to that of a monomer. The partitioning coefficient is estimated from the $C_{p, sat}$ of a comparable monomer, in this case ethyl acrylate for **R(I)** and styrene for **R(II)**, and from the C_w of their non-radical analogues, *i.e.* ethylpropionate for **R(I)** and ethylbenzene for **R(II)**. For the reactivity of these radicals, they are compared with their polymeric analogues. As a rule of thumb $k_{p, 1} \approx 4 k_p$ is used [1, 11]. For **R(I)** also the reactivity ratios of ethyl acrylate with styrene have to be taken into account, since here crosspropagation takes place. All above mentioned parameters and the resulting $k_{dM, RAFT}$ and $k_{p, 1, RAFT}$ values are shown in Table 4.4.

C

CH₃
 C
 O
 OC₂H₅ H
 C
 CH₃
 H
 R(I) poly(ethyl acrylate) R(II) poly(styrene)
 C
 CH₂
 C
 O
 OC₂H₅ H
 C
 CH₂
 H

Chapter 4

122

Table 4.4 Parameters used to calculate k_{dM}

RAFT and k_p
_{1,RAFT} of R(I) and R(II) in order to test Condition 2.

R(I) R(II)

$D_w 1.5 \cdot 10^{-7} \text{ dm}^2 \text{ s}^{-1}$ [1] $D_w 1.5 \cdot 10^{-7} \text{ dm}^2 \text{ s}^{-1}$ [1]

$C_p 6 \text{ M}$ [estimated] $C_p 6 \text{ M}$ [estimated]

$C_w 2 \cdot 10^{-1} \text{ M}$ [42] $C_w 1.2 \cdot 10^{-3} \text{ M}$ [43]

$r_s 50 \cdot 10^{-8} \text{ dm}$ $r_s 50 \cdot 10^{-8} \text{ dm}$

k_{dM}

RAFT $6 \cdot 10^4 \text{ s}^{-1}$ k_{dM}

RAFT $3.6 \cdot 10^2 \text{ s}^{-1}$

$k_p 2 \cdot 10^4 \text{ dm}^3 \text{ mol}^{-1}$

S^{-1}

[44] $k_p 237 \text{ dm}^3 \text{ mol}^{-1} \text{ s}^{-1}$ [38]

$r_2 (\text{STY-EA}) 0.13$ [45]

k_p

_{1,RAFT} $6 \cdot 10^5 \text{ dm}^3 \text{ mol}^{-1}$

S^{-1}

k_p

_{1,RAFT} $1 \cdot 10^3 \text{ dm}^3 \text{ mol}^{-1} \text{ s}^{-1}$

Using these values and the n -values from Table 4.3 for testing Condition 2 it is found that Condition 2 is met for both leaving groups. This means the system is under limit 2a conditions, also in the presence of these two RAFT agents.

The exit rate coefficients

In Limit 2a the free-radical loss is second order with respect to n . The kinetic expression is thus given by:

2
 cr spont initiator $n k_2) n^2 1) (($

$$\frac{dM}{dt} = -k_p \frac{M}{M_0} + k_{tr} \frac{M}{M_0} = (4.17)$$

in which

$$\frac{1}{M} \frac{dM}{dt} = -k_p \frac{1}{M} + k_{tr} \frac{1}{M}$$

$$k_{cr} = k_p - k_{tr} \quad (4.18)$$

The exit rate coefficient k_{cr} is obtained using the slope-and-intercept method and using NLLS-fitting of $\ln M$ versus time. For the reasons mentioned in section 4.6.1 (fast changing r_s at low conversions) and inhibitor artifacts, the first relaxation is not taken into account. The slope-and-intercept values of k_{cr} are obtained by taking the average of the exit rate coefficient obtained from each relaxation (normally 3 or 4 relaxations).

Seeded emulsion RAFT polymerizations

123

changing r_s at low conversions) and inhibitor artifacts, the first relaxation is not taken into account. The slope-and-intercept values of k_{cr} are obtained by taking the average of the exit rate coefficient obtained from each relaxation (normally 3 or 4 relaxations).

The NLLS-fitting is obtained by putting all relaxations together and fitting the combined data, as shown in Figure 4.4.

In Table 4.5 the results are shown and compared with the 'theoretically' expected exit rate coefficient from Eq. 4.18. The most right term in Eq. 4.18 involves transfer to monomer derived radicals, and the parameters used can be found in Tables 4.1 and 4.2 ($k_{tr}=0.0167 \text{ dm}^3 \text{ mol}^{-1} \text{ s}^{-1}$ is used).

Table 4.5 Theoretically calculated (Eq. 4.18) and experimentally obtained (by \odot -relaxation) Limit 2a exit rate coefficients of seeded styrene emulsion polymerizations at 50 °C in the presence of I or II.

	(I)	(II)							
[STY]/[RAFT]			$k_{cr}(\text{calc})$						
			[s ⁻¹]						
$k_{cr}(\text{exp})$			[s ⁻¹]						
(slopeintercept)			$k_{cr}(\text{exp})$						
			[s ⁻¹]						
(NLLS)			$k_{cr}(\text{calc})$						
			[s ⁻¹]						
$k_{cr}(\text{exp})$			[s ⁻¹]						
(slopeintercept)			$k_{cr}(\text{exp})$						
			[s ⁻¹]						
(NLLS)			$k_{cr}(\text{calc})$						
			[s ⁻¹]						
no RAFT	0.022	0.043	0.037	0.022	0.043	0.037			
400	0.064	0.082	0.069	0.171	0.079	0.103			
200	0.105	0.100	0.075	0.321	0.142	0.123			
100	0.188	0.199	0.166	0.817	0.186	0.158			

As expected, the exit rate coefficients increase by increasing the amount of RAFT. No significant effect of different RAFT agents is observed for k_{cr} . Also both methods for obtaining k_{cr} (slope-and-intercept and NLLS fitting) give similar results.

Figure 4.9 shows that the observed dependence of the exit rate coefficient on f_{RAFT} is linear, exactly as predicted by Eq. 4.18. Further quantitative comparison between the predictions of this equation and the data cannot be made because the values of k_p

$k_{p,RAFT}$

and the partition coefficient of R(I) and R(II) between the particle and aqueous phase, used to calculate the desorption rate coefficients of R(I) and R(II), are only rough estimates. The similarity between the exit rate coefficients for both RAFT agents, despite the different water-solubility of the leaving groups, is ascribed to fortuitous similarities of the corresponding ratios in Eq. 4.18.

Chapter 4

124

Figure 4.9 Experimentally determined Limit 2a exit rate coefficients versus the mole fraction of RAFT agents I and II of seeded styrene emulsion polymerizations at 50 °C, determined by the slope-and-intercept method and NLLS fitting.

Influence of particle size on exit rate coefficient

Eqs. 4.14 and 4.18 show that the Limit 2a exit rate coefficient should be proportional to 1 over the squared radius. This was explored further by performing experiments with a larger seed, viz. 94 nm un-swollen diameter, in which exit should be reduced. However, calculation[1] also indicates that

this size is such that zero-one kinetics might no longer be applicable. Two \odot -relaxation experiments, one without and one with I (ratio to monomer of 1:200), were performed. Using the slope-and-intercept method, values for $k_{cr} = 0.016 \text{ s}^{-1}$ (no RAFT) and 0.085 s^{-1} (with RAFT) were obtained.

The first value, for the experiments without RAFT seems to follow Eqs. 4.14 and 4.18. For the small seed, with a swollen radius of about 50 nm, $k_{cr} = 0.043 \text{ s}^{-1}$ was found. The swollen radius of the big seed is about 75 nm. Based on a 1 over the squared swollen radius proportionality a value of $0.043 \cdot (50^2/75^2) = 0.019 \text{ s}^{-1}$ is expected for k_{cr} , which is close to the experimental value of 0.016 s^{-1} .

The latter value, 0.085 s^{-1} , is similar to the value found in the smaller seed under the same conditions (*i.e.* $k_{cr} = 0.10 \text{ s}^{-1}$; ratio 1:200, 46.5 nm seed). Because this system is probably somewhere between zero-one and pseudo-bulk kinetics, for which there is no simple means of fitting a phenomenological rate coefficient to theory[1], no quantitative interpretation can be given. Qualitatively, one can see that the loss by exit should be smaller, which at first sight appears to be inconsistent with experiment.

0.000 0.002 0.004 0.006 0.008 0.010
 0.00
 0.04
 0.08
 0.12
 0.16
 0.20

I, slope-and-intercept

I, NLLS

II, slope-and-intercept

II, NLLS

k_{cr} [S-1]

f_{RAFT} [-]

Seeded emulsion RAFT polymerizations

125

However, it must be realized that intra-particle termination will be rate-determining in this non-zero-one system. Because RAFT produces small species which diffuse rapidly, and because termination in these systems is diffusion-controlled[46,47] it is apparent that the rate of radical loss by intra-particle termination will be increased. The observation that the rate of radical loss is similar in the small and large particles studied here can therefore readily be rationalized in terms of an approximate cancellation of these two effects.

4.6.5 Dilatometry runs with chemical and \odot -initiation: determination of entry rate coefficients

The entry rate coefficient for initiator-derived radicals, $\gamma_{initiator}$, can be obtained from Eq. 4.17. Using γ_{ss} (chemical) and using k_{cr} and γ_{spont} values obtained from the \odot -relaxation experiments and the slope-and-intercept method, $\gamma_{initiator}$ is given by:

γ_{spont}

γ_{ss}

2

γ_{ss} k_{cr}

$\gamma_{initiator} n 2 1$

$n k 2$

$\gamma -$

-

= γ (4.28)

Results are given in Table 4.6 and Figure 4.10.

Table 4.6 $\gamma_{\text{initiator}}$ obtained from chemically initiated experiments using k_{cr} and γ_{spont} from \ominus -relaxation experiments.

ss	n	[-]	k_{cr} [s ⁻¹]	γ_{spont} [s ⁻¹]	$\gamma_{\text{initiator}}$ [s ⁻¹]
no RAFT	0.33	0.043	$8.0 \cdot 10^{-5}$	$2.6 \cdot 10^{-2}$	
[STY]/[(I)]=400	0.11	0.082	$5.8 \cdot 10^{-5}$	$2.4 \cdot 10^{-3}$	
[STY]/[(I)]=200	0.093	0.10	$3.1 \cdot 10^{-5}$	$2.1 \cdot 10^{-3}$	
[STY]/[(I)]=100	0.065	0.20	$1.1 \cdot 10^{-5}$	$1.9 \cdot 10^{-3}$	
[STY]/[(II)]=400	0.098	0.079	$6.9 \cdot 10^{-5}$	$1.8 \cdot 10^{-3}$	
[STY]/[(II)]=200	0.074	0.14	$3.6 \cdot 10^{-5}$	$1.8 \cdot 10^{-3}$	
[STY]/[(II)]=100	0.056	0.19	$0.4 \cdot 10^{-5}$	$1.3 \cdot 10^{-3}$	

Initially there is a drastic decrease in $\gamma_{\text{initiator}}$ with increasing I and II, which then remains relatively constant. It should be noted that the entry rate coefficient for the experiments without RAFT corresponds with a value which indicates an initiator efficiency > 100%. At 100% initiator efficiency, $\gamma_{\text{initiator}}$ would be $2k_d[I]N_A/N_c =$

Chapter 4

126

$1.44 \cdot 10^{-2}$. However the experimentally determined $\gamma_{\text{initiator}}$ is very sensitive to errors in the exact particle number, k etc.. The absolute numbers are therefore not very reliable, but the trend in the data is reliable, since all values contain the same systematic errors.

It is apparent from Figure 4.11 that the RAFT agents used here also reduce the entry rate coefficient for \ominus -initiated systems, γ_{\ominus} , but only if the RAFT concentration is sufficiently high. γ_{\ominus} has been determined using Eq. 4.28 in which $\gamma_{\text{initiator}}$ is replaced by γ_{\ominus} and using ss n in the gamma source. At low RAFT concentrations γ_{\ominus} is not affected by the RAFT agents, whereas in the chemically initiated experiments with the same amount of RAFT a drastic decrease in the entry rate is observed. Now, while quantitative models for entry for chemical initiators are well established [7], this is certainly not the case for \ominus -initiation. This is because the initiation process for the latter involves several radical species: $H\cdot$, $OH\cdot$ and hydrated electrons, and these species arise in both the water and particle phases. Hence, all that can be inferred from the data in Figures 4.10 and 4.11 is that the observed decrease in entry rate coefficient for \ominus -initiation is not consistent with the effect seen with chemical initiation.

The observed reduction in entry rate coefficients is surprising, given the well established mechanism for entry in conventional systems: propagation to a z-mer, etc.. In these styrene systems, $z \sim 3$. If this mechanism were operative in the present systems, entry should not be affected by the RAFT agents used here (see Figure 4.1): they are essentially insoluble in the water phase and have a low reactivity, and thus will not affect the rate of z-mer formation (any transfer would only occur at much higher degrees of polymerization). However, still an effect is clearly seen.

Seeded emulsion RAFT polymerizations

127

Figure 4.10 (left) $\gamma_{\text{initiator}}$ versus the molar fraction of RAFT of seeded styrene emulsion polymerizations at 50 °C. (closed squares) **I**; (open squares) **II**.

Figure 4.11 (right) γ_{S} versus the molar fraction of RAFT of seeded styrene emulsion polymerizations at 50 °C. (closed squares) **I**; (open squares) **II**.

One reasonable explanation for this unexpected effect is that the xanthate RAFT agents used here are surface active, that is, they reside near the surface of the particle. Surface activity of xanthates is not unexpected since it can form a canonical structure that is ionized [28].

Scheme 4.4 Canonical structure of a xanthate-based RAFT agent.

Surface activity of **I** and **II** would mean that z-mers, whose radical locus passes through the particle surface and which themselves are also surface-active, will have a very high probability of transfer to RAFT, resulting in possible exit instead of propagation into the interior of the particle. Hence exit of the radical resulting from the transfer reaction between a z-mer and the RAFT agent at the surface will result in a decrease in the effective rate of entry, since these exiting radicals might re-enter a particle that already contains a radical, leading to termination.

(ζ -potential and conductivity measurements)

The suggestion that surface activity of the RAFT agent can explain the unexpectedly large effect on entry can be checked by directly measuring this surface

R1
O
S
S
R2
O
S
S
R2 R1 O S
R2 R1
S
0.000 0.002 0.004 0.006 0.008 0.010
1E-3
0.01
 γ_{S} [S-1]
f_{RAFT} [-]
0.000 0.002 0.004 0.006 0.008 0.010
1E-3
0.01
 $\gamma_{\text{initiator}}$ [S-1]
f_{RAFT} [-]

Chapter 4
128

activity. Should **I** and **II** act as surface active species, they should displace surfactant from the surface of the particles, increasing the conductivity in the aqueous phase and altering the charge density on the particle surface, and thus the ζ -potential. The measured conductivity and z-potential of styrene swollen latexes with different amounts of **I** and **II** are shown in Table 4.7. The pH was about 7 in all experiments.

Table 4.7 Conductivities and ζ -potentials of monomer swollen latexes with different amounts of RAFT agents (**I**) and (**II**).

(I) (II)

[STY]/[RAFT] conductivity

[∞ S cm⁻¹]

ζ -potential

[mV]

conductivity

[∞ S cm⁻¹]

ζ -potential

[mV]

no RAFT 652 -52.7 634 -52.6

400 656 -51.8 644 -50.3

100 655 -51.3 644 -51.6

50 663 -50.7 645 -50.8

These results show that, if the amount of RAFT is increased, the conductivity is increased and ζ -potentials are decreased. However, the differences are too small to conclude that there is a significant effect, but the data show a slight trend that RAFT agent to a small extent displaces the surfactant from the particle surface.

Although the explanation is consistent with the trends in the entry rate coefficient, it does not seem to drastically affect the MWD. This is simply because the MWD is determined by the average concentration of RAFT inside the particle (since the growing chain randomly samples the whole particle interior), whereas the concentration of RAFT closer to the surface specifically affects entry because the zmer enters through this surface.

4.6.6 Surface activity as the explanation for the decrease in entry rate

In the foregoing it was discussed that surface activity can explain the results at least qualitatively and also experimental data indicated that the RAFT agent is located at the surface, although no hard conclusion can be drawn from the conductivity and ζ -potential experiments. It was also observed from Figures 4.10 and 4.11 that $\lambda_{\text{initiator}}$ decreased dramatically when RAFT is present, whereas λ_{e} was unaffected, unless the RAFT concentration was very high. This is because in a e -initiated system, the

Seeded emulsion RAFT polymerizations

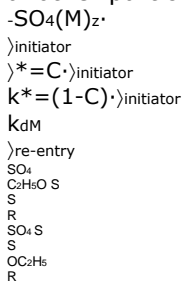
129

initiating species are uncharged, and therefore do not have the same preference to be located at the particle surface as z-mers do. Moreover, this surface activity theory is consistent with the molecular weight and exit rate data. Although the RAFT agent is located at the surface it is still 'seen' by growing radicals in the interior of the particle, and thus the molecular weight follows theory and also the exit rate increases linearly with RAFT concentration.

The question that remains is if the dramatic decrease in entry rate, as seen in Figure 4.10, can be explained quantitatively.

Let us assume that all the entering z-mers undergo transfer to a RAFT agent at the particle surface. The small radical that is formed by this reaction can either immediately exit or enter the particle. The fraction that really goes into the particle is defined as C. After entry, this small radical behaves as a 'normal' small radical. So a fraction of the entering z-mers, after transfer, exits immediately as an R· and will reenter another particle, where it can terminate. So if n is high this will lead to a lot of extra termination and, therefore, the apparent $\gamma_{\text{initiator}}$ will be lower. This is shown schematically in Figure 4.12.

Figure 4.12 Schematic representation of the effect of surface activity of RAFT on $\gamma_{\text{initiator}}$. An entering z-mer reacts with RAFT at the surface. A fraction (1-C) of the leaving group of the RAFT agent that is formed exits while a fraction C enters. The exited radical can terminate in another particle and thus the apparent $\gamma_{\text{initiator}}$ decreases.



Chapter 4

130

It can be derived that in this case Eq. 4.17 can be written as:

$2 \gamma_{\text{cr}} \gamma_{\text{initiator}} \text{spont}$

$$\frac{1}{n} \left(\frac{k_2}{k_1} \right) \left(\frac{n-1}{n} \right) \left(\frac{n-1}{n} \right) C^3 \left(1 - \frac{d\tau}{dn} - \frac{d\tau}{dn} - \frac{d\tau}{dn} + \gamma \right) = (4.29)$$

In the experiments with RAFT, n is close to 0.10. Assuming that all entering z-mers will transfer and exit (C=0), this leads to an apparent $\gamma_{\text{initiator}}$ which is 12.5% lower than in a system without surface activity. As can be seen in Figure 4.10, the entry rates drop about 90% and therefore surface activity cannot explain the observed results quantitatively.

Up to now it was assumed that the studied system was in Limit 2a, as tested by Conditions 1 and 2. However, as a result of surface-activity it might also be possible that the systems is in Limit 1, i.e. complete aqueous phase termination of exited radicals. This will occur if the RAFT at the surface is not only a barrier for z-mers but for all entering or re-entering radicals.

If limit 1 is assumed, the exit rate coefficients have to be determined using the equation for first order loss, Eq. 4.15. Again the slope and intercept method or NLLS fitting can be used to obtain exit rate coefficients. The results are shown in Figure 4.13.

Figure 4.13 k_{ct} (Limit 1 exit rate coefficient) versus molar fraction of RAFT, as determined by τ -relaxation experiments using the slope-and-intercept method and using NLLS fitting of n versus time data.

0.000 0.002 0.004 0.006 0.008 0.010

0.000

0.005

0.010

0.015

0.020

0.025

0.030

0.035 I, slope-and-intercept

I, NLLS

II, slope-and-intercept

II, NLLS

k_{dt} [S⁻¹]

f_{RAFT} [-]

Seeded emulsion RAFT polymerizations

131

Figure 4.13 shows that when a first order loss mechanism is assumed to be operative, the exit rate coefficients obtained are independent of the RAFT concentration. Based on this consideration, first order loss mechanisms can be rejected, since also in this case the exit rate coefficient should increase linearly with RAFT concentration.

4.6.7 Other explanations for the decrease in entry rate

Until now, it was assumed that the decrease in polymerization rate was solely a result of increased exit and decreased entry. This assumption was based on the fact that no retardation was observed in styrene polymerizations with the same RAFT agents in homogeneous systems, as shown in Chapter 3.

However, so far no quantitative explanation can be given for the decreased entry rate coefficient. In section 4.3.5 it was put forward that in a zero-one system no steady state on particle

level is reached and that the fraction of time a radical is present as an intermediate radical also can cause retardation. From Eq. 4.22 a 'retardation' factor Q can be calculated:

$$\cdot I \cdot R$$

$$\cdot R \cdot Q$$

$$\left| + \right|$$

$$= (4.30)$$

The polymerization rate with RAFT will thus be Q times the polymerization rate without RAFT (if effects of entry and exit are not taken into account). For a styrene polymerization at 50 °C with I and II, $k_{add} \square 2k_{tr} = 2 \cdot 0.7 \cdot 237 = 332 \text{ dm}^3 \text{ mol}^{-1} \text{ s}^{-1}$. The fragmentation rate constant k_{-add} is unknown, although the results in Chapter 3 show that in nBA solution polymerizations with I, $k_{-add} = 10^4 \text{ s}^{-1}$. For styrene polymerization, this quantity could not be determined, since in styrene polymerizations with xanthates no retardation will be observed, unless fragmentation is extremely slow. Recently, some articles have appeared that report this quantity.

Monteiro *et al.*[25] report a value of $1 \cdot 10^5 \text{ s}^{-1}$ for a styrene polymerization with a dithiobenzoate RAFT agent at 70 °C, Fukuda *et al.*[26] report a value in the order of 10^4 s^{-1} for the same system at 60 °C, while Davis *et al.*[31] report a value of $3.3 \cdot 10^{-2}$

s^{-1} for this system (note that there is a difference of 7 orders of magnitude between

the different values). In Table 4.8 the effect these parameters have on the rate of

Chapter 4

132

polymerization, expressed in retardation factor Q are shown for the RAFT concentrations used in this work.

Table 4.8 Retardation factor Q in zero-one seeded emulsion styrene polymerizations at 50 °C at different concentrations of a xanthate RAFT and different values of k_{-add} .

[STY]/[RAFT] $k_{\text{-add}} =$

$1 \cdot 10^5 \text{ s}^{-1}$

[25]

$k_{\text{-add}} =$

$1 \cdot 10^4 \text{ s}^{-1}$

[26]

$k_{\text{-add}} =$

$3.3 \cdot 10^{-2} \text{ s}^{-1}$

[31]

400 >0.999 >0.999 0.013

200 >0.999 >0.999 0.007

100 >0.999 >0.999 0.003

Table 4.8 shows that retardation without a contribution from increased exit is possible in a zero-one system, provided that the fragmentation rate is sufficiently low.

However, as mentioned before, the fragmentation rate constant reported by Davis *et al.* is much too low and unrealistic, since this value would mean that even in xanthate systems with a relatively low addition rate, polymerization would hardly proceed, which is not the case. The values reported by Monteiro and Fukuda will not result in retardation in a zero-one styrene system with a xanthate. The question remains which fragmentation rate constant can, besides increased exit, explain the retardation in rate.

If a constant and RAFT-independent entry rate is assumed, as predicted in Figure 4.1, and the experimentally determined exit rates are used, it can be calculated that the fragmentation rate has to be in the order of $5 \cdot 10^6 \text{ s}^{-1}$, in order to explain the observed values of n with RAFT (Appendix 4.2).

Fragmentation rates of this order of magnitude would also lead to retardation in homogeneous systems, assuming that the rate of termination of an intermediate radical is equal to the rate of termination of a 'normal' radical. Since no retardation is observed in homogeneous systems and because for nBA polymerizations with I it was found that $k_{\text{-add}} = 10^4 \text{ s}^{-1}$, slow fragmentation can be rejected as a contribution to the decrease in polymerization rate in these seeded emulsion polymerizations.

In conclusion, it can be said that slow fragmentation of the intermediate radical, leading to an underestimation of the true entry rate, is not the reason for the observed decrease in the entry rate.

Seeded emulsion RAFT polymerizations

133

4.7 Conclusions

The presence of RAFT agents with low transfer constants (approx. 0.7) has a large effect on the kinetics of the seeded emulsion polymerization of styrene. Using \odot -radiolysis relaxation measurements to determine the exit rate coefficient directly, this exit rate coefficient was found to increase with the amount of RAFT, showing the linear dependence on the molar ratio of RAFT to monomer as predicted by the transfer/diffusion theory for exit.

Measurements of the steady-state rate with chemical initiator showed that the entry rate coefficients decreased with the amount of RAFT.

This is inconsistent with the aqueous-phase-propagation model for entry, which successfully predicts the entry rate coefficient for ordinary emulsion polymerization systems. Based on these results, it was postulated that the RAFT agents used in this work are surface active. This is supported, but not conclusively confirmed, by measurement of the conductivity and ζ -potential of the latex in the presence of RAFT.

Surface activity seems likely because of the canonical forms of these RAFT agents. On the other hand, qualitatively the decrease in entry rate was larger than what can be explained by surface-activity alone. Other causes were considered but no closely reasoned explanation could be put forward at this stage of investigation.

4.8 References

- [1] Gilbert, R. G. **Emulsion Polymerization: A Mechanistic approach**; Academic: London, (1995)
- [2] Van den Brink, M.; Pepers, M.; Van Herk, A. M.; German, A. L. **Emulsion (Co) polymerization of styrene and butyl acrylate monitored by on-line raman spectroscopy**. *Macromol. Symposia* (2000), 150(Polymers in Dispersed Media), 121
- [3] Van den Brink, M.; Pepers, M.; Van Herk, A. M.; German, A. L. **On-line monitoring and composition control of the emulsion copolymerization of VeoVA 9 and butyl acrylate by Raman spectroscopy**. *Polymer Reaction Eng.* (2001), 9(2), 101
- [4] Lansdowne, S. W.; Gilbert, R. G.; Napper, D. H.; Sangster, D. F. **Relaxation studies of the seeded emulsion polymerization of styrene initiated by γ -radiolysis**. *J. Chem. Soc., Faraday Trans. 1* (1980), 76(6), 1344
- [5] Lichti, G.; Sangster, D. F.; Whang, B. C. Y.; Napper, D. H.; Gilbert, R. G.. **Effects of chain-transfer agents on the kinetics of the seeded emulsion polymerization of styrene**. *J. Chem. Soc., Faraday Trans. 1* (1982), 78(7), 2129
- [6] De Bruyn, H.; Gilbert, R. G.; Ballard, M. J. **Exit in the Emulsion Polymerization of Vinyl Acetate**. *Macromolecules* (1996), 29(27), 8666
- [7] Maxwell, I. A.; Morrison, B. R.; Napper, D. H.; Gilbert, R. G. **Entry of free radicals into latex particles in emulsion polymerization**. *Macromolecules* (1991), 24(7), 1629
- [8] Vorwerg, L.; Gilbert, R. G.. **Electrosteric Stabilization with Poly(Acrylic) Acid in Emulsion Polymerization: Effect on Kinetics and Secondary Particle Formation**. *Macromolecules* (2000), 33(18), 6693
- [9] Maxwell, I. A.; Morrison, B. R.; Napper, D. H.; Gilbert, R. G. **The effect of chain-transfer agent on the entry of free radicals in emulsion polymerization**. *Makromol. Chem.* (1992), 193(2), 303
- [10] Brandrup, J.; Immergut, E. H.; Editors. **Polymer Handbook, Fourth Edition**. (1998)

Chapter 4

134

- [11] Wojnarovits, L.; Takacs, E. **Rate coefficients of the initial steps of radiation induced oligomerization of acrylates in dilute aqueous solution**. *Radiat. Phys. Chem.* (1999), 55(5-6), 639
- [12] Schoonbrood, H. A. S.; **Emulsion co- and terpolymerization : monomer partitioning, kinetics and control of microstructure and mechanical properties** Ph. D. thesis, Technische Universiteit Eindhoven, Eindhoven, 1994
- [13] Leaist, D. G.; Abdu, S. M. **Ternary Mutual Diffusion Coefficients and Critical Micelle Concentrations of Aqueous Sodium Dodecyl Sulfate + Lithium Dodecyl Sulfate Solutions at 25**

- °C. J. Chem. Eng. Data (2001), 46(4), 922
- [14] Griffiths, M. C.; Strauch, J.; Monteiro, M. J.; Gilbert, R. G. **Measurement of Diffusion Coefficients of Oligomeric Penetrants in Rubbery Polymer Matrixes**. *Macromolecules* (1998), 31(22), 7835
- [15] Schoonbrood, H. A. S.; van den Boom, M. A. T.; German, A. L.; Hutovic, J. **Multimonomer partitioning in latex systems with moderately water-soluble monomers**. *J. Polym. Sci., Part A: Polym. Chem.* (1994), 32(12), 2311
- [16] Maxwell, I. A.; Kurja, J.; Van Doremaele, G. H. J.; German, A. L. **Thermodynamics of swelling of latex particles with two monomers**. *Makromol. Chem.* (1992), 193(8), 2065
- [17] Casey, B. S.; Morrison, B. R.; Maxwell, I. A.; Gilbert, R. G.; Napper, D. H. **Free radical exit in emulsion polymerization. I. Theoretical model**. *J. Polym. Sci., Part A: Polym. Chem.* (1994), 32(4), 605
- [18] Morrison, B. R.; Casey, B. S.; Lacik, I.; Leslie, G. L.; Sangster, D. F.; Gilbert, R. G.; Napper, D. H. **Free radical exit in emulsion polymerization. II. Model discrimination via experiment**. *J. Polym. Sci., Part A: Polym. Chem.* (1994), 32(4), 631
- [19] Smith, W. V.; Ewart, R. H. **Kinetics of emulsion polymerization**. *J. Chem. Phys.* (1948), 16, 592
- [20] Jovanovic, S.; Romatowski, J.; Schulz, G. V. **Molecular-weight distribution of several emulsion polymers of styrene**. *Makromol. Chem.* (1965), 85 187
- [21] Schulz, G. V.; Romatowski, J. **Emulsion polymerization of styrene with intermittent chain initiation. I. Molecular-weight distribution**. *Makromol. Chem.* (1965), 85 195
- [22] Romatowski, J.; Schulz, G. V. **Emulsion polymerization of styrene with intermittent free radicals. II. Kinetic investigations**. *Makromol. Chem.* (1965), 85 227
- [23] Nomura, M.; Minamino, Y.; Fujita, K.; Harada, M. **The role of chain transfer agents in the emulsion polymerization of styrene**. *J. Polym. Sci., Polym. Chem. Ed.* (1982), 20(5), 1261
- [24] Mendoza, J.; De La Cal, J. C.; Asua, J. M. **Kinetics of the styrene emulsion polymerization using n-dodecyl mercaptan as chain-transfer agent**. *J. Polym. Sci., Part A: Polym. Chem.* (2000), 38(24), 4490
- [25] Monteiro, M. J.; De Brouwer, H. **Intermediate Radical Termination as the Mechanism for Retardation in Reversible Addition-Fragmentation Chain Transfer Polymerization**. *Macromolecules* (2001) 34(3), 349
- [26] Kwak, Y.; Goto, A.; Tsujii, Y.; Murata, Y.; Komatsu, K.; Fukuda, T. **A Kinetic Study on the Rate Retardation in Radical Polymerization of Styrene with Addition-Fragmentation Chain Transfer**. *Macromolecules* (2002) 35(8), 3026
- [27] de Brouwer, H.; Tsavalas, J. G.; Schork, F. J.; Monteiro, M. J. **Living Radical Polymerization in Miniemulsion Using Reversible Addition-Fragmentation Chain Transfer**. *Macromolecules* (2000), 33(25), 9239
- [28] Moad, G.; Chiefari, J.; Chong, Y. K.; Krstina, J.; Mayadunne, R. T. A.; Postma, A.; Rizzardo, E.; Thang, S. H. **Living free radical polymerization with reversible addition - fragmentation chain transfer (the life of RAFT)**. *Polymer International* (2000), 49(9), 993
- [29] Prescott, S. W.; Ballard, M. J.; Rizzardo, E.; Gilbert R. G. **Successful Use of RAFT Techniques in Emulsion Polymerization: Living Character, RAFT Agent Transport and Rate of Polymerization**. *Macromolecules*, submitted
- [30] Monteiro, M. J.; de Barbeyrac, J. **Free-Radical Polymerization of Styrene in Emulsion Using a Reversible Addition-Fragmentation Chain Transfer Agent with a Low Transfer Constant: Effect on Rate, Particle Size, and Molecular Weight**. *Macromolecules* (2001), 34(13), 4416
- [31] Barner-Kowollik, C.; Quinn, J. F.; Morsley, D. R.; Davis, T. P. **Modeling the reversible addition-fragmentation chain transfer process in cumyl dithiobenzoate-mediated styrene homopolymerizations: assessing rate coefficients for the addition-fragmentation equilibrium**. *J. Polym. Sci., Part A: Polym. Chem.* (2001), 39(9), 1353
- [32] Barner-Kowollik, C.; Vana, P.; Quinn, J. F.; Davis, T. P. **Long-lived intermediates in reversible addition-fragmentation chain-transfer (RAFT) polymerization generated by γ radiation**. *J. Polym. Sci., Part A: Polym. Chem.* (2002), 40(8), 1058
- Seeded emulsion RAFT polymerizations*

135

[33] van Herk, A. M.; de Brouwer, H.; Manders, B. G.; Luthjens, L. H.; Hom, M. L.; Hummel, A. **Pulsed**

Electron Beam Polymerization of Styrene In Latex Particles. *Macromolecules* (1996), 29(3), 1027

[34] O'Donnell, J. H.; Sangster, D. F. **Principles of radiation chemistry**, London : Arnold, 1970

[35] Corpart, P.; Charmot, D.; Biadatti, T.; Zard, S.; Michelet, D. **Block polymer synthesis by controlled radical polymerization.** *PCT Int. Appl.* (1998), WO 9858974

[36] Morton, M.; Kaizerman, S.; Altier, M. W. **Swelling of latex particles.** *J. Colloid Sci.* (1954), 9, 300

[37] Gardon, J. L.. **Emulsion polymerization. I. Recalculation and extension of the Smith-Ewart Theory.** *J. Polym. Sci., Polym. Chem. Ed.* (1968), 6(3), 623

[38] Buback, M.; Gilbert, R. G.; Hutchinson, R. A.; Klumperman, B.; Kuchta, F. D.; Manders, B. G.;

O'Driscoll, K. F.; Russell, G. T.; Schweer, J. **Critically evaluated rate coefficients for free-radical polymerization. 1. Propagation rate coefficient for styrene.** *Macromol. Chem. Phys.* (1995), 196(10), 3267

[39] Kukulj, D.; Davis, T. P. **Average Propagation Rate Coefficients in the Free-Radical Copolymerization of Styrene and α -Methylstyrene Measured by Pulsed-Laser Polymerization.** *Macromolecules* (1998), 31(17), 5668

[40] Kapfenstein-Doak, H.; Barner-Kowollik, C.; Davis, T. P.; Schweer, J. **A Novel Method for the Measurement of Chain Transfer to Monomer Constants in Styrene Homopolymerizations: The Pulsed Laser Rotating Reactor Assembly.** *Macromolecules* (2001), 34(9), 2822

[41] Stickler, M.; Meyerhoff, G. **Thermal polymerization of methyl methacrylate, 1. Polymerization in bulk.** *Makromol. Chem.* (1978), 179(11), 2729

[42] Merck Catalogue 1998/1999

[43] <http://www.philipanalitica.com>

[44]] DeKock, John Ph. D. thesis, Technische Universiteit Eindhoven, Eindhoven. Average value of Eqs. 4.13 and 4.14

[45] McManus, N. T.; Penlidis, A.. **A kinetic investigation of styrene/ethyl acrylate copolymerization.** *J. Polym. Sci., Part A: Polym. Chem.* (1996), 34(2), 237

[46] Russell, G. T.; Gilbert, R. G.; Napper, D. H. **Chain-length-dependent termination rate processes in free-radical polymerizations. 1. Theory.** *Macromolecules* (1992), 25(9), 2459

[47] Scheren, P. A. G. M.; Russell, G. T.; Sangster, D. F.; Gilbert, R. G.; German, A. L. **Chain-Length-Dependent Termination Rate Processes in Free-Radical Polymerizations. 3. Styrene Polymerizations with and without Added Inert Diluent as an Experimental Test of Model.** *Macromolecules* (1995), 28(10), 3637

[48] Monteiro, M. J.; Hodgson, M.; De Brouwer, H. **The influence of RAFT on the rates and molecular weight distributions of styrene in seeded emulsion polymerizations.** *J. Polym. Sci., Part A: Polym. Chem.* (2000), 38(21), 3864

Chapter 4

136

Block copolymer synthesis using the RAFT technique

137

5

Block copolymer synthesis using the RAFT technique

Abstract

*In this chapter the application of the RAFT technique for the synthesis of polystyrene-block-poly(*n*-butyl acrylate) is described. First block copolymers are synthesized in homogeneous media. This approach has proven to be successful and the best results are obtained when the styrene block is polymerized first. Subsequently, the synthesis of block copolymers in emulsion under batch conditions is described and it is found that this approach can be applied with success. The emulsion block copolymerization process is further optimized by performing semi-batch reactions. The theory behind this semi-batch approach is provided. Experimental results show that indeed high purity block copolymers of a much lower polydispersity are being synthesized under semi-batch conditions as compared to batch operation. Finally, films made from block copolymer latexes are compared with films from random copolymer latexes and blended homopolymer latexes. The appearance and the T_g values of the films were different due to different microstructures.*

Chapter 5

138

5.1 Introduction

Polymers derived from more than one type of monomer are usually referred to as copolymers. The sequence arrangement of the constitutional units determines the type of copolymer. In a linear block copolymer the units are arranged such that one block consists of monomer one and the other block of monomer two. In addition to linear architectures, like diblock or multiblock copolymers, also more exotic structures like four arm starblock copolymers are possible. Block copolymers are used in many applications. They can for instance be used as surfactants[1], as adhesion promoters[2], as dispersing agents[3], as impact modifiers or as compatibilizers.

Before the advent of free-radical 'living' polymerization techniques, block copolymers were and still are being synthesized using anionic and other living polymerization techniques, e.g. cationic polymerization, or by non-living techniques like end-group functionalization and Ziegler-Natta catalysis[4]. These polymerization techniques suffer from a number of disadvantages. The choice of monomers that can be used is limited, the process cannot tolerate even very low levels of impurity, expensive reagents are required, and it requires special equipment and reaction conditions, which translates to expensive polymer products.

The recent development of 'living' free-radical polymerization techniques like Nitroxide Mediated Polymerization (NMP)[5], Atom Transfer Radical Polymerization (ATRP)[6,7] and Reversible Addition-Fragmentation chain Transfer (RAFT) polymerization[8] has allowed the preparation of complex polymer architectures (e.g. block, hyper-branched, star) via 'conventional' free-radical polymerization[9]. All these methods are relatively robust to impurities, can be carried out over a wide range of reaction conditions and can be used for a wide range of monomers.

In this chapter the synthesis of block copolymers in both a homogeneous system and in emulsion using RAFT will be discussed.

5.2 Synthesis of polystyrene-block-poly(*n*-butyl acrylate) in solution using RAFT

As mentioned above, RAFT is one of the new 'living' polymerization techniques that allows synthesis of complex architectures via conventional free-radical techniques. In recent years, a number of publications have appeared that describe the *Block copolymer synthesis using the RAFT technique*

139

synthesis of unusual polymers prepared from free-radical 'living' polymerization[e.g.10]. In most cases these papers deal with the synthesis of block copolymers, but synthesis of more complex architectures (stars, branches, dendrimers) are slowly being realized[11].

In this section a xanthate will be used in the synthesis of polystyrene-blockpoly(*n*-butyl acrylate) in a toluene solution. Two approaches will be tested. In the first approach styrene is polymerized first, followed by *n*-butyl acrylate (nBA). In the second approach the opposite order is followed.

First styrene, then n-butyl acrylate

First, low molecular weight polystyrene was synthesized in the presence of a low transfer constant RAFT agent, *i.e.* *O*-ethylxanthyl ethyl propionate (I, Scheme 4.2), at 70 °C. The amount of dead chains was minimized by keeping the initiator concentration very low (1 mole% of the amount of RAFT agent). The polymer formed was precipitated in methanol, filtered and washed a few times with methanol. The latter was done in order to remove monomer and RAFT residuals, to exclude their influence on the second block polymerization. Since the polymerization did not proceed to high conversion a considerable amount of un-reacted RAFT agent was still present because of the low transfer constant of the RAFT agent with styrene (see Chapter 3). The number-average molecular weight of the polymer formed, M_n , was $2.0 \cdot 10^3$ g mol⁻¹ and the polydispersity, PD, was 1.44. This low polydispersity (compared to a polydispersity of about 2.0 found in Chapter 3 for styrene homopolymerizations) is probably the result of the precipitation, in which the lowest molecular weight polymer is selectively removed. The polystyrene obtained was then used in a solution polymerization with *n*-butyl acrylate. The procedure and experimental conditions are summarized in Table 5.1. Styrene was polymerized at 70 °C and nBA at 60 °C. This was done because the polymerization of styrene at 60 °C is too slow, whilst at 70 °C nBA polymerizes too fast, making sampling difficult.

Chapter 5

140

Table 5.1 Reaction conditions and results of a block copolymerization of styrene and *n*-butyl acrylate with RAFT in solution, in which styrene is polymerized first.

First step: styrene homopolymerization

Recipe

0.016 g AIBN

10.020 g styrene
 2.116 g I (Scheme 4.2)
 10.002 g toluene
 Conditions
 70 °C
 21 hours .
 precipitation in methanol Result 46% conversion
 $M_n=2011$
 $PD=1.44$

. polystyrene (**PS1**)
 Second step: n-butyl acrylate block copolymerization

Recipe
 0.043 g AIBN
 6.412 g n-butyl acrylate
 0.508 g **PS1**
 15.080 g toluene

Conditions
 60 °C
 23.5 hours
 Result
 88% conversion
 $M_n=14636$
 $PD=2.15$

The molecular weight and polydispersity versus conversion of the second step, as obtained by GPC analysis using a refractive index (RI) detector are shown in Figure 5.1. In the ideal case, *i.e.* no homopolymer formation of the second monomer and negligible termination, the M_n is given by:

$$\frac{M_n}{M_n} = \frac{m_A}{m_B} \frac{x}{1-x} \quad (5.1)$$

in which M_n

M_n is the number average molecular weight of the first block (A), x is the fractional conversion of the second monomer (B), m_A is the total mass of the polymer A and m_B is the total initial mass of monomer B. It should be noted that the data in Figure 5.1 are based on polystyrene standards and, therefore, quantitatively might contain an error. The main error comes from the difference in refractive index of polystyrene and poly(n-butyl acrylate) in relation to THF (the mobile phase for GPC).

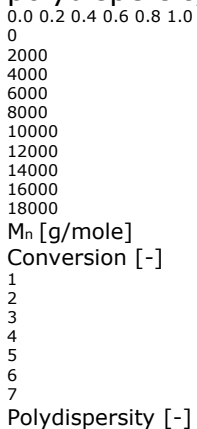
In general, the concentration detector (*i.e.* refractive index detector) of the GPC will show approximately a three times greater concentration for polystyrene than for poly(n-butyl acrylate) at the same homopolymer concentrations[12].

Block copolymer synthesis using the RAFT technique

Figure 5.1 Number average molecular weight (closed squares), M_n , and polydispersity (open circles) of the second step (n-butyl acrylate polymerization) of a block copolymerization of nbutyl acrylate and styrene. The solid line (..) represents the theoretical evolution predicted by Eq. 5.1. Also the PREDICI simulations (Appendix 5.1) of the polydispersity profiles for different transfer constants are shown. (----) $C_T=1.0$; (- - - - -) $C_T=1.31$; (· · · · ·) $C_T=1.73$. Figure 5.1 shows that M_n increases linearly with conversion and that the polydispersity initially increased and then decreased to a final value of about 2.15.

What should be noted is that the molecular weights are much lower than theoretically expected from Eq. 5.1. Correction of the molecular weights with the Mark-Houwink parameters of poly(n-butyl acrylate) only gives slightly higher molecular weights. The differences in molecular weight between theory and experiment might arise from termination of initiator-derived radicals and transfer reactions, which are not taken into account in Eq. 5.1. However, they are most probably the result of the differences in refractive index between polystyrene and poly(n-butyl acrylate), as discussed above. Low molecular weight polystyrene will give a 3 times stronger signal than an equal amount of poly(n-butyl acrylate) and, therefore, the molecular weight found will be an underestimation of the true molecular weight.

When the polydispersities are now considered, it can be seen that the polydispersity first increased to a value of about 4.5 and then decreased towards 2.15 at 88% conversion. This is not surprising, since both the newly formed block copolymer and the starting block combine to give the polydispersity. The high



Chapter 5

142

polydispersity is also due to the polydispersity of the starting polystyrene and the low transfer constant of nBA to the polystyrene-xanthate.

In Figure 5.1 PREDICI simulations (Appendix 5.1) of the polydispersity at different transfer constants, 1, 1.3 and 1.73 are shown. These simulations indicate that the experimental polydispersity profile fits that found from simulation and corresponds to a transfer constant for this RAFT polymerization between 1 and 1.3.

The results found for both the molecular weight and polydispersity profiles indicate that a block copolymer has been produced.

Additional evidence for the formation of block copolymer is obtained from the

GPC traces. Using a UV detector on the GPC, the shift of the polystyrene can be monitored. If the molecular weight of the starting polystyrene dormant species grows by the addition of nBA then the molecular weight distribution as observed from UV detection should also increase. This is due to the fact that poly(n-butyl acrylate) does not have an extinction coefficient at 254 nm, and thus is considered 'invisible'.

Therefore, a shift of the UV-detector GPC trace to higher molecular weights proves that the polystyrene molecular weight has increased, indicating block copolymer formation. In Figure 5.2a the GPC UV traces are shown.

Figure 5.2a clearly shows a shift of the GPC traces towards higher molecular weights. Since these traces have been normalized, it also shows that the amount of initially present dormant polystyrene decreases. The fact that at 88% conversion, most of the GPC signal shifted towards the high molecular weight side indicates that most of the polystyrene starting material has been converted to block copolymer and this type of block copolymer synthesis is quite effective. In Figure 5.2b the starting and final MWDs are shown.

Besides the clear shift towards higher molecular weight of the MWD obtained from the UV detector, this figure also shows that the final MWDs from UV and RI do not completely overlap as a result of unreacted polystyrenexanthate and 'dead' polystyrene. Figure 5.2b also indicates that the amount of high molecular weight nBA homopolymer is small, suggesting that the resulting polymer contains a high percentage of block copolymer.

Block copolymer synthesis using the RAFT technique

143

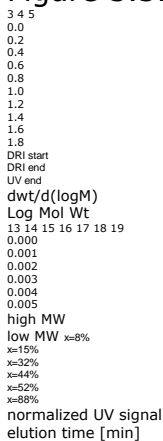
Figure 5.2 Normalized GPC UV (254 nm) traces of block copolymer of n-butyl acrylate polymerized on polystyrene (a) and the starting and final MWDs (b). Both the starting MWD and final MWDs obtained from the RI detector and the UV detector at 254 nm are shown.

Since the amount of polystyrene in the reactor is constant, the UV trace can be normalized and thus the area below the UV-signal over a designated elution time-span indicates the amount of material in the corresponding molecular weight span.

Therefore, this data can be used to estimate the transfer constant of n-butyl acrylate to dormant polystyrene chains (with a xanthate end-group), using the method described by Goto *et al.*[13-15]. It can be derived that:

$$\frac{dM}{dt} = \frac{dS}{dt} = \frac{dC_0}{dt} \quad (5.2)$$

in which S_0 is the amount of transfer agents at $t=0$, S is the amount of transfer agent, M_0 the amount of monomer at $t=0$ and M the amount of monomer. If the natural logarithm of S_0/S and the natural logarithm of M_0/M are plotted versus time, then the transfer constant is given by the ratio of the slopes of these plots. Here the amount of transfer agent, in this case dormant polystyrene chains, is estimated from the height of the low molecular weight side of the UV GPC trace. The amount of monomer can be obtained from the conversion measurements. The result is shown in Figure 5.3.



a b

Chapter 5

144

Figure 5.3 Determination of the transfer constant of n-butyl acrylate to polystyrenexanthate using the method of Goto. The transfer constant, C_T , is obtained from conversion measurements and the GPC traces in Figure 5.2 using Equation 5.2. This results in a C_T of $3.31 \cdot 10^{-5} / 3.18 \cdot 10^{-5} = 1.04$.

The transfer constant derived from the data in Figure 5.3 for n-butyl acrylate to polystyrene-xanthate is 1.04. It should be noted that this value is an underestimation and in fact will be higher. The amount of dormant polystyrene is estimated from the low molecular weight side of the GPC UV trace, which will also contain some block copolymer as a result of the broadness of the high block copolymer peak. This results in an overestimation of the amount of polystyrene-xanthate and thus an underestimation of the transfer constant. The transfer constant of n-butyl acrylate with I was determined in Chapter 3 and was found to be 1.7, which is of the same order of magnitude, especially when the underestimation of the value reported in this section is taken into account. Moreover, the transfer constant obtained here corresponds to the value obtained from the PREDICI simulations (between 1 and 1.3), as shown in Figure 5.1.

It can be concluded that the synthesis of polystyrene-block-poly(n-butyl acrylate) using a xanthate is effective when styrene is polymerized first and that the transfer constant of n-butyl acrylate to polystyrene-xanthate is of the same order of magnitude as to I. In the next section polystyrene-block-poly(n-butyl acrylate) was synthesized in the opposite order, starting with dormant poly(n-butyl acrylate).

0 3600 7200 10800 14400 18000 21600 25200
0.0
0.2

0.4
0.6
0.8
1.0
 $\ln M_0/M = 3.18 \cdot 10^{-5} t$
 $\ln S_0/S = 3.31 \cdot 10^{-5} t$
 $\ln S_0/S [-]$
time [s]
0.0
0.2
0.4
0.6
0.8
1.0
 $\ln M_0/M [-]$

Block copolymer synthesis using the RAFT technique

145

First n-butyl acrylate, then styrene

It has been shown that it is possible to produce a block copolymer of styrene and n-butyl acrylate when styrene is polymerized first. This does not automatically mean that polymerizing the monomers in the reverse order can produce the same purity of block copolymer. In block copolymerizations it is important that the first block (A) is a comparable or a better leaving group as compared to the second block (B)[16]. In simple terms, the growing B chain will add to a dormant A chain and form an intermediate radical. If B is a much better leaving group than A, the intermediate radical will go back to its originating species after most additions. This results primarily in the formation of homopolymer.

The same is also clearly shown by Eq. 3.1, which shows that the transfer rate coefficient will be decreased drastically if $k_{\text{-add}} \gg k_{\text{tr}}$. Because the transfer constants of the xanthates with styrene and n-butyl acrylate are low, as shown in Chapter 3, this is of special importance when xanthates are used as RAFT agents. Accordingly, if the transfer constant of B to dormant A chains $\ll 1$, a lot of homopolymer A will remain and the polydispersity will be broad. For styrene and n-butyl acrylate it is not expected that one of these two forms a much better leaving group as compared to the other. Therefore, it is expected that the block copolymerization can also be performed in the reverse order. To test this, an experiment was performed in which n-butyl acrylate was polymerized first in the presence of I, followed in a second step by styrene. The experimental conditions and results are given in Table 5.2.

Table 5.2 shows that the polymer formed in the first step is of low molecular weight (*i.e.* 7065 g/mol) and that the polydispersity is 1.64. The second stage polymerization produced a polymer with an M_n close to 20640 and a PD of 2.15 after 46.5 % conversion. Although the molecular weight (based on polystyrene standards) is also close to the theoretically expected molecular weight (Eq. 5.1) this is not a proof that block copolymers have been produced. In this case where butyl acrylate is polymerized first, a shift of the UV trace towards higher molecular weights is not an indication for block formation. However, the shift of the low molecular weight peak in the Refractive Index (RI) traces and RI MWD, which have been scaled to conversion, indicates that the starting block had increased in molecular weight. This is shown in Figure 5.4. It is important to note that these traces

also have to be corrected for differences between polystyrene and poly(n-butyl acrylate) in detector signal[12].
 However, since the polymer composition at a certain elution time is unknown this

Chapter 5

146

cannot be done, and, therefore, these results are only indicative and should be considered with care.

Table 5.2 Reaction conditions and results of a homogeneous blockcopolymerization of styrene and nbutyl acrylate with RAFT. First n-butyl acrylate is polymerized.

First step: n-butyl acrylate homopolymerization Recipe 0.050 g AIBN 20.185 g n-butyl acrylate 0.719 g I (Scheme 4.2) 16.100 g toluene Conditions 65 °C 20.5 hours extraction with methanol Result 100% conversion $M_n=7065$ PD=1.64 . poly(n-butyl acrylate) (**PB1**)

Second step: styrene block copolymerization

Recipe

0.040 g AIBN

16.119 g styrene

4.017 g **PB1**

16.113 g toluene

Conditions

65 °C

19.5 hours

Result

46.5% conversion

$M_n=20640$

PD=2.15

Figure 5.4 (a) GPC RI traces and (b) MWDs of a homogeneous block copolymerization where nBA is polymerized first then followed by polymerization of styrene. Both are scaled with conversion and indicate a shift of the starting block towards higher molecular weights.

Another indication of block copolymer formation is the M_n and polydispersity obtained from the UV trace. Because the UV detector at 254 nm only observes

```

12 13 14 15 16 17 18
0.000
0.002
0.004
0.006
0.008
0.010
0.012 46% conversion
6% conversion
starting poly(n-butyl acrylate)-xanthate
RI signal [arbitrary unit]
Elution time [min]
3.0 3.5 4.0 4.5 5.0 5.5 6.0
-0.5
0.0
0.5
1.0
1.5
2.0
2.5
3.0
3.5
4.0
RI MWD at
46% conversion
UV MWD at
46% conversion
starting
poly(n-butyl acrylate)-xanthate
dwt/d(logM)
Slice Log MW
  
```

a b

Block copolymer synthesis using the RAFT technique

147

polymer chains containing styrene (*i.e.* styrene homopolymer and block copolymer) and thus not the starting poly(*n*-butyl acrylate), the M_n will be higher and the polydispersity will be lower than appears from the RI trace. It was found that M_n is 29 kg mol⁻¹ with a polydispersity of 1.69. This M_n is much lower than the M_n that would be obtained if no transfer to the dormant poly(*n*-butyl acrylate) chains took place and is close to what is expected using a transfer constant of styrene to poly(*n*-butyl acrylate)-xanthate close to 1. These results indicate polymerizing butyl acrylate first can also produce a block copolymer. However, absolute proof can be obtained by HPLC, by which the disappearance of the dormant poly(*n*-butyl acrylate) can be monitored. Therefore, the polymer formed was analyzed by HPLC using a silica column and a gradient of *n*-heptane to THF. The polymer concentration that was injected was chosen such that the amount of pBA was equal for all samples. In that case, a decrease in the pBA peak indicates the formation of block copolymer. The results are shown in Figure 5.5.

Figure 5.5 HPLC chromatograms of the experiment described in Table 5.2. The amount of injected pBA was equal for all three samples. The signal of the pBA peak does not disappear, even after 46% conversion, which indicates that the formation of block copolymer is not effective.

Figure 5.5 shows that the pBA signal does not or hardly decrease, which indicates that the formation of block copolymer after 46% conversion is not effective.

These results are not in accord with the results obtained by GPC, which indicated that at least some block copolymer was formed. Since the GPC results are quantitatively

14 16 18 20 22 24 26
0

pBA

ELSD signal

Elution time [min]

0.9% conversion

6.2% conversion

46% conversion

Chapter 5

148

less reliable as a result of differences in styrene and nBA detector signals, the formation of block copolymer in this experiment, in which butyl acrylate is polymerized first, is yet to be fully resolved. Therefore, in the following parts, which will deal with block copolymerizations in emulsion, styrene will be polymerized first because in that case it has clearly been shown that block copolymer has formed.

5.3 Synthesis of polystyrene-block-poly(*n*-butyl acrylate) in emulsion

It has been shown that it is possible to synthesize polystyrene-block-poly(*n*-butyl acrylate) in solution using a xanthate as RAFT agent. In Chapter 4 it has been shown that seeded styrene polymerizations with xanthates resulted in stable polystyrene-xanthate latexes. So in principle, because both emulsion polymerization with xanthates and solution block copolymerization are possible, also block copolymerization in emulsion should be possible, which has been shown for other systems in literature[17,18]. The easiest approach would be to just add

the second monomer after full conversion of the first monomer or to use the latex of a RAFT polymerization as a seed latex.

In the previous section it was shown that a block copolymer of styrene and butyl acrylate can be synthesized by chain extension of polystyrene-xanthate with the second monomer. It was also shown that block copolymer formation can be monitored more easily when styrene is polymerized first. The formation of block copolymers when polystyrene is the starting block can be observed due to shift of the UV GPC trace toward higher molecular weights. Therefore, in the following emulsion experiments styrene was polymerized first in the presence of a xanthate and a poly(methyl methacrylate) (PMMA) seed. The PMMA seed was used such that the resulting polystyrene (PSTY) latex formed would have a controlled particle size and particle number. It should be noted that the amount of PMMA by the end of the polymerization is only a few percent (4-6%) of the PSTY, and is for our purpose considered negligible. The resulting PSTY latex was then used for chain extension with n-butyl acrylate. This approach was followed in the 2 experiments that are shown in Table 5.3. The mass ratio of styrene to nBA was 1 to 2 and 1 to 9.34 for PBL1 and PBL2, respectively.

Block copolymer synthesis using the RAFT technique

149

Table 5.3 Reaction conditions and results of a block copolymerization of styrene and n-butyl acrylate with RAFT in emulsion.

First step: styrene homopolymerization

Recipe

water 120.4 g

SDS 0.401 g

NaHCO₃ 0.046 g

pMMA seed latex 42.4 g
(5.6% solids, d=62 nm)

SPS 0.046 g

I 0.855 g

styrene 40.01

Conditions

70 °C

24 hours

Result

100% conversion

M_n=12082

PD=2.01

particle size (CHDF) d_n
=230 nm

. polystyrene-xanthate
latex (**PSL1**)

Recipe

water 121.6 g

SDS 0.37 g

NaHCO₃ 0.046 g

pMMA seed latex 40.1 g

(4.3% solids, $d_z=40$ nm)

SPS 0.046 g

I 1.52 g

styrene 40.12 g

Conditions

70 °C

21 hours

Result

100% conversion

$M_n=6917$

PD=2.10

particle size (DLS) d_v

=129 nm

. polystyrene-xanthate

latex (**PSL2**)

Second step: n-butyl acrylate block copolymerization

Recipe

water 64.8 g

SDS 0.161 g

NaHCO₃ 0.016 g

PSL1 40.01 g

SPS 0.016 g

nBA 16.02 g

Conditions

60 °C

22 hours

$m_{nBA}/m_{polystyrene}=2$

Result

100% conversion

$M_n=25655$

PD=1.80

$d_v=366$ nm

. polystyrene-blockpoly(

n-butyl acrylate)

latex (**PBL1**)

Recipe

water 140.3 g

SDS 0.3 g

NaHCO₃ 0.03 g

PSL2 20.39 g

SPS 0.03 g

nBA 40.005 g

Conditions

60 °C

6 hours

$m_{nBA}/m_{polystyrene}=9.34$

Result

100% conversion

$M_n = 46947$
 $PD = 2.76$
 $d_v = 290 \text{ nm}$
 . polystyrene-blockpoly(
 n-butyl acrylate)
 latex (**PBL2**)

Table 5.3 shows that in both experiments conversion reached 100% and that the chain extension of the polystyrene-xanthate latex with nBA resulted in an increase in molecular weight. In Figure 5.6 the evolutions of M_n and polydispersity with conversion of these 2 experiments are shown.

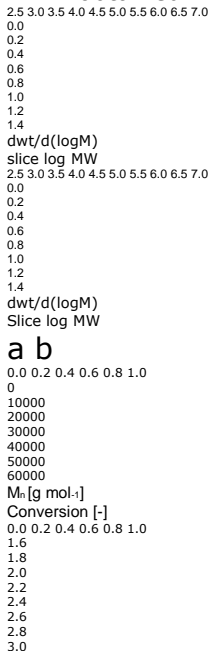
Chapter 5

150

Figure 5.6 Block copolymerizations of n-butyl acrylate on a polystyrene-xanthate latex, as described in Table 5.3 (a) M_n versus conversion and (b) polydispersity versus conversion. The lines represent the theoretical predictions according Eq. 5.1. The closed squares and solid line represent the experiment with a nBA to polystyrene weight ratio of 2 (PBL1), the open circles and dashed line represent the experiment with a nBA to polystyrene weight ratio of 9.34 (PBL2).

Similar to what was observed for the block copolymerizations in solution, M_n increases linearly with conversion and the molecular weights are lower than predicted by Eq. 5.1, which again might be the consequence of differences in RI detection of polystyrene and poly(n-butyl acrylate)[12]. Another observation that can be made is that in the second experiment, which is the one with the high nBA to polystyrenexanthate ratio, the polydispersity started to increase at $x > 0.6$. In Figure 5.7 the MWDs of the starting blocks and the final polymers are shown.

Figure 5.7 MWDs of starting polystyrene-xanthate and final block copolymers of seeded emulsion polymerizations with a nBA to polystyrene-xanthate ratio of 2 (a) and a nBA to polystyrene-xanthate ratio of 9.34 (b). The solid MWD (..) represents the starting polystyrene-xanthate, the dashed MWD (- - -) represents the MWD obtained from the UV detector and the dotted MWD (· · ·) represents the MWD obtained from the RI detector.



a b

Block copolymer synthesis using the RAFT technique

151

Figure 5.7 shows that in both experiments the MWD obtained by UV has shifted towards higher molecular weights, which indicates that block copolymer has been produced. The fact that the UV MWD and the RI MWD are largely overlapping indicates that a high percentage of the final material is block copolymer. However, it can be seen from the high molecular weight side in Figure 5.7b that in the experiment with the high nBA to polystyrene-xanthate ratio there is also some high molecular weight nBA homopolymer, which is not observed in Figure 5.7a. Figure 5.6 showed that at high conversions the polydispersity increased to approximately 2.8, whereas the number-average molecular weight is still increasing linearly (or even less). This indicates that the high molecular weight material is formed towards the end of the reaction. This could be the result of a gel effect, leading to low transfer constants of the polymeric xanthates and thus higher molecular weights. However, the fact that this high molecular weight material is not produced in the experiment with the low nBA to polystyrene-xanthate ratio indicates that another effect may also be at play.

Other possibilities include secondary nucleation, which means that new particles are formed in which no RAFT agent is present. Since the high molecular weight material is produced at high conversion, *i.e.* in a stage where all monomer is already in the particles, secondary nucleation is unlikely. Moreover, the particle number was much higher than the catastrophic region for secondary nucleation[19] and the particle sizes after the second stage correspond to the particle sizes theoretically expected. Another possibility is that the xanthate group becomes less accessible for a growing radical because of slow diffusion, phase separation, or because the xanthate groups become buried in the particle. After all, at high conversions the polymer chains become less mobile. Since for the transfer reaction in a RAFT block copolymerization diffusion of a polymer chains towards another polymer chain is required, the probability of transfer will decrease as a consequence. This might lead to the formation of high molecular weight material at high conversions. For the moment this seems the only plausible explanation.

Additional evidence for the formation of block copolymer was obtained by HPLC. The polymer formed in PSL2 and PBL2 was separated using a gradient of heptane to THF on a silica column. The chromatograms of PSL2 and PBL2 at 8%, 36% and 61% conversion, respectively, are shown in Figure 5.8.

Chapter 5

152

Figure 5.8 HPLC chromatograms of PBL2. After 61% conversion all initially present PSL2 has disappeared, which indicates that all polystyrene-xanthate has been transformed into block copolymer.

Figure 5.8 shows that at 61% conversion all initially present polystyrenexanthate has disappeared and thus has been transformed into block copolymer.

It can be concluded that via emulsion polymerization, block copolymers can be produced. Although the observed molecular weights are below the expected values and under some conditions also homopolymer has been formed, a high percentage of the final material is block copolymer. Moreover, all initially present polystyrenexanthate was transformed into blocks.

In order to optimize the block copolymer formation, semi-batch experiments have been performed. In two separate papers Monteiro *et al.* have shown that under starved feed conditions a higher percentage of block copolymer can be obtained compared to batch conditions[17,18]. They attributed this higher percentage of blocks to a lower entry efficiency (and thus less termination)[17] and to a decrease in secondary particle formation[18], respectively.

In the following section it will be shown that due to the fact that the rate of transfer over the rate of propagation is artificially increased by feeding in monomer, it is theoretically expected that the polymer will be of higher purity and narrower polydispersity. Therefore, the following section will deal with this theory and with the results of semi-batch synthesis of polystyrene-block-poly(*n*-butyl acrylate).

16 18 20 22 24 26

0

ELSD signal

Elution time [min]

PSL2

PBL2 8% conversion

PBL2 36% conversion

PBL2 61% conversion

Block copolymer synthesis using the RAFT technique

153

5.4 Synthesis of polystyrene-block-poly(*n*-butyl acrylate) in emulsion

under semi-batch conditions

Because of the low transfer constant of *n*BA and styrene with xanthates, low polydispersity block copolymers cannot be obtained under batch conditions. However,

Müller *et al.* have shown that it is theoretically possible to produce low polydispersity

material with low transfer constant species if the monomer concentration is kept

low[22], whereas Moad *et al.* have already produced low polydispersity blocks using

macromonomers under semi-batch conditions[23].

If the monomer concentration is low enough then ideally each growing radical will add no more than one monomer unit before the radical activity is transferred to another chain. This means that all chains grow more or less simultaneously, resulting in a low polydispersity. In the case of an ideal block copolymerization of *n*BA on polystyrene-xanthate, all initially present polystyrene-xanthate chains will add an equal number of monomer units to form the new block copolymer. In terms of a number distribution (concentration versus chain length) this means that during the

polymerization the whole initially present distribution will be translated over the chain length axis towards a higher molar mass. This means that an ideal living polymerization can theoretically be imitated by performing the block copolymerization under starved feed conditions, whereby the monomer feed rate and thus the monomer concentration approaches zero. Deviations from ideal behavior are caused by side reaction like transfer to monomer and polymer or termination. If a reasonable polymerization rate is desired the monomer concentration must be higher than the ideal 'zero' concentration. Moreover, the polymerization is performed in emulsion, so not all polymer chains will grow simultaneously as a result of compartmentalization. In this section, first, the above mentioned theoretical aspects of a semi-batch block copolymerization will be considered, followed by the results of a series of semibatch block copolymerizations of nBA on polystyrene (with a polydispersity of 2) with different monomer feed rates.

Ideal block copolymerization

As mentioned before, an ideal block copolymerization (all initially present chains of the first block will add the same number of monomer units) will result in a translation of the chain length distribution of the initial block over the chain length axis. In Chapter 4 and Table 5.3 it was shown that conventional seeded batch

Chapter 5

154

emulsion polymerizations with xanthates led to the formation of a polystyrenexanthate latex with a polydispersity of approximately 2. The chain length distribution of such polymer can mathematically be approximated by a Flory-Schultz distribution[19]:

$$\dots$$

$$\cdot$$

$$\dots$$

$$\cdot$$

$$- =$$

$$n M$$

$$M$$

$$\exp) M (P (5.3)$$

In Figure 5.9 the chain length distributions P(M), weight distributions W(M), GPC plots X(M) and polydispersity versus M_n of an ideal block copolymerization for varying degrees of chain extension are shown. The initially present block has an M_n of 7000 and a polydispersity of 2 and is obtained from Eq. 5.3. X(M) and W(M) are obtained from P(M) using the following relationship:

$$2 M) M (P M) M (W) M (X = = (5.4) M_n \text{ and } M_w \text{ and thus the polydispersity are obtained from P(M) and Eqs. A2.1 and A2.3 (See Appendix 2.1).$$

Figure 5.9 shows that an ideal block copolymerization can lead to narrow molecular weight material, even though the starting material has a polydispersity of 2.

For instance a chain extension from $M_n = 7000$ to $M_n=14000$ leads to a decrease in the polydispersity from 2 to 1.25 (Figure 5.9d), whereas a chain extension to $M_n = 25000$ already leads to a polydispersity of 1.08.

Block copolymer synthesis using the RAFT technique

155

Figure 5.9 Simulations of the chain length distribution $P(M)$ (a), the weight distribution $W(M)$ (b), the GPC distribution (c) and the polydispersity versus chain extension (d) for an ideal block copolymerization (*i.e.* all initially present polymer chains add the same number of monomer units in the second stage) in which the starting block has an M_n of 7000 and a polydispersity of 2 (Flory-Schultz distribution, Eq. 5.3).

In Figure 5.7d the polydispersity versus chain extension of an ideal block copolymerization is compared to a PREDICI simulation of a batch block copolymerization (Appendix 5.1) using $C_T = 10^4$ and a very low initiator concentration.

Ideal block copolymerization conditions can also be approached if the transfer constant in the RAFT process is very high. In Figure 5.9 a PREDICI simulation (Appendix 5.1) of the polydispersity versus chain extension is shown for a batch block copolymerization with a transfer constant of 10^4 and a low initiator concentration. It appears that a system having a transfer constant of this order of magnitude, which is not unrealistic for high reactivity RAFT agents[15], behaves like an ideal block copolymerization. However, in the present work xanthates are used as RAFT agents, which have a transfer constant close to 1. Therefore, ideal chain extension conditions have to be approached by performing the block copolymerization under semi-batch conditions. For a number of reasons ideal conditions cannot be fully fulfilled:

```

0.0 2.0x104 4.0x104 6.0x104 8.0x104 1.0x105 1.2x105
0
initial distribution Mn=7000
Mn=10500 (msw/msy=0.5)
Mn=14000 (msw/msy=1)
Mn=21000 (msw/msy=2)
Mn=35000 (msw/msy=4)
Mn=77000 (msw/msy=10)
W(M) [arbitrary mass]
M [g/mol]
0.0 2.0x104 4.0x104 6.0x104 8.0x104 1.0x105 1.2x105
0.0
P(M) [arbitrary concentration]
M [g/mol]
initial distribution Mn=7000
Mn=10500 (msw/msy=0.5)
Mn=14000 (msw/msy=1)
Mn=21000 (msw/msy=2)
Mn=35000 (msw/msy=4)
M
n
=77000 (m
sw
/m
sy
=10)
7000 14000 21000 28000 35000 42000 49000 56000
1.0
1.2
1.4
1.6
1.8
2.0
polydispersity [-]
Mn [g/mol]
ideal block copolymerization
PREDICI simulation of batch block copolymerization
with C
=104 and very low initiator concentration
1.0
1.2
1.4
1.6
1.8
2.0
2.5 3.0 3.5 4.0 4.5 5.0 5.5
0.000
initial distribution Mn=7000
Mn=14000 (msw/msy=1)
Mn=21000 (msw/msy=2)
Mn=35000 (msw/msy=4)
w(log M)
log(M)

```

a b

d c

156

- Side reactions like e.g. transfer and termination cannot be neglected.
- Under starved feed conditions where the feed rate is slow enough to produce low polydispersity polymer, the polymerization rate will be infinitely slow such that the reaction cannot be performed in a practical way.
- Not all chains have an equal probability to grow as a result of a broad particle size distribution.

The latter consideration is due to the fact that per unit of volume all particle sizes contain the same number of polymer chains. The smaller particles have a larger surface area per volume unit and, therefore, have a higher probability to be entered by an aqueous phase radical.

The two aforementioned ideal block copolymerization conditions, i.e. very low monomer concentration or high transfer constant, can be compared in terms of the average number of monomer units that is added between an activation and deactivation of a polymer chain. This average number of monomer units, \bar{n} , is given by:

$$\bar{n} = \frac{C_p}{C_T} \left(\frac{k_p}{k_t} \right) \quad (5.5)$$

In Table 5.4 it is calculated which monomer concentration (C_p) is required for a semi-batch block copolymerization with $C_T=1$ in order to obtain the same \bar{n} as in a batch polymerization with a high(er) transfer constant.

Table 5.4 Calculation of the particle monomer concentration (C_p) that is required to obtain the same average number of monomer units (\bar{n}) inserted per activation in a semi-batch emulsion block copolymerization with $C_T=1$ compared to a batch emulsion block copolymerization with a high(er) transfer constant.

parameters Batch \bar{n} Semi-batch $C_T=1$

$$C_T = 10^4 \quad 1.6 \cdot 10^{-2} \quad C_p = 2.5 \cdot 10^{-3} \text{ M}$$

$$C_T = 10^3 \quad 1.6 \cdot 10^{-1} \quad C_p = 2.5 \cdot 10^{-2} \text{ M}$$

$$C_T = 10^2 \quad 1.6 \cdot 10^0 \quad C_p = 2.4 \cdot 10^{-1} \text{ M}$$

$$C_T = 10^1 \quad 1.6 \cdot 10^1 \quad C_p = 1.9 \text{ M}$$

$$C_{p,sat} = 5.5 \text{ M}$$

$$FW_{monomer} = 128 \text{ g mol}^{-1}$$

$$FW_{first\ block} = 7000 \text{ g mol}^{-1}$$

$$d_{monomer} = 900 \text{ g dm}^{-3}$$

$$d_{first\ block} = 1100 \text{ g dm}^{-3}$$

Block copolymer synthesis using the RAFT technique

157

The calculations in Table 5.4 show that in the absence of side-reactions a semibatch polymerization with a low transfer constant can give the same results as a batch polymerization with a high transfer constant. For example,

the initially formed polymer of a batch polymerization with $C_T=100$ will be similar to the polymer formed in a semi-batch polymerization with $C_T=1$ and $C_P=0.24$, which shows that a high transfer constant is not essential to produce low polydispersity material. In the next section the results of semi-batch emulsion polymerizations of nBA on polystyrenexanthate will be presented.

Results

In the previous section we have seen that batch polymerization of nBA on polystyrene-xanthate latexes did lead to the formation of block copolymer which, however, was not of low polydispersity. It was also shown that, if the monomer concentration is kept low during the polymerization, it is theoretically possible to produce low polydispersity block copolymer with xanthates, even though the first block has a relatively high polydispersity of about 2. In order to test whether or not low polydispersity block copolymer can be obtained using RAFT agents with a low transfer constant, like the xanthates, a series of experiments was performed in which nBA was fed to a polystyrene-xanthate latex with an M_n of 7000 and a polydispersity of 2. The final nBA to polystyrene mass ratio is 4 to 1 in all experiments and the final solid contents of the latex is 20%. The polymerization was performed at 60 °C, the surfactant concentration was kept below the critical micelle concentration and the initiator concentration was 1 mM, such that the amount of dead chains as a result of bimolecular termination is kept low. In Figure 5.10 the monomer feed profiles and overall conversion versus time and the corresponding monomer concentration, C_p , versus overall conversion are shown.

Chapter 5

158

Figure 5.10 (a) Overall conversion versus time and monomer feed profiles for semi-batch emulsion block copolymerizations with different monomer feed rates.

The solid line (..) represents the monomer feed profile for the lowest feed rate (monomer feeding time 790 minutes), the dashed line (- - -) represents the monomer feed profile for the medium feed rate (monomer feeding time 395 minutes) and the dotted line (. . . .) represents the monomer feed profile for the fastest feed rate (monomer feeding time 197.5 minutes).

(b) The corresponding particle monomer concentration, C_p , versus the overall conversion.

Figure 5.10a shows that the semi-batch polymerizations are not completely starved feed. The measured overall conversion is not equal to the monomer feed profiles. Figure 5.10b shows that a higher monomer feed rate results in a higher monomer concentration in the particles. From the foregoing discussion about ideal block copolymerizations and from the work of Müller[22] it is therefore expected that a higher monomer feed rate will result in a higher polydispersity of the block copolymer. In Figure 5.11 the M_n and polydispersity versus conversion are shown.

Figure 5.11a shows that M_n increases with conversion. If the experimental molecular weights are compared with the theoretically expected molecular weights it is obvious that the experimental values are much lower, similar to what was found by Chambard for his block copolymerizations with ATRP[20]. At full conversion an M_n of $3.5 \cdot 10^4$ g mol⁻¹ is expected, while $2.0 \cdot 10^4$ g mol⁻¹ or lower was found. Figure 5.11b shows that the polydispersity decreases with increasing conversion.

a b
 0 20 40 60 80 100
 0.0
 0.5
 1.0
 1.5
 2.0
 2.5
 3.0
 lowest feed rate
 medium feed rate
 highest feed rate
 C_0 [M]
 overall conversion [%]
 0 180 360 540 720 1400 1500
 0
 20
 40
 60
 80
 100
 overall conversion [%]
 time [min]
 0
 20
 40
 60
 80
 100
 percentage of monomer added [%]
 0 180 360 540 720 1400 1500

Block copolymer synthesis using the RAFT technique

159

Figure 5.11 (a) M_n versus overall conversion and (b) polydispersity versus overall conversion for semibatch emulsion block copolymerizations with different monomer feed rates. The polydispersity start at 2, the polydispersity of the polystyrene block, and decreases during the polymerization. The solid line represents the theoretically expected M_n (Eq. 5.1).

If the monomer feed rate is higher, lower M_n values are found, which suggests that transfer to monomer might be the cause. Another reason can be that GPC analysis does not give reliable results for these block copolymers, which was already suggested in sections 5.2 and 5.3. Figure 5.11b shows that the polydispersity decreases with conversion and in the end relatively low polydispersity material was produced. Figure 5.11b also shows that a lower monomer feed rate results in lower polydispersities. This is not unexpected, since at lower monomer feed rates the system is closer to the ideal block copolymerization conditions. When the polydispersity profiles in Figures 5.11b and 5.9d are compared it is obvious that the block copolymerization does not proceed ideally, resulting in higher polydispersities that ideally can be obtained. This is due to the monomer concentration not approaching zero and due to side reactions like transfer and termination. However, it is obvious that the polydispersities in these semi-batch polymerizations are much lower than those in the batch polymerization of the previous section. It is therefore expected that the block copolymers produced under semi-batch conditions are much more pure, which is confirmed by the MWDs in Figure 5.12.

0 20 40 60 80 100
 8000
 10000
 12000
 14000
 16000
 18000
 20000
 M_n [g/mol]
 overall conversion [%]
a b
 0 20 40 60 80 100
 1.3
 1.4
 1.5
 1.6
 1.7
 1.8
 1.9
 2.0
 lowest feed rate
 medium feed rate
 highest feed rate
 polydispersity [-]
 overall conversion [%]

1.3
1.4
1.5
1.6
1.7
1.8
1.9
2.0

Chapter 5

160

Figure 5.12 MWDs of the starting polystyrene-xanthate block (solid line, ...) and the final block copolymer of a semi-batch polymerization (monomer fed in 790 minutes), obtained by both RI detection (dashed line, - - - -) and UV detection (dotted line, ······). Figure 5.12 shows that the UV MWD has shifted towards higher molecular weight completely, which indicates that block copolymer has formed. From the matching overlays of the UV and RI MWDs it can be concluded that the block copolymer formed is very pure. Semi-batch block copolymerization conditions are therefore preferred over batch conditions. Besides narrower molecular weight distributions it also results in purer block copolymers. Even narrower MWD material will be obtained if also the first block would have a narrow molecular weight distribution.

Semi-batch polymerizations of styrene on a polystyrene-xanthate latex, on the other hand, did not result in narrow molecular weight material. On the contrary, the polymer obtained in the end was of a high polydispersity. Probably this is the result of the high intra-particle viscosity at high conversions, which immobilized the xanthate groups at low monomer concentrations, resulting in a lowering of the transfer constant and consequently the formation of high molecular weight material in the end. When toluene, which acts as a plasticizer, was added to the monomer feed the polydispersity became much lower. These results are shown in Figure 5.13.

2.4 2.8 3.2 3.6 4.0 4.4 4.8 5.2 5.6
0.0
0.2
0.4
0.6
0.8
1.0
1.2
1.4
1.6
1.8

dwt/d(logM)

Slice log MW

Block copolymer synthesis using the RAFT technique

161

Figure 5.13 M_n (closed symbols) and polydispersity (open symbols) versus conversion for a semi-batch emulsion polymerization of styrene on a polystyrene-xanthate latex at 60 °C with and without 17 w% toluene added to the monomer feed. The amount of monomer was 3.8 times the weight of the initially present polystyrene-xanthate and fed during 790 minutes. The squares represent the results of the experiment without toluene and the circles represent the results of the experiment with 17 w% toluene added to the monomer feed. The solid line represents the theoretical M_n according to Eq. 5.1.

It can be concluded that it is possible to produce narrow molecular weight block copolymer in emulsion with xanthates and that the block copolymer is of high purity.

However, care has to be taken in choosing the right reaction conditions. A too high intra-particle viscosity might lead to less satisfying results, as was shown by the semibatch experiments with styrene on polystyrene-xanthate.

In the next section some properties of block copolymer latexes will be compared with blends of homopolymer latexes and with random copolymer latexes of the same composition.

5.5 Polystyrene-block-poly(*n*-butyl acrylate) latex films

5.5.1 Introduction

The research and development of latexes, used *e.g.* as binders in waterborne coatings or in waterborne adhesives, has focused on systems consisting of more than one monomer. The use of more than one monomer combines the specific properties of

0 20 40 60 80 100

0

4000

8000

12000

16000

20000

24000

M_n [g mol⁻¹]

conversion [%]

1

2

3

4

5

6

polydispersity [-]

Chapter 5

162

each component and reduces the need for additives. Examples include blends of latexes, copolymer latexes and two-stage latexes. Often a polymer with a low glass transition temperature (T_g) is used in combination with a polymer with a high T_g . The low T_g polymer ensures good film formation, while the high T_g polymer accounts for other properties, for instance hardness or scratch resistance. The development of 'living' free radical polymerization in emulsion has extended this field of research by introducing the possibility of creating more complex architectures *e.g.* block copolymer latexes.

This section describes the morphology, *i.e.* the geometrical arrangement of the different phases, of polystyrene-block-poly(*n*-butyl acrylate) (PSblockPB) latex films, which were synthesized using the RAFT technique, and the effect of heat treatment on the film. Polystyrene has a T_g (approx. 100 °C) much higher than the ambient film formation temperature, while the T_g of poly(*n*-butyl acrylate) (approx. -50 °C) is much lower than the ambient film formation temperature. The block copolymer films will be compared with films made from random copolymer latexes (PSrandomPB) and blends of homopolymer latexes (PSblendPB) of the same overall composition and comparable molecular weights and particle sizes. Two styrene to *n*-butyl acrylate ratios will be considered, 1/1 and 1/4, respectively.

5.5.2 The latexes and latex films

Two block copolymer latexes, two random copolymer latexes and two blends of a polystyrene latex with a poly(*n*-butyl acrylate) latex were prepared using the RAFT technique. All latexes had a solid content of approximately 20% and

the styrene to nbutyl acrylate ratio was 1/1 or 1/4, respectively. The random copolymer latex and the homopolymer latexes used to make the blends were synthesized by seeded batch emulsion polymerizations, in which I (Scheme 4.2) was used to control the molecular weight. The block copolymer latexes were synthesized by semi-batch emulsion polymerization of nBA on a polystyrene-xanthate seed ($M_n=7405 \text{ g mol}^{-1}$, $PD=1.92$, $d_v=143 \text{ nm}$). Molecular weights and particle sizes are given in Table 5.5.

Block copolymer synthesis using the RAFT technique

163

Table 5.5 Properties of the latexes used for film casting. All latexes have a solid content of 20%. Films were cast and dried at room temperature.

M_n	[g/mol]	PD	[-]	Particle size	d_v [nm]
PSblockPB 1/1	11296	1.63	193		
PSblockPB 1/4	19884	1.46	270		
PSrandomPB 1/1	18067	1.99	194		
PSrandomPB 1/4	36183	1.92	204		
pSTY 7405	1.92	143			
PSblendPB 1/1					
pBA 8403	1.59	196			
pSTY 7405	1.92	143			
PSblendPB 1/4					
PBA 29514	1.63	208			

These latexes were used to cast a thin film, just covering the bottom of a Petri

dish. The latexes were dried at room temperature for several weeks. The film formation of polymer latexes can be described as a three-stage process. In the first stage water evaporates, which results in a decrease in the inter-particle distance until the particles come in contact with each other. The second stage involves the coalescence of the particles and evaporation of the remaining interstitial water. In the third stage, the macromolecules interdiffuse across the particle-particle boundaries.

Photographs of about 1 cm^2 of the dried films on a black background are shown in Figure 5.14. Subsequently, the Petri dishes were put in an oven for 20 hours at $140 \text{ }^\circ\text{C}$, a temperature above the T_g of both polymers. The appearance of the films after this heat treatment is also shown in Figure 5.14. In Table 5.6 a description of the appearance of the films is given.

Table 5.6 Description of appearance of films cast from styrene/n-butyl acrylate latexes and dried at room temperature before and after a heat treatment of 20 hours at $140 \text{ }^\circ\text{C}$.

film before heat treatment	after heat treatment
PSblockPB 1/1	white/opaque opaque/transparent
PSrandomPB 1/1	transparent/opaque transparent
PSblendPB 1/1	white/sticky macro phase separated
PSblockPB 1/4	white/opaque opaque/transparent

PSrandomPB 1/4 transparent/opaque transparent
PSblendPB 1/4 white/sticky/phase
separation
macro phase separated

Chapter 5

164

Figure 5.14 Fotos of films (approximately 1 cm²), cast from styrene/n-butyl acrylate latexes dried at room temperature before and after a heat treatment of 20 hours at 140 °C.

PSblockPB 1/1
PSrandomPB 1/1
PSblendPB 1/1
PSblockPB 1/4
PSrandomPB 1/4
PSblendPB 1/4
before heat
treatment
after heat
treatment

Block copolymer synthesis using the RAFT technique

165

5.5.3 Discussion

All films, formed at room temperature, have a white and/or opaque appearance, which indicates that either phase separation has occurred or coalescence is incomplete. The transparency of the films, both before and after the heat treatment, decreases from random via block to the blended latexes. In the case of the block and random copolymer latexes the transparency increases as a result of the heat treatment, whereas the same heat treatment results in (further) phase separation when the films of the blended latexes are considered, showing transparent and white domains. These results are another indication that truly block copolymers were produced. After all, the heat treatment was performed far above the T_g of both polystyrene and PBA and therefore the films of the blended latexes and the block copolymer latexes should be identical after the heat treatment if the block copolymer latexes were in fact no block copolymers but just a blend of two homopolymers.

However, because of a covalent bond between the polystyrene part and the PBA part the block copolymer latexes do not show phase separation on the same macroscopic scale as observed for the blended latexes. The absence of macroscopic phase separation with block copolymers does not exclude the possibility that micro-phase separation has occurred. After all, also on a microscopic scale phase separation is possible. This can be tested using differential scanning calorimetry (DSC). In the case that a block copolymer phase separates on a microscopic level, DSC measurements will result in two T_g values, close to the values found for the macro phase separated

blended latexes, *i.e.* the T_g values of the homopolymers. The absence of micro phase separation will result in a single T_g , close to the T_g of a random copolymer of the same composition. The T_g values found by DSC measurements of the room temperature dried films are shown in Table 5.7. It has to be noted that the T_g values found from the first and second heating scan were identical.

Table 5.7 T_g values of various styrene/n-butyl acrylate latex films, obtained by DSC.

Film	T_g 1 [°C]	T_g 2 [°C]
PSblockPB 1/1	no T_g	no T_g
PSblockPB 1/4	-47	no second T_g
PSrandomPB 1/1	15	no second T_g
PSrandomPB 1/4	-25	no second T_g
PSblendPB 1/1	-47	97
PSblendPB 1/4	-48	92

Chapter 5

166

Table 5.7 shows that the T_g values of the block copolymer films do not correspond to the T_g values of the random copolymers with the same overall composition. This indicates that in the block copolymer films, on a microscopic level, phase separation has occurred and the morphology might consist of small domains of either polystyrene in a PBA matrix or *vice versa* or might be lamellar. For PSblockPB 1/1 strangely enough no T_g is found. For PSblockPB 1/4 only 1 T_g is found, which corresponds to the low temperature T_g of the blends, for which both a low and high temperature T_g were found. The fact that only 1 T_g is found for the PSblockPB 1/4 and that the films are transparent might indicate that the polystyrene domains are very small.

It has been shown that it is possible to prepare block copolymers latexes with unique film properties. After a heat treatment far above the T_g , the block copolymer films keep a homogeneous appearance, whereas the films of the latex blends show macroscopic phase separation. The block copolymer latexes probably phase separate on a microscopic level and the morphology might consist of inclusions of one phase in a matrix of the other phase or might be lamellar. Therefore, no macroscopic phase separation is observed with the block copolymers. The microscopic phase separation is confirmed by the DSC results. After all, for the block copolymers no T_g 's are found that correspond to those for the random copolymer latexes.

The unique film properties of the block copolymer latexes can, for instance, be exploited in heat resistant high impact applications. After all, even after heating far above the T_g , a morphology of *e.g.* soft domains in a hard matrix can be maintained, whereas a blend of homopolymers leads to macroscopic phase separation.

5.6 Conclusions

It has been demonstrated that block copolymers can be prepared using RAFT

agents (xanthates) of low reactivity. Experiments, performed in solution, have shown that chain extension of polystyrene-xanthate with n-butyl acrylate resulted in the formation of block copolymers. The opposite order of synthesizing the same block copolymers, *i.e.* chain extension of poly(n-butyl acrylate)-xanthate with styrene, could not be demonstrated with certainty.

Block copolymer synthesis using the RAFT technique

167

Preparation of block copolymer latexes has also proven to be possible. A batch emulsion polymerization of n-butyl acrylate on a polystyrene-xanthate latex, also synthesized via batch emulsion polymerization using xanthates, resulted in a block copolymer latex. The process was further optimized by performing semi-batch emulsion polymerization, in which the second monomer was slowly fed to the reactor.

This resulted in very pure block copolymers of relatively low polydispersity. Finally it has been demonstrated that films of the block copolymer latexes have some unique properties as compared to blends of homopolymer latexes and random copolymer latexes of the same composition. The block copolymer films have an homogeneous appearance, even after a heat treatment, while DSC measurements revealed that the T_g 's did not correspond to the random copolymers, indicating phase separation on a microscopic level. The blended latexes, on the other hand, phase separated on a macroscopic level, while the random copolymer latexes resulted in homogeneous films with a single T_g .

5.7 Experimental

5.7.1 Materials

Styrene (STY) and n-butyl acrylate (BA) were purchased from Aldrich and purified of inhibitor by passing through an inhibitor-removal column (Aldrich). All other materials were from Aldrich (unless otherwise stated) and used as received.

5.7.2 Homogeneous polymerizations

Appropriate amounts of monomer, initiator (AIBN), RAFT agent of polymeric RAFT agent and solvent were mixed in a round-bottom flask equipped with a magnetic stirrer and reflux condenser, all under an argon atmosphere. Oxygen was removed from the mixture by bubbling through nitrogen. After that the flask was submerged in an oil bath, which was at reaction temperature. Conversion was determined gravimetrically.

5.7.3 Batch emulsion polymerizations

All ingredients except initiator solution were loaded in the 250 mL jacketed glass reactor, equipped with a reflux condenser, and stirred at 300/400 rpm for 1 hour at reaction temperature under an argon atmosphere. After that, the initiator solution was

added. Samples were taken using a syringe with a long needle through a rubber septum and conversion was determined by gravimetry. The same samples were used for GPC analysis afterwards.

5.7.4 Semi-batch emulsion polymerizations

All ingredients except initiator solution and a large part of the nBA monomer were loaded in the 250 mL jacketed glass reactor, equipped with a reflux condenser, and stirred overnight by a magnetic stirrer under an argon atmosphere and at room temperature. At that stage the reactor typically contained: 0.024 g NaHCO₃, 0.203 g SDS, 66.2 g purified water, 2 grams of nBA and 33.5 g of polystyrene-xanthate seed latex (13.1% solids). The reactor was heated at 60 °C and the initiator solution, 0.0235 g sodium persulfate in 3 g water, was added. About 15 minutes later the remaining monomer (15.7 mL) was added using a Metrohm Dosimat syringe pump at a rate of 0.02, 0.04 and 0.08 mL/min, respectively. Samples were taken using a syringe with a long needle through a rubber septum and conversion was determined by gravimetry. The same samples were used for GPC analysis afterwards.

5.7.5 GPC

The dried polymer was dissolved in tetrahydrofuran (THF, Biosolve) to a concentration of 1 mg/mL. The solution was filtered over a 0.2 mm PTFE syringe-filter. Analyses were carried out using two PLGel (Mixed-C) columns (Polymer Laboratories) at 40 °C. A Waters 486 UV-detector, operated at 254 nm, and a Waters 410 refractive index detector were used for detection. THF was used as eluent at a flow-rate of 1 ml/min. Narrow-distribution polystyrene standards (Polymer Laboratories) with molecular weights ranging from 580 to 7.1·10⁶ g/mol were used to calibrate the GPC set-up.

The molecular weights of the block copolymers were in some cases, when considered as BA homopolymers, corrected with Mark-Houwink parameters given in literature[21]: $a=0.716$ and $K=11.4 \cdot 10^{-5} \text{ dL} \cdot \text{g}^{-1}$ for polystyrene and $a=0.700$ and $K=12.2 \cdot 10^{-5} \text{ dL} \cdot \text{g}^{-1}$ for poly(n-butyl acrylate).

5.7.6 HPLC

HPLC analyses were performed using an Alliance Waters 2690 Separation Module, equipped with a PL-EMD 960 ELD Detector and a 2487 Waters dual UV detector, operating at 254 and 280 nm. The block copolymers were analysed using a Zorbax Si

column, thermostatted at 35 °C using a gradient from pure n-heptane (Biosolve) to THF (Biosolve) in 40 minutes. Typically 10 μ L of dried sample dissolved in THF at 5 mg/g THF were injected.

5.7.7 DSC

Glass transition temperatures were measured using a Perkin-Elmer Pyris 1. All polymers were dried at room temperature for several weeks and subsequently for at least 2 days under vacuum, also at room temperature. The temperature program was as follows: -70 °C to 150 °C, 5 minutes isothermally at 150 °C, back to -70 °C, 5 minutes isothermally at -70 °C and back to 150 °C, all at 10 °C min⁻¹.

5.8 References

- [1] Piirma, I. **Polymeric surfactants**; Dekker: New York, (1992)
- [2] Schellekens, M. A.J. **Adhesion promoting polyolefin block copolymers : macromolecular design based on living radical polymerization** Ph.D. thesis, Technische Universiteit Eindhoven, Eindhoven, 2002
- [3] Duivenvoorde, F. L. **Pigment dispersing in powder coatings : synthesis and use of block copolymer dispersing agents** Ph.D. thesis, Technische Universiteit Eindhoven, Eindhoven, 2000
- [4] Janes W.H.; Allport D.C. **Block copolymers**; Applied Science Publishers: London, (1973)
- [5] Georges, M. K.; Moffat, K. A.; Veregin, R. P. N.; Kazmaier, P. M.; Hamer, G. K. **Narrow molecular weight resins by a free radical polymerization process; the effect of nitroxides and organic acids on the polymerization**. Polym. Mater. Sci. Eng. (1993) 69, 305
- [6] Kato, M.; Kamigaito, M.; Sawamoto, M.; Higashimura, T. **Polymerization of Methyl Methacrylate with the Carbon Tetrachloride/ Dichlorotris- (triphenylphosphine)ruthenium(II)/ Methylaluminum Bis(2,6-di-tert-butylphenoxide) Initiating System: Possibility of Living Radical Polymerization**. Macromolecules (1995), 28(5), 1721
- [7] Wang, J. S.; Matyjaszewski, K. **Controlled/"Living" Radical Polymerization. Halogen Atom Transfer Radical Polymerization Promoted by a Cu(I)/Cu(II) Redox Process**. Macromolecules (1995), 28(23), 7901
- [8] Chiefari, J.; Chong, Y. K.; Ercole, F.; Krstina, J.; Jeffery, J.; Le, T. P. T.; Mayadunne, R. T. A.; Meijs, G. F.; Moad, C. L.; Moad, G.; Rizzardo, E.; Thang, S. H. **Living Free-Radical Polymerization by Reversible Addition-Fragmentation Chain Transfer: The RAFT Process**. Macromolecules (1998), 31(16), 5559
- [9] Matyjaszewski, K. (Ed.) **Controlled Radical Polymerization**; ACS Symposium Series No. 685; Washington DC, 1997
- [10] De Brouwer, H.; Schellekens, M. A. J.; Klumperman, B.; Monteiro, M. J.; German, A. L. **Controlled radical copolymerization of styrene and maleic anhydride and the synthesis of novel polyolefin-based block copolymers by reversible addition-fragmentation chain-transfer (RAFT) polymerization**. J. Polym. Sci., Part A: Polym. Chem. (2000), 38(19), 3596
- [11] Stenzel-Rosenbaum, M.; Davis, T. P.; Chen, V.; Fane, A. G. **Star-polymer synthesis via radical reversible addition-fragmentation chain-transfer polymerization**. J. Polym. Sci., Part A: Polym. Chem. (2001), 39(16), 2777
- [12] Tortosa, K.; Smith, J. A.; Cunningham, M. F.. **Synthesis of polystyrene-block-poly(butyl acrylate) copolymers using nitroxide-mediated living radical polymerization in miniemulsion**. Macromol. Rapid Comm. (2001), 22(12), 957
- [13] Goto, A.; Terauchi, T.; Fukuda, T.; Miyamoto, T. **Gel permeation chromatographic determination of activation rate constants in nitroxide-controlled free radical polymerization. Part 1. Direct analysis by peak resolution**. Macromol. Rapid Comm. (1997), 18(8), 673

- [14] Fukuda, T.; Goto, A. **Gel permeation chromatographic determination of activation rate constants in nitroxide-controlled free radical polymerization. Part 2. Analysis of evolution of polydispersities.** *Macromol. Rapid Comm.* (1997), 18(8), 683
- [15] Goto, A.; Sato, K.; Tsujii, Y.; Fukuda, T.; Moad, G.; Rizzardo, E.; Thang, S. H. **Mechanism and kinetics of RAFT-based living radical polymerizations of styrene and methyl methacrylate.** *Macromolecules* (2001), 34(3), 402
- [16] Chong, Y. K.; Le, T. P. T.; Moad, G.; Rizzardo, E.; Thang, S. H. **A More Versatile Route to Block Copolymers and Other Polymers of Complex Architecture by Living Radical Polymerization: The RAFT Process.** *Macromolecules* (1999), 32(6), 2071
- [17] Monteiro, M. J.; Sjöberg, M.; Van der Vlist, J.; Gottgens, C. M. **Synthesis of butyl acrylate-styrene block copolymers in emulsion by reversible addition-fragmentation chain transfer: effect of surfactant migration upon film formation.** *J. Polym. Sci., Part A: Polym. Chem.* (2000), 38(23), 4206
- [18] Monteiro, M. J.; de Barbeyrac, J. **Free-Radical Polymerization of Styrene in Emulsion Using a Reversible Addition-Fragmentation Chain Transfer Agent with a Low Transfer Constant: Effect on Rate, Particle Size, and Molecular Weight.** *Macromolecules* (2001), 34(13), 4416
- [19] Gilbert, R. G. **Emulsion Polymerization: A Mechanistic approach;** Academic: London, (1995)
- [20] Chambard, G. **Control of monomer sequence distribution. Strategic approaches based on novel insights in atom transfer radical copolymerisation.** Ph. D. thesis, Technische Universiteit Eindhoven, Eindhoven, 2000
- [21] Beuermann, S.; Paquet, D. A., Jr.; McMinn, J. H.; Hutchinson, R. A. **Determination of freeradical propagation rate coefficients of butyl, 2-ethylhexyl, and dodecyl acrylates by pulsed laser polymerization.** *Macromolecules* (1996), 29(12), 4206
- [22] Müller, A. H. E.; Yan, D.; Litvinenko, G.; Zhuang, R.; Dong, H. **Kinetic analysis of "living" polymerization processes exhibiting slow equilibria. 2. Molecular weight distribution for degenerative transfer (Direct activity exchange between active and "dormant" species) at constant monomer concentration.** *Macromolecules* (1995), 28(22), 7335
- [23] Krstina, J.; Moad, C. L.; Moad, G.; Rizzardo, E.; Berge, C. T.; Fryd, M. **A new form of controlled growth free radical polymerization.** *Macromol. Symp.* (1996), 111, 13

Appendices

Appendix 2.1 Calculation of M_n and M_w from two distributions

The number average molecular weight is given by:

•

•

• 8

=

8

=

8

=

==

1 i

i

1 i

i i

1 i

i

n

N

N M

N

w

M (A2.1)

thus

• • 8

=

8

=

• • =

1 i

i i n

1 i

i N M M N w (A2.2)

The weight average molecular weight is given by:

•

• •

8

=

8

=

8

==

1 i

i i

1 i

2

i i

1 i

i i

w

M N

M N

w
 M_w
 M (A2.3)

thus 8

$=$
 8
 $=$
 8
 $=$
 8
 $=$

$\cdot \cdot = \cdot \cdot =$

$1 i$
 $i n w$
 $1 i$
 $i w$
 $1 i$
 2
 $i i$
 $1 i$

$i i N M M w M M N M w$ (A2.4)

the total number of chains of distribution A, $\cdot 8$

$= 1 i$

$i N$, is defined as N_A .

The number average molecular weight of the sum of two distributions A and B (nitroxide end-capped chains and dead chains) then is given by:

$B A$
 $B B_n$
 $A A$
 n
 $B A$
 $B A$
 n

$N N$

$N M N M$

$N N$

$w w$

M

+

$\cdot + \cdot =$

+

$+ =$ (A2.5)

for the weight average molecular follows:

$B B_n$
 $A A$
 n
 $B B_n B$

w

$A A$

n

$A w$

w

$N M N M$

$N M M N M M$

M

$\cdot + \cdot$

$\cdot \cdot + \cdot \cdot =$ (A2.6)

Appendices

172

Appendix 3.1 Calculation <kt> (QBASIC)

```
100 INPUT "Number average degree of polymerization Pn (Mn/FW)"; Pn
110 FOR wp = 0 TO .3 STEP .05
111 Dmon# = 100 * EXP(-19.982 - 4.4073 * wp + 8.2787 * wp * wp - 13.719
* wp *
wp * wp)
120 FOR i = 1 TO 10 * Pn STEP 1
125 DI# = Dmon# / (i ^ (.49 + 1.75 * wp))
126 RI# = EXP(-1 * i / Pn)
127 sigmari# = sigmari# + RI#
130 FOR j = 1 TO 10 * Pn STEP 1
140 DJ# = Dmon# / (j ^ (.49 + 1.75 * wp))
150 RJ# = EXP(-1 * j / Pn)
160 ktij# = 5.69E+15 * (DI# + DJ#)
170 sigmasigma# = sigmasigma# + ktij# * RI# * RJ#
180 NEXT j
190 NEXT i
200 avkt# = sigmasigma# / (sigmari# ^ 2)
205 PRINT wp
210 PRINT "average kt:"; avkt# / 1E+08; "*1E8"
220 sigmari# = 0: sigmasigma# = 0
230 NEXT wp
```

Appendix 3.2 Calculation Q (QBASIC)

```
50 kp = 22900
60 kadd = 79200
70 kd = .0000095
85 kminadd = 120
90 kt = 1E+08
95 kti = 1E+08
96 ktii = 1E+08
110 M = 8.65
115 PS = .0865
120 I = .001
200 PspEST# = (((kd * I) / kt) ^ .5) * .5
205 PIEST# = (2 * PspEST# * kminadd + 2 * ktii * PspEST# * PspEST#) /
(kadd * PS
- kti * PspEST#)
210 PICALC# = (2 * kd * I + 2 * kminadd * PspEST#) / (2 * kt * PIEST# +
kadd *
PS + kti * PspEST#)
220 PspCALC# = kadd * PICALC# * PS / (2 * kminadd + kti * PICALC# + 2 *
ktii *
PspEST#)
221 check# = ABS(1 - (PspCALC# / PspEST#))
240 IF check# < .000000001# THEN GOTO 300
255 PspEST# = PspCALC#
260 GOTO 205
300 PI = PICALC#
310 PSP = PspCALC#
350 RP = kp * PI * M
360 RPMAX = kp * M * (((kd * I) / kt) ^ .5)
370 apparentkp = (RP / RPMAX) * kp
375 PRINT "PI"; PI
376 PRINT "PSP"; PSP
377 PRINT "PI max"; (((kd * I) / kt) ^ .5)
380 PRINT "real kp"; kp
390 PRINT "apparent kp"; apparentkp
400 PRINT "reduction factor"; apparentkp / kp
```

Appendix 3.3 Simple model (Matlab)

```

dydt(1)=-kp*y(1)*y(5); %M
dydt(2)=-kd*y(2); %I
dydt(3)=-kadd*y(3)*y(5)+2*kfrag*y(6); %X
dydt(4)=kt*y(5)*y(5)+kti*y(5)*y(6)+ktii*y(6)*y(6); %Pd
dydt(5)=2*f*kd*y(2)+2*kfrag*y(6)-kadd*y(5)*y(3)-2*kt*y(5)*y(5)-
kti*y(5)*y(6);
%Pr
dydt(6)=kadd*y(5)*y(3)-2*kfrag*y(6)-kti*y(5)*y(6)-2*ktii*y(6)*y(6); %Pi

```

Appendix 3.4 Full model (Matlab)

```

% 1 I
% 2 P
% 3 R
% 4 M
% 5 XR
% 6 XP
% 7 PXR
% 8 PXP
% 9 RXR
% 10 D
dydt(1)=-kd*y(1);
dydt(2)=2*f*kd*y(1)-kaddpr*y(2)*y(5)-
kaddpp*y(2)*y(6)+kminaddpxr*y(7)+2*kbetapxp*y(8)+kpstar*y(4)*y(3)-
2*kt*y(2)*y(3)-2*kt*y(2)*y(2)-kti*(y(7)+y(8)+y(9))*y(2);
dydt(3)=kbetapxr*y(7)-kpstar*y(4)*y(3)-kaddr*y(3)*y(5)-
kaddrp*y(3)*y(6)+2*kbetarxr*y(9)-2*kt*y(3)*y(2)-2*kt*y(3)*y(3)-
kti*(y(7)+y(8)+y(9))*y(3);
dydt(4)=-kp*y(2)*y(4)-kpstar*y(3)*y(4);
dydt(5)=-kaddpr*y(2)*y(5)+kminaddpxr*y(7)-
kaddr*y(3)*y(5)+2*kbetarxr*y(9);
dydt(6)=-kaddpp*y(2)*y(6)+kbetapxr*y(7)+2*kbetapxp*y(8)-
kaddrp*y(3)*y(6);
dydt(7)=kaddpr*y(2)*y(5)-kbetapxr*y(7)-kminaddpxr*y(7)+kaddrp*y(3)*y(6)-
kti*(y(2)+y(3))*y(7)-2*ktii*y(7)*y(7)-2*ktii*y(7)*(y(8)+y(9));
dydt(8)=kaddpp*y(2)*y(6)-2*kbetapxp*y(8)-kti*(y(2)+y(3))*y(8)-
2*ktii*y(8)*y(8)-
2*ktii*y(8)*(y(7)+y(9));
dydt(9)=kaddr*y(3)*y(5)-2*kbetarxr*y(9)-kti*(y(2)+y(3))*y(9)-
2*ktii*y(9)*y(9)-
2*ktii*y(9)*(y(7)+y(8));
dydt(10)=kt*y(2)*(y(2)+y(3))+kt*y(3)*y(3)+kti*y(7)*(y(2)+y(3))+kti*y(8)*
(y(2)+y(
3))+kti*y(8)*(y(2)+y(3))+ktii*y(7)*(y(7)+y(8)+y(9))+ktii*y(8)*(y(8)+y(9)
)+ktii*y
(9)*y(9);

```

Appendix 4.1 Seeded emulsion polymerization rate (QBASIC)

```

1 INPUT "filename"; filename$
2 OPEN "o", #1, filename$
3 PRINT #1, "time "; "conversion "; "nbar "; "ru "; "rs "; "rho "; "kcr
":
25 CLS
29 GOTO 2000
120 tottrad = .0000001
130 twokdi = 2 * kd * ci
140 rholst = 1E+12
145 REM ** start iteration loop **
150 im(1) = twokdi / (kpaq(1) * cw + ktaq * tottrad)
160 tnew = im(1)
170 FOR x = 2 TO z - 1
180 im(x) = kpaq(x - 1) * cw * im(x - 1) / (kpaq(x) * cw + ktaq *
tottrad)
190 tnew = tnew + im(x)
200 NEXT x
210 rhomm = kpaq(z - 1) * cw * im(z - 1) / (nc / 6.02E+23)
220 IF ABS(1 - (rhomm / rholst)) < .00001 THEN GOTO 1000
225 GOTO 230: PRINT rholst / rhomm, tnew:
230 rholst = rhomm
240 tottrad = tnew
245
250 GOTO 150
1000 rhomm = kpaq(z - 1) * cw * im(z - 1) / (nc / 6.02E+23)
1010 rhomax = twokdi / (nc / 6.02E+23)
1020 f = rhomm / rhomax
1025 CLS
1070 rho = rhomm
1100 rs = 1E-09 * ru * ((1000 * dm / (1000 * dm - cp * m0)) ^ (1 / 3))
1110 kdm = 3 * dw * cwR * .0001 / (rs * rs * cp)
1400 REM ***** limit 2a *****
1410 kcr = ktr * kdm / kp1
1420 nbarlimit2a = .5 * (((rho / kcr) ^ 2) + 2 * rho / kcr) ^ .5) - .5
* rho /
kcr
1430
1900 GOTO 3000
2000 kd = .000001 [initiator decomposition rate coefficient]
2010 z = 3 [critical degree of polymerization for entry]
2020 ktaq = 1.1E+09 [aqueous phase termination rate coefficient]
2030 nc = 1E+17 [number of particles per liter]
2040 cw = .0043 [monomer aqueous phase saturation concentration]
2045 cwR = .0012 [R aqueous phase saturation concentration]
2050 ci = .0012 [initiator concentration]
2060 kpaq(1) = 1000 [propagation rate coefficient in water of 1-mer]
2070 kpaq(2) = 500 [propagation rate coefficient in water of 2-mer]
2075 kp = 237 [monomer propagation rate coefficient]
2080 dw = .000015# [diffusion coefficient in water]
2090 ru0 = 23.25 [initial unswollen particle radius]
2095 ru = ru0 [unswollen particle radius]
2100 dm = .909 [monomer density]
2110 m0 = 104.15 [monomer molecular weight]
2120 ktr = .0167 [transfer to monomer rate coefficient]
2130 kt = 1.1E+09 [termination rate coefficient]
2140 kp1 = 1000 [propagation rate coefficient of transfer derived
radical]
2150 cp = 6 [particle monomer concentration]

```

```

2160 seedpol = .313 [weight seed polymer]
2165 dseedpol = 1.15 [density seed polymer]
2170 monomer = 12.32 [weight monomer]
2180 dnewpol = 1.05 [density of polymer formed]
2182 vwater = .0481 [volume of water]

```

Appendices

175

```

2185 time = 0
2186 conversion = 0
2187 A = kp * cp * nc / (6.02E+23 * (monomer / (vwater * m0)))
2188 timestep = 1
2189 nbar = 0
2200 GOTO 120
3000 dn = ((rho * (1 - 2 * nbar)) - 2 * kcr * nbar * nbar) * timestep
3010 nbar = nbar + dn
3020 dx = A * nbar * timestep
3030 time = time + timestep
3040 conversion = conversion + dx
3050 ru = ru0 * (((seedpol / dseedpol) + (conversion * monomer /
dnewpol)) /
(seedpol / dseedpol)) ^ (1 / 3))
3055 rsnm = rs * 1E+09
3060 IF time > 1000 THEN timestep = 10
3070 PRINT time; nbar; conversion; ru; rsnm
3071 PRINT #1, time; conversion; nbar; ru; rsnm; rho; kcr:
3075 IF conversion > .3 THEN GOTO 4000
3080 GOTO 1100
4000 END

```

Appendix 4.2 Retardation by intermediate radical termination in emulsion (Matlab)

```

N0=1; % number of particles containing no radicals
N1p=0; % number of particles containing 1 polymeric radical
N1m=0; % number of particles containing 1 monomeric radical
N1i=0; % number of particles containing 1 intermediate radical
N1r=0; % number of particles containing 1 RAFT derived radical
rhore=kdm*y(3); %rho re-entry monomer derived radical
rhorer=kdmRAFT*y(5); %rho re-entry RAFT derived radical
dydt(1)=(rhoi+rhot+rhore+rhorer)*(y(2)+y(3)+y(4)+y(5)-y(1)) +kdm*y(3)
+kdmRAFT*y(5); %N0
dydt(2)=(rhoi+rhot)*y(1) -(rhoi+rhot+rhore+rhorer)*y(2) -ktr*Cp*y(2)
+kp1*Cp*y(3) +kp1RAFT*Cp*y(5) -kadd*CpRAFT*y(2) +kfrag*y(4); %N1p
dydt(3)=rhore*y(1) -(rhoi+rhot+rhore+rhorer)*y(3) -kdm*y(3)+ ktr*Cp*y(2)
-
kp1*Cp*y(3); %N1m
dydt(4)=kadd*CpRAFT*y(2) -2*kfrag*y(4) -(rhoi+rhot+rhore+rhorer)*y(4);
%N1i
dydt(5)=rhorer*y(1) -(rhoi+rhot+rhore+rhorer)*y(5) -kdmRAFT*y(5) -
kp1RAFT*Cp*y(5) +kfrag*y(4); %N1m

```

Appendix 5.1 PREDICI simulation of a block copolymerization

In order to simulate a block copolymerization first a reaction scheme has to be chosen. Because here xanthates are used as RAFT agents the role of the intermediate radical can safely be neglected and addition and fragmentation is considered as a single transfer reaction. Further it is assumed that all termination is via combination. The following reaction scheme and rate parameters have been used in the simulations:

Appendices

176

$I + 2M \xrightarrow{2 PBR_1 k_i, \text{eff}}$

$PSR_i + M \cdot PBLR_{i+1} k_p$
 $PBR_i + M \cdot PBR_{i+1} k_p$
 $PBLR_i + M \cdot PBLR_{i+1} k_p$
 $PBR_i + PSS_j \cdot PBS_i + PSR_j k_{tr}$
 $PBLR_i + PBS_j \cdot PBLR_i + PBR_j k_{tr}$
 $PSR_i + PBS_j \cdot PSS_i + PBR_j k_{tr}$
 $PBR_i + PBS_j \cdot PBS_i + PBR_j k_{tr}$
 $PBLR_i + PBLR_j \cdot PBLR_i + PBLR_j k_{tr}$
 $PSR_i + PBLR_j \cdot PSS_i + PBLR_j k_{tr}$
 $PBR_i + PBLR_j \cdot PBS_i + PBLR_j k_{tr}$
 $PSR_i + PSS_j \cdot PSS_i + PSR_j k_{tr}$
 $PBLR_i + PSS_j \cdot PBLR_i + PSR_j k_{tr}$
 $PSR_i + PBR_j \cdot PBLD_{i+j} k_t$
 $PSR_i + PBLR_j \cdot PSBSD_{i+j} k_t$
 $PBR_i + PBLR_j \cdot PBLD_{i+j} k_t$
 $PSR_i + PSR_j \cdot PSD_{i+j} k_t$
 $PBLR_i + PBLR_j \cdot PSBSD_{i+j} k_t$
 $PBR_i + PBR_j \cdot PBD_{i+j} k_t$

I = initiator M = monomer (B)

PBR = polymeric B radical
 PSR = polymeric starting block (S) radical
 PBLR = polymeric block copolymer

PSS = dormant S block
 PBS = dormant B polymer
 PBLR = dormant block copolymer
 PSD = dead S polymer
 PBD = dead B polymer
 PBLD = dead block copolymer
 PSBSD = dead SBS triblock copolymer

Starting conditions:
 The concentration of monomer and initiator and the initial distribution (concentration versus chain length) of the starting block. The latter can be obtained experimentally by GPC or can be simulated using e.g. PREDICI.

Remark:
 PREDICI calculates the chain length distributions of all chains. In this model the copolymer composition is not taken into account. For a block copolymer the molar mass can thus be calculated by multiplying the chain length by $F_A F_{WA} + F_B F_{WB}$ (F_i is the molefraction i in the polymer, F_{Wi} is the monomer i molar mass), assuming that the copolymer composition of the block copolymer is equal over the whole distribution. For simplicity, since $F_B > F_A$, it was assumed that the molar mass of a 'block copolymer unit' is equal to F_{WB} .

Summary
 177

Summary

The discovery of 'living' free-radical polymerization techniques has broadened the scope of the polymer chemist considerably in the last decade. The extend

of control over the macromolecular structure, which formerly could only be achieved by conventional living polymerization techniques, like anionic polymerization, could now be obtained by free-radical polymerization. This brings along a number of advantages.

Radical polymerization is robust to impurities and the monomer choice is much more extensive than anionic polymerization. The other main advantage is that radical polymerization can also be carried out in an aqueous environment ('Green' Chemistry), which is known as emulsion polymerization. This brings some extra advantages, like the absence of organic solvent and the low viscosity of the product.

It goes without saying that combination of the advantages of 'living' radical polymerization and emulsion polymerization in a single process will lead to a wider range of macromolecular architectures both on a polymer composition scale as well as on a nanoscale (latex particle morphology). Research described in this thesis will utilize these two historical areas of free-radical polymerization to prepare nanoparticles with controlled polymer composition. Two techniques have been investigated: Nitroxide-Mediated Controlled Radical Polymerization (NMCRP) and Reversible Addition-Fragmentation chain Transfer (RAFT).

The reaction temperature of an emulsion polymerization is limited to the boilingpoint of water, unless the polymerization is performed at high pressure requiring expensive reactors, while for most polymerizations controlled by nitroxides temperatures above 100 °C are required. After the process was described, computer simulations have been performed in order to determine which parameters are required for a successful application of NMCRP at 90 °C. Furthermore, the effects of compartmentalization and heterogeneity on the NMCRP kinetics were analyzed. A set of four alkoxyamines was tested for their applicability at 90 °C, both in a bulk polymerization and in a miniemulsion polymerization. Although this resulted in low polydispersity polymer, the results were not satisfying, especially because the rate of polymerization was too low. Therefore, at this stage of the investigation it was decided to continue with another and more promising 'living' free-radical polymerization technique for aqueous polymerizations: RAFT.

Summary

178

RAFT is characterized by a reversible exchange of the radical activity between

the polymer chains. The faster this exchange proceeds, the more equally all polymer chains grow and the more controlled the polymerization proceeds. The transfer constant depends on this rate of exchange. The transfer constant has been determined using two methods, the Mayo method and the *ln* CLD method. By means of an extensive analysis it was made clear that both methods give reliable results. The RAFT agents that were used, the xanthates, have, as compared with many other RAFT agents, a low transfer constant of approximately 1 with a small temperature dependency. With the aid of the transfer constant and kinetic parameters from literature it was possible to simulate the rate of polymerization and the molar mass distribution of homogeneous styrene RAFT polymerization under various conditions. The results agreed well with those found experimentally. For *n*-butyl acrylate this appeared to be more complex. The values from literature resulted in an overestimation of the rate of polymerization, probably because transfer to polymer becomes important. Moreover, the leaving group of the RAFT agent seemed to play an important role. When this was an ethylbenzene radical, retardation was observed with increasing amounts of RAFT agent, while for another type of radical no effect has been observed. This could be attributed to the slow re-initiation rate of the ethylbenzene radical. The RAFT process has also been performed in a seeded emulsion polymerization. It appeared that the rate of polymerization of styrene decreased with increasing amount of RAFT agent, whereas in a homogeneous system the rate of polymerization was not affected by the RAFT agent. Extensive analysis indicated that this result was to be expected, since the exit rate parameter was expected to increase and the entry rate parameter to remain constant. It was found from τ -relaxation experiments in combination with dilatometry that indeed the exit rate parameter increased linearly with the amount of RAFT agent. Subsequently, it appeared from chemically initiated experiments that also the entry rate parameter decreased drastically. Among others, surface-activity is put forward as a possible explanation. Qualitatively this explanation is plausible, however, quantitatively it was not. Eventually, the gained knowledge has been applied to actually create macromolecular architectures in aqueous dispersions in the form of block copolymers of styrene and *n*-butyl acrylate. First, these blocks were synthesized in a homogeneous medium. The best results were obtained when styrene was polymerized

first, followed by n-butyl acrylate. It has been shown that indeed real block copolymer had formed. By monitoring the rate of polystyrene homopolymer consumption compared to n-butyl acrylate, the transfer constant of n-butyl acrylate to polystyrenexanthate could also be determined. Comparison of experimental data with simulations for polydispersity versus conversion could also be used for this purpose. Both methods resulted in a similar transfer constant of approximately 1. Subsequently, styrene in the presence of a RAFT agent was polymerized in an emulsion. The resulting polystyrene-xanthate latex was then used as a seed latex for the n-butyl acrylate polymerization and resulted in the formation of a block copolymer latex. Next, this process was further optimized. It is described how, from a theoretically point of view, the transfer constant can be apparently increased by lowering the monomer concentration. From experiments, in which n-butyl acrylate was slowly added to the polystyrene-xanthate latex, it indeed appeared that block copolymers of a very high purity and lower polydispersity were obtained.

Finally, the film-properties of the produced block copolymer latexes, as well as the effect of an increased temperature on these properties, have been compared with those of random copolymer latexes and blends of homopolymer latexes, all of the same overall monomer composition. It appeared that the three systems have different properties, which with the aid of DSC could be ascribed to differences in microstructure.